Biodegradable Glass Ceramics for Bone Regeneration

Anabela Gregório Dias

Tese submetida à Faculdade de Engenharia da Universidade do Porto para candidatura à obtenção do grau de Doutor em Ciências de Engenharia

Faculdade de Engenharia
Universidade do Porto
2005

… to Mário.

I had always the opinion,
that there is something more important than gold.
Glass, for example, I consider for more important

Ernst Rössler

Many people said that is the intellect that does a great scientist.
They were wrong, is the character.

Albert Einstein

Contents

Acknowledgments *i*

Publications *v*

Abstract *ix*

Resumo *xi*

Résumée *xiii*

Aim and structure of the thesis *xv*

Chapter 1 – Literature overview

1. General outline 1

2. Bone tissue 2

3. Bone grafts 3

3.1. Synthetic bone graft substitutes (alloplastics) 6

3.1.1. Ceramic-based bone graft substitutes 6

3.1.1.1. Synthetic hydroxyapatite-based materials 8

3.1.1.2. Synthetic tricalcium phosphate-based materials 9

3.1.1.3. Glass-based materials 9

3.1.2. Medical Applications 9

4. Glasses 11

4.1. Principles of glass formation 12

4.1.1. Structure of phosphate glasses 13

5. Glass ceramics 15

5.1. Casting and controlled crystallization method 16

5.1.1. Bulk and surface crystallization 18

5.2. Sintering and crystallization by glass powder method 19

Chapter 2 - Physicochemical characterization

2.1. *In vitro* degradation studies of calcium phosphate glass ceramics prepared by controlled crystallization 35

2.2. Crystallization studies of biodegradable $CaO-P_2O_5$ glass with MgO and TiO_2 for bone regeneration applications 51

2.3. *In situ* thermal and structural characterization of bioactive calcium phosphate glass ceramics containing TiO_2 and MgO oxides: High Temperature-XRD studies 57

2.4. Physicochemical degradation studies of calcium phosphate glass ceramic containing TiO_2 and MgO oxides 73

Chapter 3 - In vitro and in vivo biological evaluation

3.1. Biological activity of two glass ceramics in the meta- and pyrophosphate region: a comparative study 87

3.2. *In vitro* studies of calcium phosphate glass ceramics with different solubility using human bone marrow cells 93

3.3. *In vivo* performance of biodegradable calcium phosphate glass ceramics using a rabbit model: histological and SEM observation 111

Chapter 4 - General conclusions 125

Acknowledgments

Firstly, I would like to express my sincere gratitude to my supervisor, Prof. José Domingos Santos, and co-supervisor, Prof. Maria Ascensão Lopes, for their guidance, ideas, encouragement and unconditional support during the development of this work, which made it all possible.

Sincere thanks to Prof. Maria Helena Fernandes, to whom I am grateful for all availability, patience and encouragement.

I am grateful to Dr. Iain Gibson and Dr. Jan Skakle, for assistance in the X-ray diffraction analysis. I will always remember them for their kind and helpful welcome during my stay in Scotland.

I am thankful to Prof. A. Osaka, Dr. S. Takashima, Dr. K. Tsuru and Dr. S. Hayakawa for their support in several characterization studies as well as *in vivo* experiments. I am also grateful for their warm welcome and help during my stay in Japan.

I also would like to acknowledge the heads and staff of the following institutions for helping me and providing all the support needed to get through my work:

In Portugal:

- Instituto de Engenharia Biomédica (INEB), Laboratório de Biomateriais, Porto
- Departamento de Engenharia Metalúrgica e Materiais (DEMM-FEUP), Faculdade de Engenharia, Universidade do Porto, Porto

- Faculdade de Medicina Dentária da Universidade do Porto (FMDUP), Porto
- Centro de Materiais da Universidade do Porto (CEMUP), Porto
- Departamento de Engenharia Cerâmica e do Vidro (DECV-UA), Universidade de Aveiro, Aveiro

In Scotland:

- Department of Chemistry, University of Aberdeen
- School of Medical Sciences, College of Life Sciences and Medicine, Institute of Medical Sciences, University of Aberdeen

In Japan:

- Biomaterials Lab., Faculty of Engineering, Okayama University
- Research Center for Biomedical Engineering, Okayama University
- Animal Center for Medical Research, Okayama University

My sincere thanks to Ana Paula Filipe, Cristina Ribeiro, Ana Queiroz, Miguel Oliveira, Cristina Barrias, Cristina Martins, Susana Sousa and Judite Barbosa for their patience, encouragement and friendship and some other colleagues and friends that have helped me in getting through my work: Prof. Fernando Jorge Monteiro, Prof. Mário Barbosa, Pedro Granja, Marcelo Prado, Isabel Amaral, Carlos Fonseca, Meriem Lamghari, Sofia Rodrigues, Manuela Brás, Januário Lima, Virgínia Fonseca, Sónia Couto, Vanessa Maltieira, Eva Frias (INEB), Julanda, Sílvia, D. Nina, D. Amélia, Sr. Ramiro, D. Fernanda, D. Fátima (DEMM-FEUP), Prof. Teresa Duarte and Emília Soares (DEMEGI-FEUP), Margarida Amaral and Alexandra Lemos (DECV-UA), Dr. Carlos Sá and Daniela Silva (CEMUP), Prof. Américo Afonso, Mrs. Ana Mota, Prof. Adelina Costa and Prof. Lurdes Pereira (FMD-UP), Yuki Shirosaki, Yuri Nakamura, Takeshi Yabuta, Takahiro Kawai, Roxana Jaco, Adeliz (Japan), Delfina Vasconcelos and Li Wang.

To my close friends Leonor and Zé Carlos for their friendship, support and encouragement.

Finally, I also wish to express my sincere gratitude to my husband Mário, for his infinite patience and encouragement; it would have been difficult to reach my objective without your help. Thank you so much!!

To my family in general, but especially to my parents Lindalva and Almerindo for their support, encouragement and patience. Thank you!!

This thesis has been possible by the financial support from Fundação para a Ciência e Tecnologia, through the PhD grant PRAXIS XXI/BD/21458/99.

Publications

Based on the experimental work that has led to this thesis, the following publications were written:

International Journals (SCI):

1. A.G. Dias, M.A. Lopes, I.R. Gibson, J.D. Santos

"*In vitro* degradation studies of calcium phosphate glass ceramics prepared by controlled crystallization"

Journal of Non-Crystalline Solids 330 (2003) 81-89.

2. A.G. Dias, M.A. Costa, M.A. Lopes, J.D. Santos, M.H. Fernandes

"Biological activity of two glass ceramics in the meta- and pyrophosphate region: a comparative study"

Key Engineering Materials 254-256 (2004) 825-828.

3. A.G. Dias, K. Tsuru, S. Hayakawa, M.A. Lopes, J.D. Santos, A. Osaka

"Crystallization studies of biodegradable $CaO\text{-}P_2O_5$ glass with MgO and TiO_2 for bone regeneration applications"

Glass Technology 45 (2) (2004) 78-79.

4. A.G. Dias, M.A. Lopes, J.D. Santos

"Protein adsorption effect on *in vitro* acellular biodegradation of $CaO-P_2O_5$ glass ceramics"

Materials Science Forum 455-456 (2004) 398-401.

5. A.G. Dias, M.A. Lopes, J.D. Santos, M.H. Fernandes

"The influence of pre-incubation treatment in the *in vitro* biological performance of degradable $CaO-P_2O_5$ glass ceramics"

Key Engineering Materials 284-286 (2004) 565-569.

6. A.G. Dias, J.M. Skakle, I.R. Gibson, M.A. Lopes, J.D. Santos

"*In situ* thermal and structural characterization of bioactive calcium phosphate glass ceramics containing TiO_2 and MgO oxides: High Temperature - XRD studies"

Journal of Non-Crystalline Solids 351 (2005) 810-817.

7. A.G. Dias, M.A. Lopes, A.T. Trigo Cabral, J.D. Santos, M.H. Fernandes

"*In vitro* studies of calcium phosphate glass ceramics with different solubility using human bone marrow cells"

Journal of Biomedical Material Research, *in press*.

8. A.G. Dias, M.A. Lopes, A. Mota, A. Afonso, K. Tsuru, S. Hayakawa, S. Takashima, Y. Kurabayashi, A. Osaka, J. D. Santos

"*In vivo* performance of biodegradable calcium phosphate glass ceramics using the rabbit model: histological and SEM observation"

Journal of Biomaterials Applications, i*n press*.

International Conference Proceedings Books:

1. A.G. Dias, M.A. Lopes, I.R. Gibson, J.D. Santos

"Degradable $CaO-P_2O_5$ glass ceramics prepared by controlled crystallization"

17^{th} European Conference on Biomaterials, Barcelona, Espanha, 2002.

2. A.G. Dias, M.A. Lopes, K. Tsuru, S. Hayakawa, A. Osaka, J. D. Santos, A. Afonso

"In *vivo* evaluation of glass ceramic materials with different solubilities"

II Iberian Congress on Biomaterials and Biosensors, Évora, Portugal, 2004.

Abstract

The aim of this work was to develop and characterize new calcium phosphate glass ceramics that would degrade in a controlled manner in the body environment, which could ultimately be used in regenerative surgery.

Two glasses MK5 (45CaO-45P_2O_5-5MgO-5K_2O, mol%) and MT13 (45CaO-37P_2O_5-5MgO-13TiO_2, mol%) were prepared in the meta-, pyro- and orthophosphate regions and crystallized to obtain MK5B and MT13B glass ceramics, respectively. The MK5B glass ceramic was prepared by controlled crystallization of base glass blocks whereas MT13B was prepared by sintering and crystallization of base glass powder discs. As a result of the heat treatment used to convert glass into glass ceramic, four crystalline phases were precipitated in the glassy matrix: $KCa(PO_3)_3$, β-$Ca(PO_3)_2$, β-$Ca_2P_2O_7$ and $Ca_4P_6O_{19}$ phases for MK5B and $CaTi_4(PO_4)_6$, TiP_2O_7, α- and β-$Ca_2P_2O_7$ phases for MT13B. These two glass ceramics showed distinct *in vitro* and *in vivo* behaviour, which could be attributed to the different crystalline phases that were found in their microstructure.

The *in vitro* biological performance of the MK5B and MT13B glass-ceramics was assessed by direct cell culture methods using MG63 osteoblast-like cells and human bone marrow osteoblastic cells. The results demonstrated that the cells were able to adhere and proliferate on both MK5B and MT13B surfaces, but the latter showed an enhanced biological performance. Experimental findings demonstrated that the MT13B glass ceramic had a stable surface throughout the experiment time whereas MK5B had a highly unstable surface with dissolution/precipitation processes occurring throughout the culture time, causing an initial inhibition on cell attachment and subsequent proliferation. These differences might be attributed to the significant differences in the surface degradation,

which was directly correlated to the crystalline phase composition. Both glass ceramics were composed of distinct but relatively soluble phases, except the relatively insoluble $CaTi_4(PO_4)_6$ phase, which jointly with the residual glassy phase led to each glass ceramic having a unique degradation behaviour.

The *in vivo* biological response using a rabbit model showed that MT13B and MK5B had different *in vivo* degradation behaviour, however both materials demonstrated osteoconductive behaviour. The higher degradation rate observed in MK5B compared to MT13B caused a delay in new bone formation, which might be overcome for longer implantation periods.

The results demonstrated that the initial composition of mother glass used and the heat treatments applied were efficient in preparing glass ceramic biomaterials. This work also showed that by modifying the initial composition of the mother glass as well as using different heat treatment cycles, significant changes in the microstructure and properties could be achieved. Therefore, glass ceramics materials with significant different degradation rates may be prepared covering several potential clinical applications.

Resumo

O presente trabalho teve como objectivo desenvolver e caracterizar novos vidros cerâmicos de fosfato de cálcio, com degradação controlada em ambiente fisiológico, tendo em vista a sua utilização em medicina regenerativa.

Foram preparados dois vidros, MK5 (45CaO-45P_2O_5-5MgO-5K_2O, %mol) e MT13 (45CaO-37P_2O_5-5MgO-13TiO_2, %mol) na região meta-, piro- e ortofosfato, sendo posteriormente convertidos nos vidros cerâmicos MK5B e MT13B através de tratamento térmico. O MK5B foi obtido por cristalização controlada de amostras de vidro, enquanto o MT13B foi obtido por sinterização e cristalização de pós de vidro. Como resultado dos tratamentos térmicos, quatro fases cristalinas foram precipitadas na matriz vítrea, i.e. $KCa(PO_3)_3$, β-$Ca(PO_3)_2$, β-$Ca_2P_2O_7$ e $Ca_4P_6O_{19}$ no vidro cerâmico MK5B, e $CaTi_4(PO_4)_6$, TiP_2O_7, α- e β-$Ca_2P_2O_7$ no vidro cerâmico MT13B. Estes dois vidros cerâmicos apresentaram comportamentos distintos quer em ensaios *in vitro* quer *in vivo*, os quais devem ser atribuídos às diferentes fases cristalinas presentes nas respectivas microestruturas.

O comportamento biológico *in vitro* foi analisado pelo método de contacto directo com células, tendo-se utilizado a linha celular osteosarcoma MG63 e células osteoblásticas humanas. Os resultados mostraram que as células aderiram e proliferaram na superfície dos vidros cerâmicos MK5B e MT13B. O vidro cerâmico MT13B apresentou uma superfície estável ao longo do tempo de cultura, enquanto que o vidro cerâmico MK5B apresentou uma superfície altamente instável, resultante de fenómenos de dissolução/precipitação superficial, o que conduziu a uma inibição inicial na adesão das células e na subsequente proliferação. Esta diferença de comportamentos foi relacionada com a composição fásica

dos dois materiais. Os vidros cerâmicos MK5B e MT13B são constituídos por fases cristalinas relativamente solúveis no ambiente fisiológico, com excepção da fase $CaTi_4(PO_4)_6$ que é praticamente insolúvel.

O comportamento biológico *in vivo* dos dois vidros cerâmicos foi avaliado através de ensaios de cirurgia experimental, utilizando o coelho como modelo animal. Ambos materiais apresentaram comportamento bioactivo, embora com algumas diferenças acentuadas. A alta taxa de degradação do vidro cerâmico MK5B pareceu causar um atraso na formação óssea inicial, condicionando o comportamento biológico *in vivo* deste material.

Este trabalho demonstrou que modificando a composição inicial do vidro e o ciclo de tratamento térmico, induzem-se alterações significativas no microestrutura e propriedades físico-químicas e biológicas dos materiais. Vidros cerâmicos com taxas de degradação significativamente diferentes podem ser obtidos, os quais são susceptíveis de abranger um leque alargado de aplicações clínicas.

Résumée

L'objectif de ce travail a été le développement et la caractérisation de nouvelles céramiques de verre et de phosphate de calcium en cours de dégradation controlée dans le corps humain, destinées à une utilisation en chirurgie régénérative.

Deux verres, MK5 ($45CaO\text{-}45P_2O_5\text{-}5MgO\text{-}5K_2O$, mol%) et MT13 ($45CaO\text{-}37P_2O_5\text{-}5MgO\text{-}13TiO_2$, mol%), sont préparés dans les régions méta-, pyro- et orthophosphate, et cristallisés afin d'obtenir respectivement les vitro-céramiques MK5B et MT13B. MK5B est préparée par cristallisation controlée de bloques de verre basique, tandis que la MT13B est préparée par sintérisation et cristallisation de disques de poudres du verre basique.

Les résultats des traitements thérmiques utilisés pour transformer les verres en vitro-céramiques montrent quatre phases cristallines précipitées sur la matrice vitreuse: $KCa(PO_3)_3$, $\beta\text{-}Ca(PO_3)_2$, $\beta\text{-}Ca_2P_2O_7$ et $Ca_4P_6O_{19}$ dans le cas de MK5B et $CaTi_4(PO_4)_6$, TiP_2O_7, α- et $\beta\text{-}Ca_2P_2O_7$ dans le cas de MT13B. Ces deux vitro-céramiques présentent des comportements différents a la fois *in vitro* et *in vivo*. Ceci peut être attribué à plusieurs phases cristallines présentes dans leurs microstructures.

Le potentiel ostéogénique de MK5B et de MT13B a été évalué *in vitro* en utilisant les cellules ostéoblastique de la lignée MG63 et les cellules stromales de moelle osseuse. Les résultats ont démontré que les cellules sont capables d'adhérer et de proliférer sur les deux types de vitro-céramiques. Cependant, MT13B montre une meilleur adhésion et prolifération. Les résultats expérimentaux ont prouvé que la vitro-céramique MT13B présente une surface stable pendant toute la durée des expériences, alors que MK5B a une surface assez instable, oú des processus de dissolution/ précipitation pouvaient avoir lieu

pendant toute la durée de la période de culture provoquant une inibition initiale de l'attachement des cellules et de leur prolifération. Ces différences peuvent être attribuées au changement de comportement qui existe au cours la dégradation de surface. Ce comportement est directement lié à la composition chimique des phases cristallines. Les deux vitro-céramiques sont composées de phases relativement solubles bien que différentes, à l'exception de $CaTi_4(PO_4)_6$ dont la présence, avec d'autres phases vitreuses résiduelles, rend unique le comportement de dégradation de chacune des vitro-céramiques.

Les études *in vivo* chez le modèle lapin ont démontré que MT13B et MK5B ont des niveaux de dégradations différents, même si tout les deux sont ostéoconducteurs. Un taux de dégradation plus élevé a été observé chez MK5B, en comparaison avec celui de MT13B ce qui a provoqué un retardement de la formation d'os nouveau. Ce délai peut être annulé lors des périodes d'implantation plus longues.

Les résultats ont démontré que la composition initiale du verre original utilisé et le traitement thérmique appliqué sont éfficaces pour la préparation de biomatériaux vitro-céramiques. Ce travail a aussi montré que par modification de la composition du verre original ou par changement de traitement thérmique on peut obtenir des microstructures et des proprietés assez différentes. Il est donc possible de postuler que les vitro-ceramiques avec des niveaux de dégradation différents peuvent être préparées pour plusieurs applications cliniques.

Aim and structure of the thesis

In this work it was attempted to develop and characterize calcium phosphate glass ceramics materials with controlled degradation behaviour to be used as bone scaffolds for regenerative surgery applications. Two glasses in the CaO-P_2O_5-MgO system with the incorporation of K_2O and TiO_2 oxides were used as a starting point to prepare glass ceramics with different degradation rates. The glass ceramic MK5B ($45CaO$-$45P_2O_5$-$5MgO$-$5K_2O$, mol %) was shown to be highly resorbable whereas the glass MT13B ($45CaO$-$37P_2O_5$-$5MgO$-$13TiO_2$, mol %) was much less resorbable as a consequence of the crystalline phases precipitated in the mother glass matrix during the heat treatment.

This thesis is composed of four chapters. *Chapter 1* consists of a brief overview of the literature, and is organised into four divisions: bone tissue, bone grafts, glasses and glass ceramics.

Chapters 2 and 3 describe the experimental part of the work. Each chapter is prepared using a compilation of work already published and accepted as papers in international refereed journals and in international conferences.

In *chapter 2* the preparation and physicochemical characterization of the calcium phosphate glass ceramics MK5B and MT13B is described. MK5B was prepared by two heat treatment steps applied to block glass samples and MT13B by sintering discs of glass powder. The composition of the crystalline phases precipitated in the glassy matrix as a

result of heat treatments at different temperatures was determined by X-ray diffraction and the sequence of phase crystallization was studied using *in situ* high temperature X-ray diffraction (HT-XRD) analysis. The glass ceramics were also characterized using FTIR/Raman and X-ray photoelectron spectroscopy.

The *in vitro* acellular degradation studies of glass ceramics were performed to asses their resorbability potential according to standard ISO 10993:14 - *Biological evaluation of medical devices - Part 14: Identification and quantification of degradation products from ceramics*. This standard protocol that was used for the chemical degradation studies consisted of two tests. The first test consisted of an extreme soaking solution conducted at pH 3.0 uses a citric acid buffer solution that mimics the acid environment produced by osteoclasts. The second test simulates a more frequently encountered *in vivo* pH 7.4 using Tris[hydroxymethyl]aminomethane-HCl (TRIS-HCl) buffer. The tests were performed at 37ºC for up to 6 weeks. The weight loss and ions released were evaluated as a function of degradation time.

In *chapter 3* the biological evaluation of the MK5B and MT13B glass ceramics is described using *in vitro* and *in vivo* testing. The *in vitro* biological activity of the glass ceramics was evaluated by using MG63 osteoblast-like and human bone marrow osteoblastic cells. Cell morphology, proliferation and differentiation and the ability to form a mineralized extracellular matrix onto the materials surface were assessed. The *in vivo* biodegradation and tissue response induced by the presence of MK5B and MT13B glass ceramics were also shown in this chapter. The *in vivo* studies were followed over a period of 12 weeks using a rabbit model. A mixed granulometry ranging from 250-355 μm and 355-425 μm with a ratio of 1/1 was implanted in the tibiae of the rabbits and the tissue reaction at the implantation site as well as the biodegradation were evaluated as function of the implantation time.

The last *chapter 4* of this thesis presents general conclusions of the performed research, outlining the most important aspects.

The author did all of the experimental work described in this thesis, except the preparation of slices for histological studies, in which she was helped by Mrs. Ana Mota (FMDUP).

Chapter 1

Literature overview

1. General outline

Human beings are undeniably the most complex organism on this planet. The human body is a single structure but it is composed of billions of smaller structures, with the four major ones being cells, tissues, organs and systems[1,2].

The average life expectancy has been increasing progressively through time. Nevertheless, some difficulties arise as a result of a longer lifespan. The quality of life often deteriorates between 60 and 90 years due to the gradual degradation of our connective tissue (skeletal system). The need to repair or replace the deteriorated skeletal system has led to the development of bone graft substitutes[3,4]. Over the years, the use of these substitutes became standard. The range of applications continues to grow as medical research keeps exploring new scientific frontiers for diagnosing, treating, curing and preventing bone diseases. This continuous knowledge is needed to develop innovative methods, new materials as well as adjustment of existing bone grafts. At present, the design of proactive materials is highlighted. These materials elicit specific, desired, and timely responses from surrounding cells and tissues. To do this, they are either designed with structures similar to living tissues or are combined with specific molecules to promote rapid and total healing[5-7]. Undoubtedly, bone grafts substitutes have had a major impact on the practice of modern medicine and patient care in both saving and improving the quality of human life.

2. Bone tissue

Bone is a living, growing specialized form of connective tissue. As a part of the human skeleton, bone tissue provides a rigid framework that support and protects the internal organs[1,8-12].

Bone tissue is essentially constituted of an extracellular matrix and three main cell types. The extracellular matrix is a composite of inorganic (contains ≅ 65%) and organic (contains ≅ 35 %) phases. The components of the inorganic part are calcium-containing minerals, and it is the mineral content that accounts for the rigidity and strength of the bone tissue while still maintaining some degree of elasticity. The organic part of the extracellular matrix is basically composed of collagen type I and numerous non-collagenous proteins. This organic matrix is calcified by the deposition of crystals of the mineral phase, which is a highly substituted hydroxyapatite[8,9,11,12].

The three main cell types involved in the development, growth and remodelling of bone are osteoblasts, osteocytes, and osteoclasts[9,10,12-15]. The osteoblasts are fully differentiated cells responsible for the production of the extracellular bone matrix and its mineralization. It originates from less differentiated precursor cells known as osteoprogenitor or mesenchymal stem cells. These are usually found in the growing portions of bones, including the periosteum[10,12,13,16,17].

The osteocytes are the most abundant cell type in bone. They are responsible for bone matrix maintenance by secreting enzymes and maintaining its mineral content. Osteocytes derive from osteoblasts and they are not on the bone surface but regularly entrapped throughout the extracellular matrix[10,12,17-20].

Osteoclasts are giant multinucleated cells responsible for bone resorption. They originate from haematopoietic stem cells and are usually found upon bone surfaces which are undergoing bone resorption[10,13,21-24].

Bone development continues throughout adulthood in a constant remodelling process, involving the equilibrium between the resorption of bone by the osteoclasts, as well as the formation of new bone by the osteoblasts[9,13-15,17,25,26]. During the bone remodelling process, osteoclasts (bone resorption cells) remove old bone tissues by resorption, whereas osteoblasts (bone forming cells) work to refill the resorption cavities with new bone tissue.

These two processes are tied together and are responsible for the renewal of the skeleton, necessary for the maintenance of bone tissue integrity and mineral homeostasis[10-14].

The first bone formed during bone development or in the repair of fracture healing, tumours and some metabolic diseases is an immature and primitive bone called *woven bone*. The immature bone is gradually replaced by organised mature bone, *lamellar bone*. This kind of structure constitutes most of the mature skeleton. At the macrostructure level, lamellar bone is distinguished into cortical (or compact) and cancellous (or trabecular) bone[10,13,17,25,27]. They differ by the spatial orientation of its elements, organic and mineral, and by its characteristic locations in the skeleton. Compact bone represents nearly 80% of the skeleton mass, and comprises the outer parts of bones; it consists of a thick, hard and dense layer of calcified tissue. Trabecular bone only represents 20% of the skeletal mass, and fills the inner space of bones that consists of a network of thin calcified trabeculae. This bone occurs near the end of long bones and between the surfaces of flat bones[9,12,13,27].

Bone executes several functions, which can be categorised as mechanical, metabolic and protective[11-13,27]. Mechanically it acts as support and a site of muscle attachment for locomotion. Metabolically, bone acts as a reserve of ions for the entire organism, especially calcium and phosphate, and protectively it shields vital organs and bone marrow. The mechanical and protective functions are mainly performed by cortical bone and the metabolic functions are supported by trabecular bone.

3. Bone grafts

Bone graft is the term commonly used to refer to a wide range of materials used in surgical methods to stimulate new bone formation. It provides a framework through which the host bone can regenerate and heal[3,28,29]. Many medical situations call for the use of bone grafts. Among them are gaps in bone caused by trauma, facture or disease as well as abnormal skeletal development[3,30]. The types of bone grafts available to treat such problems essentially includes autografts, banked allografts and xenografts as well as a wide range of synthetic materials (alloplastics) such as ceramics, polymers and composites[3,29].

For many years the *autograft* has been considered as the gold standard for bone repair and

regeneration. It is defined as tissue transplanted from one site (donor site) to another (recipient site) within the same patient[28-30]. It is immunologically safe, thus limiting rejection concerns. These grafts provide all three requirements for the best bone regeneration: scaffold for osteoconduction, growth factors for osteoinduction and progenitor cells for osteogenesis[3,4,28]. The use of autogenous bone grafting, however is associated with various uncontrollable factors. The harvest of the autograft implies an extra and invasive surgical procedure and therefore post-operative continuous pain at the donor site or even donor site morbidity may occur. Wound infection, haematoma and hypersensitivity are other possible difficulties associated with autologous bone grafting. Another disadvantage is the limited amount of bone available for harvesting. The common donor site is the iliac crest, although bone from the tibia, fibula, distal end of the radius and posterior portions of the spine can also be used[4,30-32].

The *allograft* is defined as a tissue graft between individuals of the same species but with different genetic composition. The use of this graft type can solve some of the drawbacks related with autologous bone grafting since the second surgical procedure is eliminated and the quantity of tissue is available in large amounts[31,33,34]. Nevertheless, this alternative is associated with some problems including the risk of disease transmission[4] to the recipient and immunogenicity[35]. To lessen the potential risks to the recipient, allografts are intensively treated prior to preservation for storage, using the processes of freeze-drying, irradiation and demineralisation. However, these processes contribute to increased costs and diminished mechanical and biologic properties while the possibility of disease transmission still remains[4,31,34,36].

The *xenograft* (xenogenic bone graft) is defined as a tissue graft from a donor of a different species than the recipient. This kind of graft material allows the extraction of larger amounts of bone with a specific microstructure, reduces morbidity by eliminating the donor site and can be used as bone graft expanders by mixing them with autogenous bone[29,34]. Xenografts can be derived from mammalian bones and coral exoskeletons. Bovine derived bone has been commonly used[37,38], even though other sources such as porcine or murine bone are available. Xenogeneic bone was popular in the 1960's but fell into disfavour due to reports of patients developing autoimmune diseases following bovine bone transplants[39,40]. The re-introduction of these products in the 1990's arose after the development of methods to deproteinate bone particles, which reduces the antigenicity making these implants more tolerable to host tissues[36]. However, the use of bovine

xenograft is still a concern due to the possibility of future bovine spongiform encephalopathy from potentially slow virus transmission in bovine-derived products.

Despite the benefits of bone-derived grafts, their limitations have driven the search for synthetic alternatives[4,31,32,41-43]. Many researches have attempted to develop synthetic bone graft to provide an alternative to bone-derived grafts based on three basic criteria for successful grafting[3,4,29,42]:

(1) Osteoconduction to provide a structural framework and environment that supports the migration, attachment and growth of osteoblasts and osteoprogenitor cells into the graft

(2) Osteoinduction to recruit and stimulate osteoprogenitor stem cells or non-differentiated stem cells to differentiate into osseous forming cells

(3) Osteogenesis to provide bone formation by transplanted living cells

Depending on the purpose of the bone graft, one or more of the above described properties may be more desirable than others. Besides providing these characteristics, the bone grafts should be easy to use clinically and cost-effective.

Nowadays, many of the bone grafts under clinical evaluation use synthetic materials as an alternative to the bone-derived grafts, for instance: synthetic ceramics, polymers and composites[4,32,41,42]. However, none of the above mentioned possess osteogenic properties and normally they also lack intrinsic osteoinductivity[31,32,41,42,44]. The awareness of these failings has driven the conception of new strategies. The two main strategies that have emerged are the stimulation of bone formation using osteoinductive bone substances and the creation of biomaterials composed of an osteoconductive scaffold and osteogenic tissue. In the first strategy the osteoinductive bone substances mostly used are bone morphogenetic proteins (BMP), transforming growth factors β (TGFs β), insuline growth factors (IGFs), platelet derived growth factors (PDGF´s), fibroblast growth factors (FGFs) and vascular endothelial growth factors (VEGFs)[4,45-47]. The second strategy lies in the construction of a bone graft substitute combining the osteoconductive scaffold with osteogenic cells of the patient. In addition to the osteoconductive scaffold providing a

scaffold for the formation of new bone, it will function as a carrier for the cells as well as a dynamic delivery system for osteoinductive bone substances. Combining these concepts, namely an osteoconductive scaffold with osteoinductive growth factors and osteogenic cells may even exceed the current requirements of bone-derived grafts[7,48-53].

3.1. Synthetic bone graft substitutes (alloplastics)

Synthetic bone graft substitutes offer many advantages over applications using bone-derived grafts, including unlimited supply, purity of the material and absence of disease[32,54]. The wide variety of compositions allows the surgeons to choose a specific combination of strength, elasticity and durability for a given procedure and therefore to simplify the operative practice[4,54].

There are two main categories of synthetic bone graft substitutes: ceramic- and polymer-based. Each class has a distinct profile of properties in terms of strength, flexibility and ability for tissue ingrowth that influences the decision of which material should be used for each specific purpose.

The *ceramic-based class* includes calcium phosphates, calcium sulphates, bioactive glasses, either alone or mixed with other materials[29,55,56]. The *polymer-based class* comprises degradable polymers used alone or in combination with other materials[29,54,55,57]. Biodegradable polymers are used in a variety of surgical applications, and more recently the use of bioresorbable polymers has expanded to include scaffolds for tissue engineering in various geometric forms including porous membranes, porous blocks and microspheres. Most of the biodegradable polymers in use in tissue engineering at present belong to the polyhydroxyl acid family, namely polyglycolic acid (PGA) and polylactic acid (PLA) or copolymers of both[58,59]. When these materials are used as bone grafts, either alone or as a composite, they are designed to form osteoconductive surfaces.

3.1.1. Ceramic-based bone grafts substitutes

Ceramics are materials composed of metallic and non-metallic elements held jointly by ionic and/or covalent bonds[55,56]. The use of ceramics as bone graft substitutes, particularly calcium phosphates, is motivated because they are the main inorganic constituent of hard

tissues in the body[2,56,60]. Additionally, calcium phosphates are osteoconductive, which is one of the characteristics required in a bone graft. They are generally used in dense, granular or porous form as well as coatings of metal prosthesis and implants, or as a component of a composite.

The success of using ceramics as bone graft substitutes depends upon the interaction between the implant and host tissue. When implanted in living tissues, all materials elicit a response from the host and generally both tissue and material undergo physical and/or chemical modifications. Based on these modifications, ceramics can be classified as[43,56,61-67]:

(1) Nearly inert ceramics

(2) Surface reactive ceramics (bioactive)

(3) Bioresorbable ceramics

The nearly inert ceramics such as alumina and carbons are chemically stable and elicit minimal response with surrounding tissue, maintaining its characteristics throughout the entire period of implantation in the organism[55,62,64].

The surface reactive ceramics are midway between nearly inert and resorbable in behaviour. This kind of ceramic elicits a biological response to facilitate a direct chemical bond between the material surface and the surrounding tissues. Some of the materials included in this group are bioactive glasses (Bioglass®), glass-ceramics (Ceravital, Cerabone A/W) and hydroxyapatite [HA; $Ca_{10}(PO_4)_6(OH)_2$][55,62,68-71].

Bioresorbable ceramics are designed to degrade progressively with time and be replaced with natural host tissue, without toxicity and rejection. This biodegradation may be caused by three factors[55,65,72,73]:

(1) Physicochemical dissolution, which depends on the solubility product of the material and the local pH of its environment

(2) Physical disintegration into small particles as a result of preferential chemical attack of grain boundaries

(3) Biological factors, such as phagocytosis

Bioresorbable materials may show some complications in the clinical use, such as:

(1) Maintenance of strength and stability of the interface during biodegradation and replacement by the natural host tissue

(2) Matching resorption rates to the repair rates of body tissues. This point is very important, since some materials dissolve too quickly and some too slowly

Since a great concentration of ions or/and particles of a bioresorbable material is released, it is important that it consists only of metabolically tolerable substances, which restricts its compositional design and therefore the mechanical behaviour and eventually its final applications.

3.1.1.1. Synthetic hydroxyapatite-based materials

Hydroxyapatite (HA) is one of the most biocompatible materials and has been used as a bone graft for a long time. The synthetic hydroxyapatite materials resemble the mineral part of bone, but they present some differences such as ion substitutions that alter the interaction between the mineral and organic phases of bone, and ultimately the properties of bone. For that reason, some ions have been intentionally added to the hydroxyapatite structure. These ions include carbonate ions substituting both hydroxyl and phosphate groups, fluoride ions substituting hydroxyl groups, silicate ions substituting phosphate groups, as well as magnesium ions substituting calcium[55,61,74-79].

An ideal bone graft ought to present an adequate resorption rate to be substituted as new bone is synthesised and remodelled. Most hydroxyapatite implant materials are osteoconductive, however they resorb very slowly. Therefore, different approaches have been used in order to overcome this disadvantage. For example, hydroxyapatite can be modified and combined with other materials for improve functionality and faster resorption[55,78,80-82].

3.1.1.2. Synthetic tricalcium phosphate-based materials

Tricalcium phosphate [TCP; $Ca_3(PO_4)_2$] has four polymorphs, α, β, γ and super α[55]. The most clinically used polymorph is β-TCP. The α-polymorph is more reactive in aqueous solutions than the β-polymorph, therefore more soluble[55,83]. Besides its profile of biocompatibility and osteoconductive ability, TCP has a higher solubility and resorption rate than hydroxyapatite ceramics[78,84,85]. Due to their relative solubility TCP is generally used in circumstances where structural support is less important.

3.1.1.3. Glass-based materials

Glass-based materials are considered surface reactive ceramics[86,87]. When implanted, the materials undergo dissolution and release ions into the surrounding environment with consequent local pH changes. The composition of the materials controls their surface reactivity. These kind of materials do not become encapsulated when implanted, but closely adhere to the surrounding living bone tissues[88,89].

Almost all of the bioactive glasses and glass ceramics used contain large amounts of SiO_2. Two of the most well known implants are Bioglass® and Ceravital®[71,90-92]. Nevertheless, it is common knowledge that silica-free calcium phosphate glass-based materials also have high potential for being used as bone graft substitutes.

3.1.2. Medical applications

The research on the bone graft field started to focus on the development of synthetic substitutes for particular applications, such as craniofacial, oral/maxillofacial and orthopaedic surgery[4,7,27,29,30,93]. Table 1 shows a list of some of the most used commercially available ceramic-based grafts. These substitutes are available in different forms such as blocks, granules, cements and gels. The block and granule types are the most commercialized on the market. Blocks are normally used in situations of trauma, interbody spinal fusion, and non-unions. Granules are generally used for posterior/lateral spinal fusion, filling cystic voids, as well as for hip and knee revisions. One of the factors influencing the physician's choice of bone graft is the cost-effectiveness. Granules have a

significant price advantage over the other forms of bone grafts[27,29].

Table 1 – Some commercially available ceramic-based graft materials[7,29,30,41,94,95].

Product name	Characteristics	Company
Hydroxyapatite		
Ceros 80	Dense polycrystalline HA	Straumann Ltd, UK
Biocoral	Natural mineral skeletons of scleractinian corals	Inoteb, France
Pro Osteon	Coralline macroporous HA	Interpore Int., USA
Osteograft	Crystalline HA	CeraMed, USA
Calcitite	Dense crystalline HA	Calcitek, USA
Tricalcium phosphate		
Chronos/Ceros 82	Tricalcium phosphate	Mathys, Suisse
Biosorb	Tricalcium phosphate	SBM S.A, Lourdes
Vitoss	Ultraporous TCP	Orthovita, USA
Cerasorb	Tricalcium phosphate	Curasan AG, Germany
Bioactive glasses		
Bioglass	Bioactive glass: 45% SiO_2, 24% CaO, 24.5% Na_2O, 6% P_2O_5, mol%	Novabone, USA
Ceravital	Group of glasses and glass ceramics of various compositions	E.Pfeil & H.Brömer, Germany
Biogran	Bioactive glass	Orthovita, USA

4. Glasses

The nature of glass and the glass transition mechanism is probably the deepest and most interesting unsolved problem in solid state theory. Glasses have found to share two distinguishing characteristics: (1) time-dependent glass transformation behaviour and (2) no long range atomic order. Based in these features, a glass can be defined as "*an amorphous solid completely lacking in long range, periodic atomic structure and exhibiting a region of glass transformation behaviour* [96-100].

Traditionally glass transformation behaviour is discussed on the basis of either enthalpy or volume versus temperature diagrams, such as that shown in Figure 1.

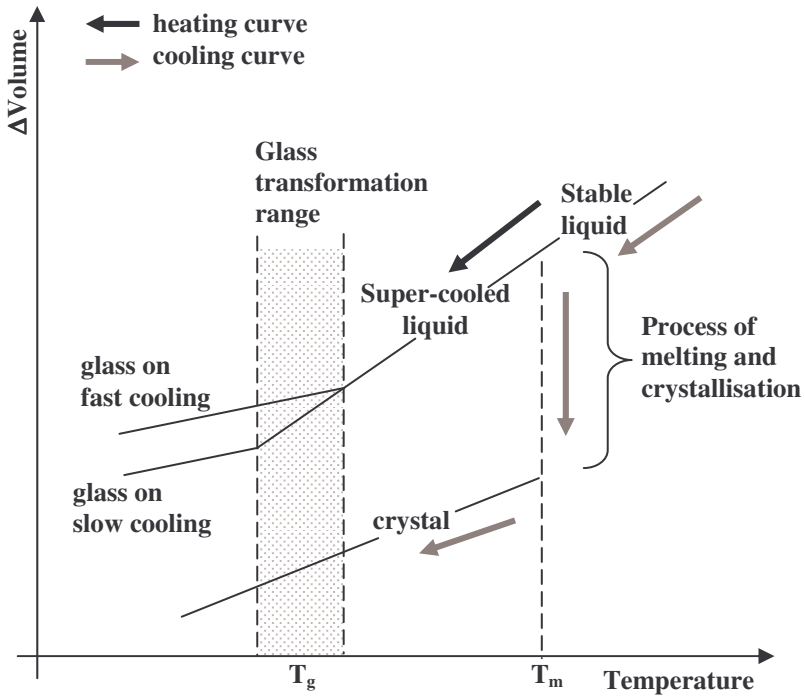

Figure 1 – Changes associated with heating and cooling in systems liable to glass formation.

Depending on the cooling rate, when a liquid is cooled to below its *melting temperature* (T_m), it can either form a crystalline state or a super-cooled liquid (Figure 1). The transition from a super-cooled liquid to a solid glass is known as the *glass transformation region* and the corresponding temperature is called *glass transition temperature* - T_g [101-104]. Since the

temperature at which glass transition occurs is dependent on cooling rate, when a slow rate is used the structural units have more time to reorganize and therefore T_g is lower. On the other hand, if a rapid cooling rate is used the transition into a glass occurs at a higher temperature, owing to the lower time available for the molecular structural arrangement.

4.1. Principles of glass formation

Among the several theories initially proposed for glass formation, the statements by Zachariasen have become the basis for the models for glass structures termed the *random network theory*. Zachariasen noted the following characteristics in glass forming oxides: (1) the material contains a high proportion of cations which are surrounded by either oxygen triangles or oxygen tetrahedral, (2) these polyhedra are connected only by their corners, and (3) some oxygen atoms are linked to only two such cations and do not form additional bonds with other cations[97,99,105-108].

Complementary studies that were performed to explain glass formation classify oxides into three groups: *network forming oxides*, *intermediate oxides* and *network modifying oxides. Intermediate oxides* are those oxides that do not form glasses by themselves, however they are incorporated into the network of the glass formers[97,99,106,108]. *Network modifying oxides* can also take part in glass formation by acting to modify the glass network, therefore modifying the glass properties. These oxides do not form networks although they occupy interstitial sites in the structure of a glass network. They are essentially the alkali or alkaline earth metal oxides. The addition of these oxides to the glass network results in its weakness due to the formation of non-bridging oxygens within the glass, i.e. disrupt the network continuity. Examples of such network modifiers are: Na_2O, K_2O, Li_2O, CaO and MgO.

Recent theories of glass formation not only address the question of why one specific material will form a glass, but also form a glass processing approach. The new approach to glass formation, known as the *kinetics theory* of glass formation, has largely replaced the earlier structural theories. Virtually any material will form a glass if cooled so rapidly that insufficient time is provided to allow the reorganization of the structure into the periodic arrangement required by crystallization[96-99,108-112].

4.1.1. Structure of phosphate glasses

Phosphate glasses consist of a polymer-like, regular tetrahedral structure based on [PO_4] groups, with their structure generally described using Q^n terminology, where n represents the number of bridging oxygen atoms per [PO_4] tetrahedron. The networks of phosphate glasses can be classified according to the ratio of oxygen to phosphorus ions [O]/[P], which establishes the connections between the P-tetrahedra through bridging oxygens[99,113-116]. The most polymerized glass forms a cross-linked Q^3 network (ordered structure), with each tetrahedron connected to three others. The introduction of components to the glass network, such as modifier oxides, reduces the polymerization between the tetrahedra due to the creation of non-bridging oxygens in the phosphate network. This depolymerization weakens the glass structure and consequently changes the final properties of the glass[99,113-115,117]. The resulting depolymerization of the glass network with the addition of an alkali oxide (R_2O) can be described by the following reaction, illustrated schematically in Figure 2:

$$2\ Q^n + R_2O \rightarrow 2\ Q^{n-1}$$

Considering the addition of modifier oxides to the glass structure and consequently increasing the [O]/[P] ratio, glasses with different structures can be obtained[113,115], (Table 2):

(1) Glasses with ratios in the region of 2.5 and 3.0 are known as branched *ultraphosphate*s (Q^3 and Q^2). Q^3 structures have three bridging and one non-bridging oxygens per phosphate tetrahedron

(2) When the ratio is equal to 3, the *metaphosphates* (Q^2) are formed. Their structure becomes a collection of tetrahedral chains and rings. Technically, the glasses formed in the region between 3.0 and 3.5 are designated as long-chained *polyphosphates*, however generally they are also referred to as metaphosphates. Their structures are comprised of chains of tetrahedra linked at two corners terminated at each end by a tetrahedra sharing only one corner (Q^2 chains terminated by Q^1 tetrahedra). Q^2 structures have two bridging and two non-

bridging oxygens per phosphate tetrahedron

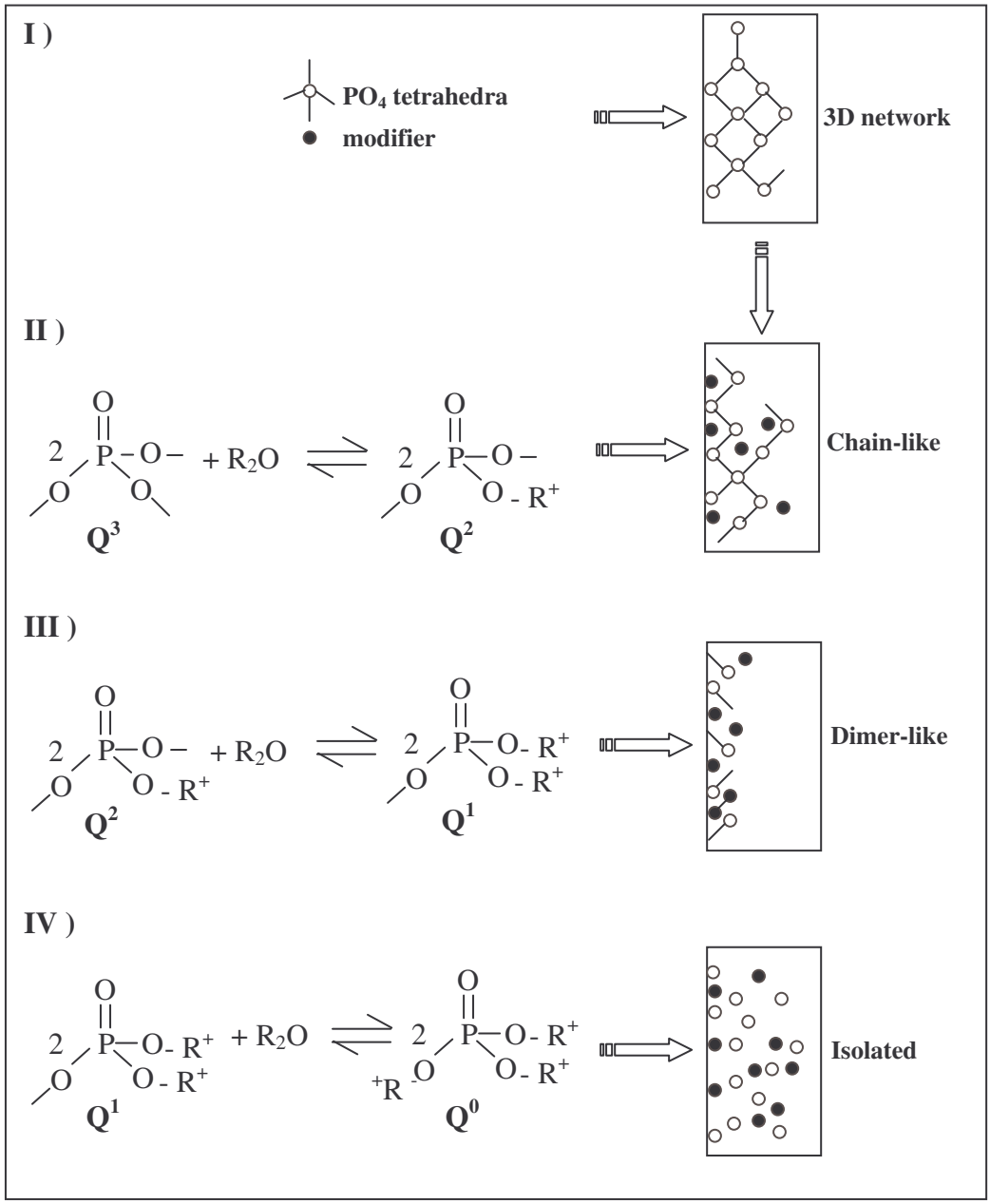

Figure 2 – Effect of [O]/[P] ratio on phosphate network structures

(3) Increasing the ratio to 3.5 will result in a *pyrophosphate* structure (Q^1), where the tetrahedra are only linked at one corner. Q^1 structures have one bridging and three non-bridging oxygens per phosphate tetrahedron

(4) Increasing the ratio to 4.0, the network become completely depolymerized with

the tetrahedra isolated, and this structure is designated as *orthophosphate* (Q^0). Q^0 structures have no bridging and four non-bridging oxygens per phosphate tetrahedron

Phosphate glasses can be prepared with a wide variety of modifiers and additives, allowing the properties of the final glass to be tailored for specific applications.

Table 2 – Glasses with different structures based on the [O]/[P] ratio.

Regions	**xR_2O (or R'O) (1-x) P_2O_5 glasses**	**[O]/[P] ratio**	**Q^n groups**
Ultraphosphate	$0 \leq x < 0.5$	$2.5 < [O]/[P] < 3.0$	Q^2 and Q^3
Metaphosphate	$x = 0.5$	$[O]/[P] = 3.0$	Q^2
	$0.5 < x < 0.67$	$3.0 < [O]/[P] < 3.5$	Q^1 and Q^2
Pyrophosphate	$x = 0.67$	$[O]/[P] = 3.5$	Q^1
	$0.67 < x < 0.75$	$3.5 < [O]/[P] < 4.0$	Q^1 and Q^0
Orthophosphate	$x = 0.75$	$[O]/[P] = 4.0$	Q^0

5. Glass ceramics

Glass ceramics are polycrystalline materials composed of one or more glassy and crystalline phases. They are usually obtained by forming a base glass, most commonly by the conventional technique of melting, which is next heat treated at an adequate temperature cycle to be converted into a glass ceramic material. The control of heat treatment cycle in the preparation of glass ceramics is of extreme importance in order to achieve a final microstructure with desirable properties[118-125].

Particular additives may be incorporated into the base glass composition to induce the nucleation of phases with specific physico-chemical properties in the glass ceramic

formation. More specifically, it allows the preparation of glass ceramic materials with the presence of biocompatible and bioresorbable phases. The characteristics of the final constituent phases and microstructure of the glass ceramic establish its properties and main applications. There are three main techniques used for the preparation of glass ceramic materials[120,126]:

(1) Casting and controlled crystallization

(2) Sintering and crystallization of glass powder

(3) Sol-gel

The later sol-gel technique will not be reviewed in this description.

5.1. Casting and controlled crystallization method

Controlled crystallization is a fundamental process in the preparation of glass ceramic materials. It is based on the preparation of glass by the conventional technique of melting and casting. The glass is first melted and then cast into a block. Afterwards, it is annealed to release the internal stresses, followed by a heat treatment of crystallization (Figure 3).

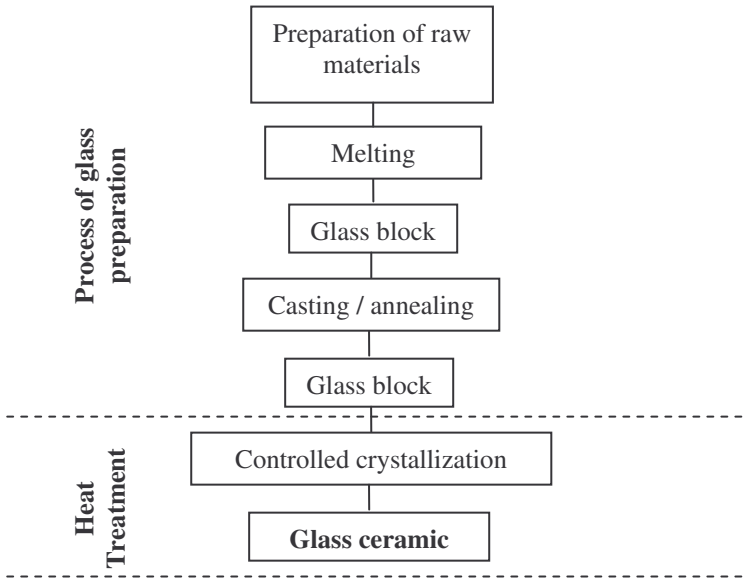

Figure 3 – Procedure for the preparation of a glass ceramic by the conventional route.

The heat treatment used to attain a glass ceramic material involves two mechanisms: nucleation and crystal growth[108,120,127-131].

Nucleation is the key process in controlling crystallization, since it is the initial step of a phase transformation. Since the phase transformation does not occur spontaneously throughout the base glass, the presence of a nucleus it needed on which the crystal subsequently grows. If the formation of nuclei does not happen, crystal growth can not occur and therefore the crystallization is avoided[120,122,132]. This process can either occur via homogeneous nucleation or heterogeneous nucleation.

In *homogeneous nucleation* the initial stage occurs spontaneously within the melt with no preferential sites for nucleus formation, i.e. occurs randomly in space and time. The composition of the melt and crystal are the same[120,132-134].

The *heterogeneous nucleation* involves formation of the nuclei of a new phase on the surface of a pre-existing surface, such as foreign surfaces, grain boundaries, impurities, crucible wall, bubbles, i.e. occurs from specific sites in the sample [120,132,135].

In this kind of nucleation a component designated as nucleating agent can be added in small percentages into the base glass facilitating the nucleation process. They act as a catalyst in the glassy matrix, as they reduce the energy barrier for nucleation[99,122,136,137]. The ability of tailoring the glass ceramic microstructure by using various additives allows an excellent control of the properties of the final material.

The heat treatment used in the preparation of glass ceramics, which interferes with the nucleation and the growth stages, can lead to two situations: uncontrollable and controllable crystallization[122]:

(1) If the nucleation and growth curves overlap in a certain temperature range T_2-T_3 (Figure 4a), the control of the crystallization process is limited or even impossible. This phenomenon takes place when nucleation and crystal growth occur simultaneously in a single-step heat treatment (Figure 5a)

(2) On the other hand, if the overlap of two processes is minimized, nucleation and growth curves are separated and a controllable crystallization is achieved (Figure 4b). The glass is heated to the nucleation temperature, between T_1 and

T_2, to allow nuclei formation. After a certain period of time, the temperature is increased to the range of T_3 and T_4 for crystal growth. Following this, the sample is then again cooled to room temperature. This two-step heat treatment is used to prepare glass ceramics in a controlled way (Figure 5b).

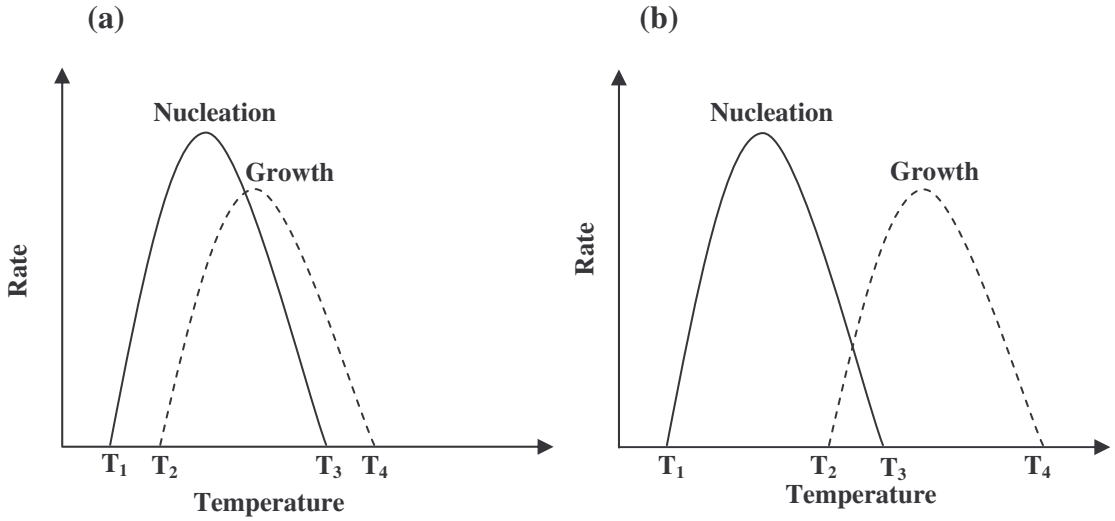

Figure 4 – Nucleation and crystal growth temperatures. **(a)** uncontrollable and **(b)** controllable crystallization.

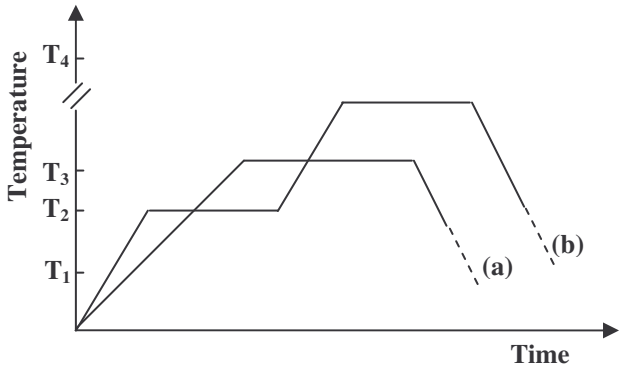

Figure 5 - Single-step heat treatment **(a)** and two-step heat treatment **(b)**.

5.1.1. Bulk and surface crystallization

The crystallization process can occur within bulk glass or on its surface, referred to as bulk and surface crystallization, respectively[108,120,138].

If crystallization occurs from nuclei dispersed throughout the bulk of the base glass, then it is termed *bulk crystallization*. Both homogeneous and heterogeneous nucleation may occur during bulk crystallization (Figure 6).

If the crystallization process is initiated on the surface of the glass sample through heterogeneous nucleation, it is called *surface crystallization.* The crystals grow from the surface towards the centre of the glass sample. Homogeneous nucleation does not lead to surface crystallization.

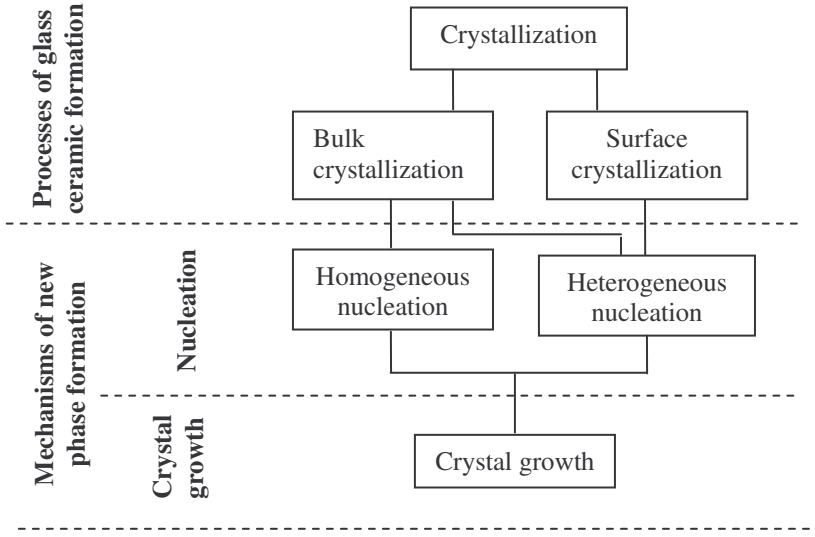

Figure 6 – Bulk and surface crystallization.

5.2. Sintering and crystallization by glass powder method

Glass sintering with subsequent heat treatment of crystallization (powder technology route) is also a useful method in the preparation of glass ceramic materials. Compared with the well-known conventional process, this method allows the preparation of complex shapes as well as glass ceramic composite materials. This procedure is based on the preparation of a base glass that is first melted and then quenched as a frit. Subsequently, the frit is crushed and milled to obtain a glass powder with a small range of particle size. Afterwards, the glass powder is compacted at room temperature to shape the final material and then subjected to an adequate heat treatment for sintering and crystallization (Figure 7). These two steps (sintering and crystallization) can either occur separately in two stages or

simultaneously as one stage. Depending on the order of events of the powder sintering process, glass ceramic materials with different properties can be obtained. If the sintering stage ends before crystallization begins, extremely dense and low porosity materials are obtained. On the other hand, if the crystallization stage occurs before or simultaneously with the sintering one, porous and heterogeneous materials are obtained[139-141].

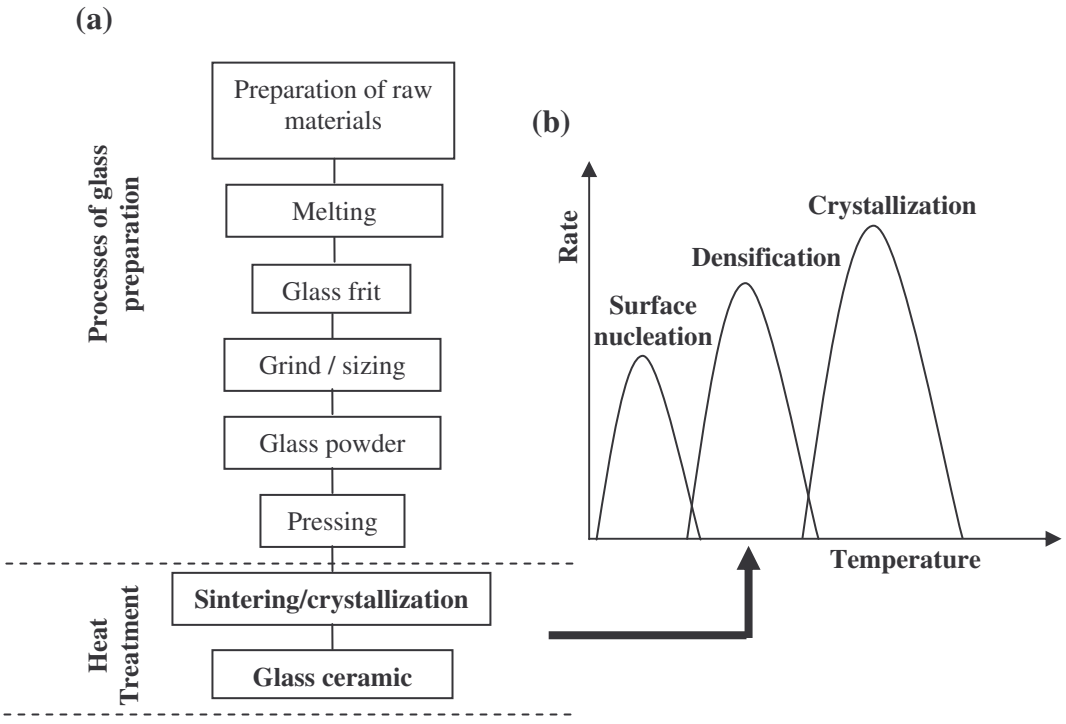

Figure 7 – Procedure for the preparation of a glass ceramic by the powder technology route **(a)** and a sequence for the densification process **(b)**.

References

1. Wynsberghe, D.V., Noback, C.R., Carola, R., Human anatomy and physiology. 3rd ed. 1995. McGraw-Hill.

2. Ackerman, U., The essentials of human physiology. 1992. Mosby Year Book.

3. Parikh, S.N. Review: Bone graft substitutes - past, present, future. Journal of Post-graduation in Medicine, 2002; **48**(2): 142-148.

4. Damien, C.J., Parsons, J.R. Bone-graft and bone-graft substitutes: Review of current technology and applications. Journal of Applied Biomaterials, 1991; **2**(3): 187-208.

5. Dee, K.C., Bizios, R. Mini-review: Proactive biomaterials and bone tissue engineering. Biotechnology and Bioengineering, 1996; **50**(4): 438-442.

6. Puleo, D., Dee, K.C., Bizios, R. Current challenges in cell-biomaterial interactions - Preface. Biomaterials, 1999; **20**(23-24): 2201-2201.

7. Laurencin, C.T., Ambrosio, A.M.A., Borden, M.D., Cooper, J.A. Tissue engineering: Orthopedic applications. Annual Review of Biomedical Engineering, 1999; **1**: 19-46.

8. Noda, M., ed. Cellular and molecular biology of bone. 1993. Academic Press Inc.

9. Marks, S.C., Hermey, D.C. The structure and development of bone, In: Principles of bone biology, Bilezikian, J.P., Raisz, L.G., Rodan, G.A., Editors. 1996, Academic Press: New York.

10. Vaughan, J., The physiology of bone. 1996. Oxford University Press. London.

11. Rodan, G.A. Introduction to bone biology. Bone, 1992; **13**: S3-S6.

12. Fernandes, M.H. Mecanismos de regulação do metabolismo ósseo. Acta Médica Portuguesa, 1998; **11**: 41-52.

13. Hill, P.A., Orth, M. Review: Bone remodelling. British Journal of Orthodontics, 1998; **25**: 101-107.

14. Rodan, G.A. Bone homeostasis. Proceedings of the National Academy of Sciences of the United States of America, 1998; **95**(23): 13361-13362.

15. Rodan, G.A. Control of bone formation and resorption: Biological and clinical perspective. Journal of Cellular Biochemistry, 1998: 55-61.

16. Aubin, J.E., Liu, F. The osteoblast lineage, In: Principles of bone biology, Bilezikian, J.P., Raisz, L.G., Rodan, G.A., Editors. 1996, Academic Press: New York.

17. Simmons, D.J., Grynpas, M.D., The osteoblast and osteocyte. 1990. The Telford Press.

18. Nijweide, P.J., Burger, E.H., Nulend, J.K., Plas, A.V.D. The osteocyte, In: Principles of bone biology, Bilezikian, J.P., Raisz, L.G., Rodan, G.A., Editors. 1996, Academic Press: New York.

19. Baiotto, S., Zidi, M. Theoretical and numerical study of a bone remodeling model: The effect of osteocyte cells distribution. Biomechanics and Modelling in Mechanobiology, 2004: S10237-S10262.

20. Tate, M.L.K., Adamson, J.R., Tami, A.E., Bauer, T.W. The osteocyte. International Journal of Biochemistry & Cell Biology, 2004; **36**(1): 1-8.

21. Suda, T., Udagawa, N., Takahashi, N. Cells of bone: osteoclast generation, In: Principles of bone biology, Bilezikian, J.P., Raisz, L.G., Rodan, G.A., Editors. 1996, Academic Press: New York.

22. Väänänen, K. Osteoclast function: biology and mechanisms, In: Principles of bone biology, Bilezikian, J.P., Raisz, L.G., Rodan, G.A., Editors. 1996, Academic Press: New York.

23. Wang, X., Puran, S. The toughness of cortical bone and its relationship with age. Annals of Biomedical Engineering, 2004; **32**(1): 123-135.

24. Boyle, W.J., Simonet, W.S., Lacey, D.L. Osteoclast differentiation and activation. Nature, 2003; **423**(6937): 337-342.

25. Stein, G.S., Lian, J.B., Stein, J.L., Wijnen, A.J.V., Frenkel, B., Montecino, M. Mechanism regulating osteoblast proliferation and differentiation, In: Principles of bone biology, Bilezikian, J.P., Raisz, L.G., Rodan, G.A., Editors. 1996, Academic Press: New York.

26. Teitelbaum, S.L. Bone resorption by osteoclasts. Science, 2000; **289**(5484): 1504-1508.

27. Davies, J.E., ed. Bone engineering. 2000. Copyright: Toronto.

28. Yoshikawa, T. Bone reconstruction by cultured bone graft. Materials Science & Engineering C-Biomimetic and Supramolecular Systems, 2000; **13**(1-2): 29-37.

29. Bone graft substitutes. ed. Laurencin, C.T. 2003. ASTM International.

30. Parikh, S.N. Bone graft substitutes in modern orthopedics. Orthopedics, 2002; **25**(11): 1301-1309.

31. Gazdag, A.R., Lane, J.M., Glaser, D., Forster, R.A. Alternatives to autogeneous bone graft: efficacy and indications. Journal of the American Academy of Orthopaedic Surgeons, 1995; **3**(1): 1.

32. Betz, R.R. Limitations of autograft and allograft: New synthetic solutions. Orthopedics, 2002; **25**(5): S561-S570.

33. Mathes, D.W., Randolph, M.A., Lee, W.P.A. Strategies for tolerance induction to

composite tissue allografts. Microsurgery, 2000; **20**(8): 448-452.

34. Tomford, W.W. Bone allografts: past, present and future. Cell and Tissue Banking, 2000; **1**: 105-109.

35. Rush, D. Insights into subclinical rejection. Transplantation Proceedings, 2004; **36**(2): 71S-73S.

36. Iwamoto, Y., Sugioka, Y., Chuman, H., Masuda, S., Hotokebuchi, T., Kawai, S., Yamamoto, M. Nationwide survey of bone grafting performed from 1980 through 1989 in Japan. Clinical Orthopaedics and Related Research, 1997(335): 292-297.

37. Block, J.E., Poser, J. Does xenogeneic demineralized bone-matrix have clinical utility as a bone-graft substitute. Medical Hypotheses, 1995; **45**(1): 27-32.

38. Jensen, S.S., Aaboe, M., Pinholt, E.M., Hjorting-Hansen, E., Melsen, F., Ruyter, I.E. Tissue reaction and material characteristics of four bone substitutes. International Journal of Oral Maxillofacial and Implantology, 1996; **11**: 55-66.

39. Pierson, A.P., Bigelow, D., Hamonic, M. Bone grafting with boplant. Results in thirthy-three cases. Journal of Bone Joint Surgery, 1968; **50B**: 364-368.

40. Buchart, H. The biology of bone graft repair. Clinical Orthopaedics, 1983; **174**: 28-42.

41. Vaccaro, A.R. The role of the osteoconductive scaffold in synthetic bone grafts. Orthopedics, 2002; **25**(5): S571-S578.

42. Lane, J.M., Tomin, E., Bostrom, M.P.G. Biosynthetic bone grafting. Clinical Orthopaedics and Related Research, 1999(367): S107-S117.

43. Hench, L.L. Biomaterials: a forecast for the future. Biomaterials, 1998; **19**(16): 1419-1423.

44. Laurencin, C.T. Advancements in tissue engineered bone substitutes. Current Opinion in Orthopedics, 1999; **10**(6): 445-451.

45. Yuan, H.P., Zou, P., Yang, Z.J., Zhang, X.D., De Bruijn, J.D., De Groot, K. Bone morphogenetic protein and ceramic-induced osteogenesis. Journal of Materials Science-Materials in Medicine, 1998; **9**(12): 717-721.

46. Boden, S.D. Bioactive factors for bone tissue engineering. Clinical Orthopaedics and Related Research, 1999(367): S84-S94.

47. Khan, S.N., Tomin, E., Lane, J.M. Clinical applications of bone graft substitutes.

Orthopedic Clinics of North America, 2000; **31**(3): 389-398.

48. Vacanti, C.A., Bonassar, L.J. An overview of tissue engineered bone. Clinical Orthopaedics and Related Research, 1999(367): S375-S381.

49. Goldstein, S.A., Patil, P.V., Moalli, M.R. Perspectives on tissue engineering of bone. Clinical Orthopaedics and Related Research, 1999(367): S419-S423.

50. Chapekar, M.S. Tissue engineering: Challenges and opportunities. Journal of Biomedical Materials Research, 2000; **53**(6): 617-620.

51. Laurencin, C.T., Katti, D.S. Repair and restore with tissue engineering. Ieee Engineering in Medicine and Biology Magazine, 2003; **22**(5): 16-17.

52. Winn, S.R., Uludag, H., Hollinger, J.O. Carrier systems for bone morphogenetic proteins. Clinical Orthopaedics and Related Research, 1999; **367**: S95-S106.

53. Principles of tissue engineering. 2rd ed. 2000. Academic Press.

54. Ratner, B.D., Bryant, S.J. Biomaterials: Where we have been and where we are going. Annual Review of Biomedical Engineering, 2004; **6**: 41-75.

55. Ratner, B.D., Hoffmam, A.S., Schoen, F.J., Lemons, F.J., eds. Biomaterials science: an introduction to materials in medicine. 2nd ed. 2004. Elsevier Academic Press.

56. Hench, L.L., Wilson, J., eds. An introduction to bioceramics. Advanced Series in Ceramics. 1993, **Vol. 1**. World Scientific Publishing: Singapore.

57. Moukwa, M. The development of polymer-based biomaterials since the 1920s. Jom-Journal of the Minerals Metals & Materials Society, 1997; **49**(2): 46-50.

58. Robbins, M.M., Vaccaro, A.R., Madigan, L. The use of bioabsorbable implants in spine surgery. Neurosurgery Focus, 2004; **16**(3): 1-7.

59. Cohen, S.R., Holmes, R.E., Meltzer, H.S., Levy, M.L., Beckett, M.Z. Craniofacial reconstruction with a fast resorbing polymer: a 6 to 12 month clinical follow-up review. Neurosurgical Focus, 2004; **16**(3): 1-3.

60. Dorozhkin, S.V.,Epple, M. Biological and medical significance of calcium phosphates. Angewandte Chemie-International Edition, 2002; **41**(17): 3130-3146.

61. Lemons, J.E. Ceramics: Past, present, and future. Bone, 1996; **19**(1): S121-S128.

62. Dubok, V.A. Bioceramics - Yesterday, today, tomorrow. Powder Metallurgy and Metal

Ceramics, 2000; **39**(7-8): 381-394.

63. Hench, L.L., Clark, A.E. Reaction mechanisms at bioceramic interfaces. American Ceramic Society Bulletin, 1970; **49**(4): 481-&.

64. Hench, L.L. Bioceramics from concept to clinic. Journal of the American Ceramic Society, 1991; **74**(7): 1487-1510.

65. Dee, K.C., Puleo, D.A., Bizios, R., An introduction to tissue-biomaterial interactions. 2002. John Wiley & Sons, Inc.

66. Yamamuro, T. In: Bone grafts, derivatives & substitutes, Urist, M.R., O'Connor, B.T., Burwell, R.G., Editors. 1994, Butterworth Heinemann.

67. Hench, L.L. Bioceramics and the origin of life. Journal of Biomedical Materials Research, 1989; **23**(7): 685-703.

68. Hench, L.L., Wilson, J. Bioactive glasses: present and future. In Bioceramics. 1998, World Scientific Publishing Co., New York, USA.

69. Nakamura, T., Yamamuro, T., Higashi, S., Kokubo, T., Itoo, S. A new glass-ceramic for bone-replacement - evaluation of its bonding to bone tissue. Journal of Biomedical Materials Research, 1985; **19**(6): 685-698.

70. Yamamuro, T. A-W glass ceramic: Clinical applications, In: An Introduction to Bioceramics, Hench, L.L.,Wilson, J., Editors. 1993, World Scientific Publishing: Singapore.

71. Ducheyne, P., Qiu, Q. Bioactive ceramics: the effect of surface reactivity on bone formation and bone cell function. Biomaterials, 1999; **20**(23-24): 2287-2303.

72. Knaack, D., Goad, M.E.P., Aiolova, M., Rey, C., Tofighi, A., Chakravarthy, P., Lee, D.D. Resorbable calcium phosphate bone substitute. Journal of Biomedical Materials Research, 1998; **43**(4): 399-409.

73. LeGeros, R.Z. Biodegradation and bioresorption of calcium phophate ceramics. Clinical Materials, 1993; **14**: 65-88.

74. Kim, S.R., Lee, J.H., Kim, Y.T., Riu, D.H., Jung, S.J., Lee, Y.J., Chung, S.C., Kim, Y.H. Synthesis of Si, Mg substituted hydroxyapatites and their sintering behaviours. Biomaterials, 2003; **24**(8): 1389-1398.

75. Nelson, D.G.A., Featherstone, J.D.B. Preparation, analysis and characterization of

carbonated apatites. Calcified Tissue International, 1982; **34**: S69-S81.

76. Yasukawa, A., Ouchi, S., Kandori, K., Ishikawa, T. Preparation and characterization of magnesium-calcium hydroxyapatites. Journal of Materials Chemistry, 1996; **6**(8): 1401-1405.

77. Jha, L.J., Best, S.M., Knowles, J.C., Rehman, I., Santos, J.D., Bonfield, W. Preparation and characterization of fluoride-substituted apatites. Journal of Materials Science-Materials in Medicine, 1997; **8**(4): 185-191.

78. Bagambisa, F.B., Joos, U., Schilli, W. Mechanisms and structure of the bond between bone and hydroxyapatite ceramics. Journal of Biomedical Materials Research, 1993; **27**(8): 1047-1055.

79. Gibson, I.R., Best, S.M., Bonfield, W. Chemical characterization of silicon-substituted hydroxyapatite. Journal of Biomedical Materials Research, 1999; **44**(4): 422-428.

80. Santos, J.D., Reis, R.L., Monteiro, F.J., Knowles, J.C., Hastings, G.W. Liquid-phase sintering of hydroxyapatite by phosphate and silicate glass additions - structure and properties of the composites. Journal of Materials Science: Materials in Medicine, 1995; **6**(6): 348-352.

81. Ioku, K., Yoshimura, M., Somiya, S. Microstructure and mechanical-properties of hydroxyapatite ceramics with zirconia dispersion prepared by post-sintering. Biomaterials, 1990; **11**(1): 57-61.

82. Lopes, M.A., Glass reinforced hydroxyapatite composites: structural, physicochemical characterisation and biological performance. Universidade do Porto, 1999, Porto.

83. Yin, X., Stott, M.J. α- and β-tricalcium phosphate: a density functional study. Physical Review, 2003; **B**(68): 205205.

84. Ravaglioli, A.,Krajewski, A., Bioceramics. 1992. Chapman & Hall. London.

85. Lopes, M.A., Santos, J.D., Monteiro, F.J., Ohtsuki, C., Osaka, A., Kaneko, S., Inoue, H. Push-out testing and histological evaluation of glass reinforced hydroxyapatite composites implanted in the tibia of rabbits. Journal of Biomedical Materials Research, 2001; **54**(4): 463-469.

86. Hyakuna, K., Yamamuro, T., Kotoura, Y., Oka, M., Nakamura, T., Kitsugi, T., Kokubo, T., Kushitani, H. Surface-reactions of calcium-phosphate ceramics to various

solutions. Journal of Biomedical Materials Research, 1990; **24**(4): 471-488.

87. Koerten, H.K., Van der Meulen, J. Degradation of calcium phosphate ceramics. Journal of Biomedical Materials Research, 1999; **44**(1): 78-86.

88. Lu, J.X., Gallur, A., Flautre, B., Anselme, K., Descamps, M., Thierry, B., Hardouin, P. Comparative study of tissue reactions to calcium phosphate ceramics among cancellous, cortical, and medullar bone sites in rabbits. Journal of Biomedical Materials Research, 1998; **42**(3): 357-367.

89. Gatti, A.M., Zaffe, D. Bioactive glasses and chemical bond. Biomaterials, 1992: 97-107.

90. Gross, U., Kinne, R., Schmitz, H.J., Strunz, V. The response of bone to surface-active glasses and glass-ceramics. Crc Critical Reviews in Biocompatibility, 1988; **4**(2): 155-179.

91. Hench, L.L. Bioactive glasses and glass-ceramics, In: Bioceramics. 1999.

92. Hench, L.L., Paschall, H.F., Paschall, M., McVey, J. Histological responses at bioglass and bioglass-ceramic interfaces. American Ceramic Society Bulletin, 1973; **52**(4): 432-432.

93. Carotenuto, G., Spagnuolo, G., Ambrosio, L., Nicolais, L. Macroporous hydroxyapatite as alloplastic material for dental applications. Journal of Materials Science-Materials in Medicine, 1999; **10**(10-11): 671-676.

94. Bauer, T.W., Muschler, G.F. Bone graft materials. Clinical Orthopaedics and Related Research, 2000; **371**: 10-27.

95. Tadic, D., Epple, M. A thorough physicochemical characterisation of 14 calcium phosphate-based bone substitution materials in comparison to natural bone. Biomaterials, 2004; **25**(6): 987-994.

96. Gutzow, I., Avramov, I., Kastner, K. Glass formation and crystallization. Journal of Non-Crystalline Solids, 1990; **123**(1-3): 97-113.

97. Kurkjian, C.R.,Prindle, W.R. Perspectives on the history of glass composition. Journal of the American Ceramic Society, 1998; **81**(4): 795-813.

98. Porai-Koshits, E.A. Genesis of concepts on structure of inorganic glasses. Journal of Non-Crystalline Solids, 1990; **123**(1-3): 1-13.

99. Shelby, J.E., Introduction to glass science and technology. 1997. The Royal Society of

Chemistry. UK.

100. Mackenzie, J.D. State of the art and prospects of glass science. Journal of Non-Crystalline Solids, 1982; **52**(1-3): 1-8.

101. Seyler, R.J., ed. Assignment of the glass transition. 1994. ASTM: Philadelphia.

102. Lacevic, N., Glotzer, S.C. Approach to the glass transition studied by higher order correlation functions. Journal of Physics-Condensed Matter, 2003; **15**(31): S2437-S2446.

103. Sokolov, A.P. The glass transition: general scenario and crossover temperature. Journal of Non-Crystalline Solids, 1998; **235**: 190-195.

104. Sokolov, A.P. The glass transition: new ideas in an age-old field. Endeavour, 1997; **21**(3): 109-113.

105. Smyth, H.T. The structure of glass, In: Introduction to Glass Science, Pye, L.D., Stevens, H.J., LaCourse, W.C., Editors. 1972, Plenum Press: New York.

106. Zachariasen, W.H. The atomic arrangement in glass. Journal of American Chemical Society, 1932; **54**: 3841-3851.

107. Imaoka, M. Glass formation range and glass structure, In: Advances in glass technology, Society, T.A.C., Editor. 1962, Plenum Press: New York.

108. Vogel, W., Structure and crystallization of glasses. 1971. Pergamon Press.

109. Di Marzio, E.A., Yang, A.J.M. Configurational entropy approach to the kinetics of glasses. Journal of Research of the National Institute of Standards and Technology, 1997; **102**(2): 135-157.

110. Zarzycki, J. Glass structure. Journal of Non-Crystalline Solids, 1982; **52**(1-3): 31-43.

111. Bray, P.J., Geissberger, A.E., Bucholtz, F., Harris, I.A. Glass structure. Journal of Non-Crystalline Solids, 1982; **52**(1-3): 45-66.

112. Evans, D.L. Glass structure: The bridge between the molten and crystalline states. Journal of Non-Crystalline Solids, 1982; **52**(1-3): 115-128.

113. Brow, R.K. Review: the structure of simple phosphate glasses. Journal of Non-Crystalline Solids, 2000; **263**(1-4): 1-28.

114. Kulaev, I.S., Vagabov, V.M., Kulakovskaya, T.V. The chemical structures and properties of condensed inorganic phosphates, In: The biochemistry of inorganic

polyphosphates. 2004, John Wiley & Sons.

115. Wazer, J.R.V., Phosphorus and its compounds. 1958; **Vol. 1**. Interscience. New York, USA.

116. Martin, S.W. Review of the structures of phosphate-glasses. European Journal of Solid State and Inorganic Chemistry, 1991; **28**(1): 163-205.

117. Elliot, S.R., Rao, C.N.R., Thomas, J.M. The chemistry of the noncrystalline state - Review. Angewandte Chemie-International Edition, 2003; **25**(1): 31-46.

118. Zanotto, E.D. The applicability of the general theory of phase transformations to glass crystallization. Thermochimica Acta, 1996; **280**: 73-82.

119. Sarkisov, P.D., Mikhailenko, N.Y., Orlova, L.A. Glass ceramic materials in the context of contemporary material science. Glass and Ceramics, 2003; **60**(9-10): 261-265.

120. Strnad, Z., Glass ceramic materials. Glass Science and Technology 8. 1986. Elsevier. New York.

121. Fernandes, M.H.F.V. Bioactive glasses and glass-ceramics. Glass-Art & Science, 1999: 1-5.

122. Stewart, D.R. Concepts of glass-ceramics, In: Introduction to Glass Science, Pye, L.D., Stevens, H.J., LaCourse, W.C., Editors. 1972, Plenum Press: New York.

123. Avrami, M. Kinetics of phase change. III - Granulation, phase change and microstructure. Journal of Chemical Physics, 1941; **9**: 177-184.

124. Avrami, M. Kinetics of phase change. I - General theory. Journal of Chemical Physics, 1939; **7**: 1103-1112.

125. Avrami, M. Kinetics of phase change. II - Transformation-time relations for random distribution of nuclei. Journal of Chemical Physics, 1940; **8**: 212-224.

126. McMillan, P.W. The crystallization of glasses. Journal of Non-Crystalline Solids, 1982; **52**(1-3): 67-76.

127. Weinberg, M.C. Glass-formation and crystallization kinetics. Thermochimica Acta, 1996; **280/281**: 63-71.

128. Weinberg, M.C. A few topics concerning nucleation and crystallization in glasses. Journal of Non-Crystalline Solids, 1999; **255**(1): 1-14.

129. Weinberg, M.C., Poisl, W.H., Granasy, L. Crystal growth and classical nucleation theory. Comptes Rendus Chimie, 2002; **5**(11): 765-771.

130. Bergeron, C.G. General aspects of the crystallization of glass, In: Introduction to Glass Science, Pye, L.D., Stevens, H.J., LaCourse, W.C., Editors. 1972, Plenum Press: New York.

131. Granasy, L., James, P.F. Non-classical theory of crystal nucleation: application to oxide glasses: review. Journal of Non-Crystalline Solids, 1999; **253**: 210-230.

132. Holand, W., Rheinberger, V., Schweiger, M. Control of nucleation in glass ceramics. Philosophical Transactions of the Royal Society of London Series a-Mathematical Physical and Engineering Sciences, 2003; **361**(1804): 575-588.

133. Fokin, V.M., Zanotto, E.D., Schmelzer, J.W.P. Homogeneous nucleation versus glass transition temperature of silicate glasses. Journal of Non-Crystalline Solids, 2003; **321**(1-2): 52-65.

134. Zanotto, E.D., Weinberg, M.C. Trends in homogeneous crystal nucleation in oxide glasses. Physics and Chemistry of Glasses, 1989; **30**(5): 186-192.

135. Messing, G.L., Mcardle, J.L., Shelleman, R.A. The need for controlled heterogeneous nucleation in ceramic processing. In Materials Research Society - Symposia Proccedings. 1986.

136. Denry, I.L., Holloway, J.A. Effect of sodium content on the crystallization behavior of fluoramphibole glass ceramics. Journal of Biomedical Materials Research (Appl. Biomater), 2002; **63**: 48-52.

137. Salama, S.N., Salman, S.M., Darwish, H. The effect of nucleation catalysts on crystallization characteristics of aluminosilicate glasses. Ceramics - Silikáti, 2002; **46**(1): 15-23.

138. Muller, R., Zanotto, E.D.,Fokin, V.M. Surface crystallization pf silicate glasses: nucleation sites and kinetics. Journal of Non-Crystalline Solids, 2000; **274**: 208-231.

139. Siligardi, C., D'Arrigo, M.C., Leonelli, C. Sintering behavior of glass-ceramic frits. American Ceramic Society Bulletin, 2000; **79**(9): 88-92.

140. Prado, M.O., Zanotto, E.D. Glass sintering with concurrent crystallization. Comptes Rendus Chimie, 2002; **5**(11): 773-786.

141. Boccaccini, A.R., Stumpfe, W., Taplin, D.M.R., Ponton, C.B. Densification and crystallization of glass powder compacts during constant heating rate sintering. Materials Science and Engineering a-Structural Materials Properties Microstructure and Processing, 1996; **219**(1-2): 26-31.

Chapter 2

Physicochemical characterization

This section describes the physicochemical characterization of calcium phosphate glass ceramics which is presented as follows:

2.1. *In vitro* degradation studies of calcium phosphate glass ceramics prepared by controlled crystallization *Journal of Non-Crystalline Solids 330 (2003) 81-89.*

2.2. Crystallization studies of biodegradable $CaO\text{-}P_2O_5$ glass with MgO and TiO_2 for bone regeneration applications Glass *Technology 45 (2004) 78-79.*

2.3. In situ thermal and structural characterization of glass ceramics containing TiO_2 and MgO oxides *Journal of Non-Crystalline Solids 351 (2005) 810-817.*

2.4. Physicochemical degradation studies of calcium phosphate glass ceramic containing TiO_2 and MgO oxides.

2.1. *In vitro* degradation studies of calcium phosphate glass ceramics prepared by controlled crystallization

A. G. Dias[1,2], M. A. Lopes[1,2], I. R. Gibson [3], J. D. Santos[1,2*]

[1]Instituto de Engenharia Biomédica (INEB), Laboratório de Biomateriais, Rua do Campo Alegre 823, 4150-180 Porto, Portugal

[2]Universidade do Porto, Faculdade de Engenharia, Departamento de Engenharia Metalúrgica e Materiais, Rua Dr. Roberto Frias, 4200-465 Porto, Portugal

[3]Department of Biomedical Sciences, Institute of Medical Sciences, University of Aberdeen, Foresterhill, Aberdeen AB25 2ZD, U.K.

Journal of Non-Crystalline Solids 330 (2003) 81- 89.

ABSTRACT

Calcium phosphate glass ceramics with incorporation of small additions of two oxides, MgO and K_2O were prepared in the metaphosphate and pyrophosphate region, using an appropriate two-step heat treatment of controlled crystallization defined by differential thermal analysis results. Identification and quantification of crystalline phases precipitated from the calcium phosphate glass were performed using X-ray diffraction and Rietveld analysis. The β-$Ca_2P_2O_7$ (β-DCP), $KCa(PO_3)_3$, β-$Ca(PO_3)_2$ and $Ca_4P_6O_{19}$ phases were detected in the glass ceramics. In order to evaluate the degradation of the glass ceramics prepared, degradation studies were carried out during 42 days in Tris – HCl solution at 37ºC, pH 7.4, using granules in the range of 355 – 415 μm. The materials presented a weight loss ranging up to 12%. The ions leached during the immersion mainly originated from the $KCa(PO_3)_3$ phase, probably due to the presence of K^+ ion in the calcium metaphosphate, and the residual glassy phase. The structural changes at the surface of materials during degradation have been analyzed by Fourier transform infrared spectroscopy and X-ray diffraction. Results showed that significant surface changes occurred with immersion time, with the decrease of $KCa(PO_3)_3$, β-$Ca_2P_2O_7$ and β-$Ca(PO_3)_2$ phases occurring at different periods of immersion. This study has demonstrated an easy way to prepared calcium phosphate materials with specific calcium phosphate phases and crystallization, and therefore specific degradation rates.

INTRODUCTION

The capacity of the human body to regenerate bone components that are lost, damaged or diseased is limited in several situations, so synthetic materials to fill bone defects have been developed[1,2]. Calcium phosphate materials have some outstanding properties, namely similarity in composition to bone mineral and osteoconductivity[3-5]. Products in the bone graft market based on hydroxyapatite and tricalcium phosphate have been used clinically. However, the success of these materials is limited mainly due to low toughness, low elasticity, low ability to be resorbable and lack of osteogenic properties[6]. To overcome the low mechanical properties several silicate glasses and glass ceramics have been developed and products such as Bioglass®, Bioverit® and Ceravital® have been available commercially for a long time. Nevertheless, all these materials still show a lack of both osteogenic properties and complete biodegradability after implantation.

Bioresorbable glass ceramics containing large amounts of biodegradable calcium phosphate crystals are believed to be one of the best approaches to obtain materials of great interest for bony defects associated with or without the release of biological therapeutic molecules[7,8].

Phosphate glasses consist of a polymer-like, regular tetrahedral structure based on $[PO_4]$ groups, with their structure generally described using Q^n terminology, where n represents the number of bridging oxygens per tetrahedron[9,10]. Depending on the [O]/[P] ratio as set by glass composition, the phosphate glasses can be made with a series of structures: (a) cross-linked network of Q^3 tetrahedra (vitreous P_2O_5), (b) polymer-like metaphosphate chains of Q^2 tetrahedra, (c) "invert" glasses based on small pyro- (Q^1) and orthophosphate (Q^0) anions. The addition of a modifier oxide leads to the creation of non-bridging oxygens in the glass that result in a depolymerization of the phosphate network, with oxygen atoms breaking the P-O-P links. This breakage in the structure of phosphate glass weakens and reduces their durability[10-12].

Phosphate-based glasses seem to be used as bioresorbable materials because of their solubility behaviour[13,14], since their solubility may be controlled by altering their chemical composition[15]. Some studies have reported that using appropriate heat-treatment the microstructure can be controlled by controlling the phases and sizes of crystals that are precipitated in the glasses[16,17].

The aim of this work was to develop glass ceramics from the system $CaO\text{-}P_2O_5\text{-}MgO\text{-}K_2O$

with compositions located mainly between the metaphosphate (Q^2) and the pyrophosphate (Q^1) region (3.0 < O/P < 3.5). A two-step heat treatment, defined by differential thermal analysis (DTA), was used to achieve nucleation and crystal growth in a controlled manner. *In vitro* acellular degradation studies were performed to assess their resorbability potential according to standard ISO 10993-14.

MATERIALS AND METHODS

Preparation of glass samples

A phosphate glass (MK5) was prepared with a composition of $45CaO\text{-}45P_2O_5\text{-}5K_2O\text{-}5MgO$ (mol %), using the following analytical chemicals: $CaCO_3$, $MgHPO_4.3H_2O$, K_2CO_3 and H_3PO_4 (85%). The glass was obtained by melting in a platinum crucible at 1450ºC for 1h. The melt was quickly poured into a steel mould preheated at 370ºC, and then annealed for 30 min at 25ºC above the glass transition temperature, as determined by DTA analysis.

Preparation of glass ceramic samples

Differential thermal analysis (DTA) of the amorphous glass was performed to determine the exothermic and endothermic heat changes such as the glass transition temperature (T_g), crystallization temperature (T_c) and melting temperature (T_m). The analyses were carried out in a DTA-50 (Shimadzu) using an inert nitrogen atmosphere, a heating rate of 15ºC/min and a temperature scanning up to 1200ºC. Alumina (Al_2O_3) was used as a reference. Volume crystallization was achieved through an efficient two-step heat treatment, as previously reported by Zhang and Santos[8], and results are shown in Fig. 1.

Three different heat treatments were performed leading to MK5B, MK5C and MK5E glass ceramics. The corresponding temperatures for each heat treatment (T_1 and T_2) are listed in Table 1.

Materials characterization

The density of the glass and glass ceramics was determined using Archimedes principle with water as the immersion liquid. All measurements were performed in triplicate.

A JEOL scanning microscope (JSM-35C) with energy dispersive X-ray (EDS)

spectroscopy (VOYAGER, Noran Instruments) was used to characterize the microstructures of studied materials before and after the heat-treatment. The precipitated phases were examined at a magnification of 4000× using an accelerating voltage of +15 KeV on samples ground and polished down to a 1 μm finishing using diamond paste.

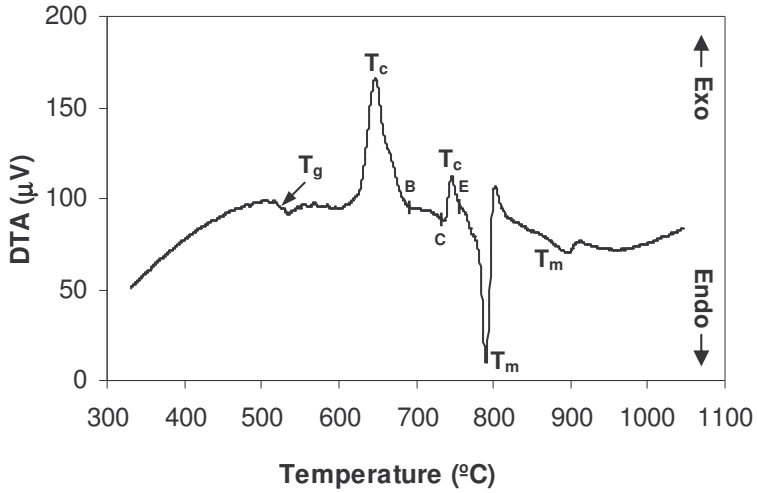

Figure 1 - DTA curve of the calcium phosphate glass MK5. Points B, C and E correspond to three different temperatures used in the heat treatments to obtain crystallization: 690, 739 and 756ºC. T_g, T_c and T_m stand for glass transition, crystallization temperature and melting temperature, respectively.

Table 1 - Temperatures used in the heat treatment cycle applied to amorphous glass to obtain glass ceramics.

Glass ceramic	T_1 [a] (ºC)	T_2 [b] (ºC)
MK5B	575	690
MK5C	575	739
MK5E	575	756

[a] Nucleation temperature
[b] Crystal growth temperature.

X-ray diffraction (XRD) and Rietveld analysis were used to identify and quantify the crystalline phases that precipitated from the mother glass. For X-ray diffraction measurements, samples were ground to a fine powder and analyzed using a Siemens D 5000 diffractometer, using flat plate geometry and Cu K_α radiation. Data were collected using a scintillation counter and a graphite diffracted beam monochromator, from 10 to 70º (2θ), with a step size of 0.02º and a counting time of 5 s per step. Quantitative phase analysis was performed by the Rietveld method using General Structure Analysis Software

(GSAS, Los Alamos National Laboratory). The weight fraction of each crystalline phase is calculated from an equation that accounts for the scale factor of each phase and the number of formula units, the mass of formula units and the cell volume of each phase[18].

The samples used in the degradation testing were ground to a small particle size in order to be analyzed by Fourier transform infrared spectroscopy (transmission mode) using a system 2000 FTIR spectrometer (Perkin Elmer). The resolution used was 4 cm^{-1} and the number of scans was not less than 100.

Degradation testing

The degradation testing was performed according to ISO 10993-14 - "Biological evaluation of medical devices- Part 14: Identification and quantification of degradation products from ceramics". Granules with a size between 355 and 415μm were used as obtained by automated controlled sieving technique. Tests were carried out in Tris[hydroxymethyl]aminomethane-HCl (Tris-HCl) solution (pH 7.4) at 37ºC, with a mixing speed of 120 rpm, using triplicate samples. At the end of each period of immersion time (0.5, 3, 7, 14, 28 and 42 days), granules were separated from solution by filtration (0.2μm), washed in deionised water and dried to constant weight. A relative weight loss percentage of samples was calculated from the following equation:

$$\text{Weight loss } (\%) = [(W_0 - W_t)/W_0] \times 100$$

where W_0 and W_t stand for initial weight and weight after a specific immersion time, respectively.

The concentration of calcium, magnesium and potassium ions in the soaking solution was measured by flame atomic absorption spectroscopy (AAS) (Unicam, Model Solar). The phosphorus concentration was measured from total phosphate groups by ultraviolet spectroscopy using the molybdenum blue method (Philips, Model PU 8620, UV-Vis Nir). The pH value at the end of each immersion time was measured at 37 ± 0.1ºC.

RESULTS

A typical DTA curve obtained at a heating rate of 15ºC/min for MK5 glass is shown in

Figure 1. Two exothermic peaks can be observed due to crystallisation phenomena at onset temperatures of 627 and 739ºC, and two endothermic peaks at onset temperatures of 773 and 896ºC correspond to melting. The latter two peaks are suggested to be due to the partial melting of crystalline phases or residual glass matrix. The temperature of glass transition at mid point (T_g) was 534ºC.

Figure 2 shows the XRD patterns of glass samples after the three different heat treatments (nucleation and crystal growth) used. The patterns are almost the same for all three heat treatments and show the precipitation of four phases: β-$Ca_2P_2O_7$, $Ca_4P_6O_{19}$, $KCa(PO_3)_3$ and β-$Ca(PO_3)_2$.

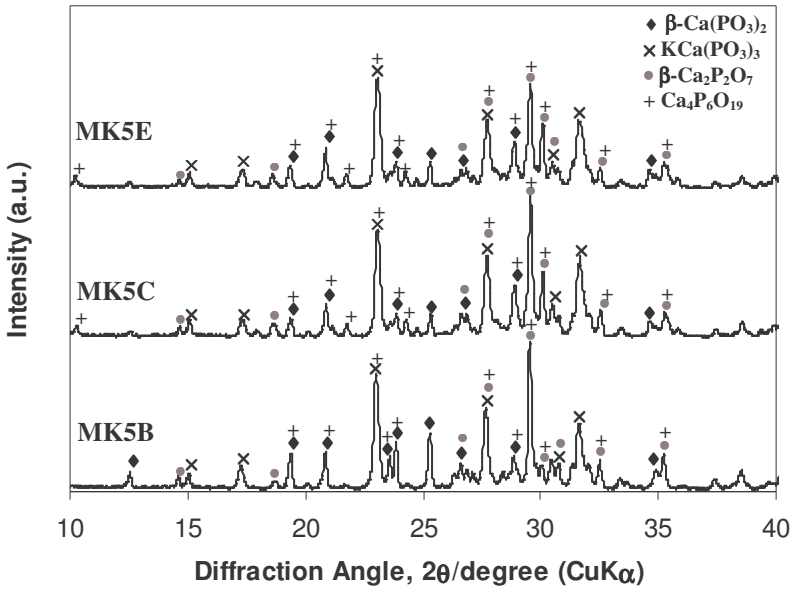

Figure 2 - XRD patterns of the three glass ceramics prepared, MK5B, MK5C and MK5E.

Table 2 shows the percentage of each precipitated phase in the crystallized materials obtained by applying the Rietveld analysis to XRD patterns. The predominant phase in all samples prior to soaking was β-$Ca_2P_2O_7$, with the other phases ranging in content from 0 to 20%. The sample MK5B appeared to have negligible $Ca_4P_6O_{19}$ but contained significantly more β-$Ca(PO_3)_2$ than MK5C or MK5E. All samples appeared to have a comparable content of amorphous glassy phase, as indicated by a broad amorphous band in the diffraction pattern. Comparing the area under the amorphous background with the area of the crystalline peaks would indicate that the fraction of amorphous phase content in all samples was low (<10%).

Table 2 - Relative percentage of precipitated phases before and after 7 and 42 days of immersion, determined by Rietveld analysis.

	Immersion time (days)	β-$Ca_2P_2O_7$	β-$Ca(PO_3)_2$	$KCa(PO_3)_3$	$Ca_4P_6O_{19}$
MK5B	0	73	18	7	2
	7	50	34	5	10
	42	65	26	4	5
MK5C	0	77	8	7	8
	7	52	37	4	7
	42	57	28	5	10
MK5E	0	70	12	9	9
	7	52	26	7	15
	42	67	20	4	9

On soaking for 7 days, the relative weight fractions of the β-$Ca_2P_2O_7$ and $KCa(PO_3)_3$ phases decreased for all three samples, with a concomitant increase in the relative weight fractions of the other two phases, most notably the β-$Ca(PO_3)_2$ phase. This behaviour corresponds to the dissolution (loss) of the β-$Ca_2P_2O_7$ and $KCa(PO_3)_3$ phases during soaking, with the relative increase of the other two phases. Soaking for 42 days seems to have resulted in a further decrease in the relative weight fraction of the $KCa(PO_3)_3$. In contrast, the relative weight fraction of the β-$Ca_2P_2O_7$ phase increased from 7 to 42 days soaking, with a decrease in the weight fraction of the β-$Ca(PO_3)_2$ phase.

The above results were confirmed by SEM analysis since the crystalline phases precipitated in different regions of the microstructure of the glass could be easily distinguished at a magnification of 4000×, as shown in Figure 3.

Glass samples before crystallization presented a microstructure completely amorphous (Fig. 3A) whereas crystallized samples showed volume crystallization (Figs 3B-3D). The phases denoted by *1* and *2* contain only Ca and P elements, but showed different Ca/P ratio. The phase denoted by *3* contains all elements presented in the amorphous glass Mg, P, K and Ca, and the phase denoted by *4* contains only P, Ca and K elements. The areas denoted by *1* may correspond to β-$Ca(PO_3)_2$ and $Ca_4P_6O_{19}$ since the Ca/P atomic ratio was ≅ 0.5-0.6(6).

The areas denoted by *2* may correspond to the β-$Ca_2P_2O_7$ phase, since the Ca/P atomic ratio was ≅ 1. The areas denoted by *3* should correspond to the glassy residual matrix since it is composed of all elements that were present in the mother glass; this area appears to be

phosphate-rich, which would correlate with this region corresponding to the residual glassy phase. Finally, areas denoted by *4* may correspond to the K-containing phase.

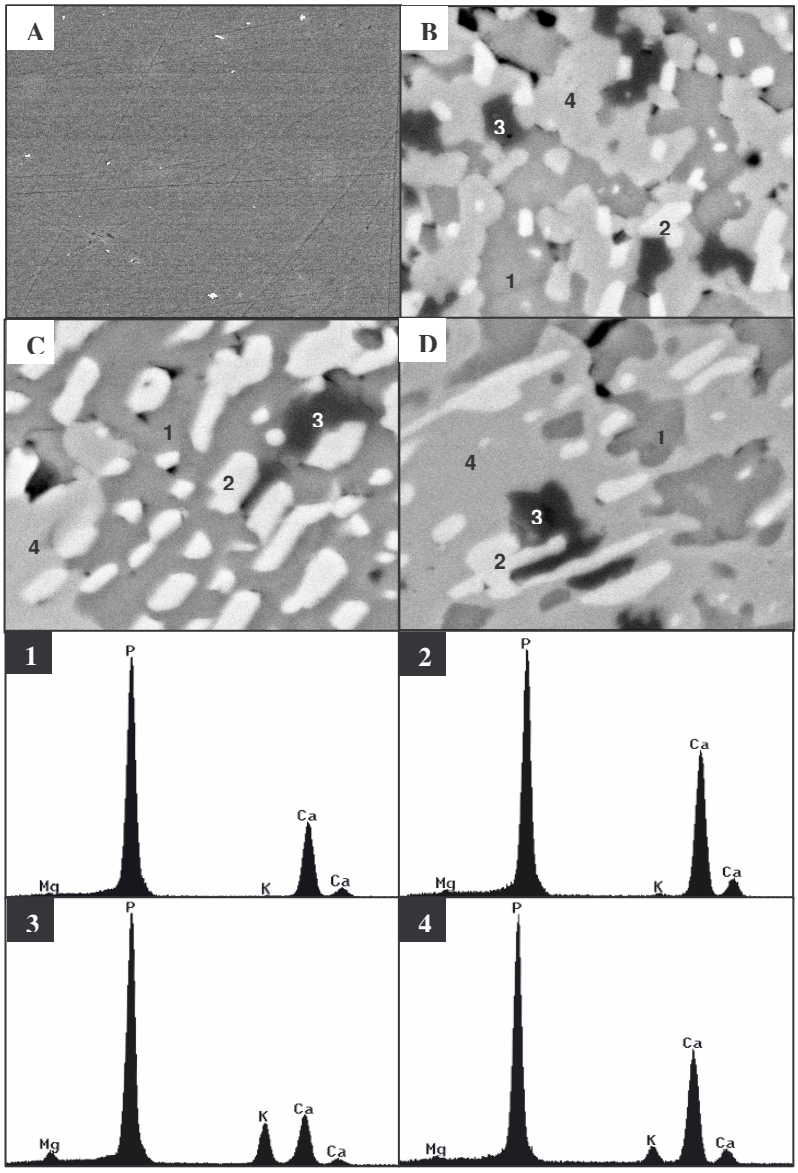

Figure 3 - Micrographs obtained by SEM and EDS spectra of the labelled regions (1-4) (4000×). (A) Glass MK5 (B) MK5B, (C) MK5C and (D) MK5E.

The specific volume of the glass MK5 and glass ceramics (MK5B, MK5C and MK5E) samples was shown to be 2.60 ± 0.03 g/cm^3 with no statistically significant difference.

The variation of weight loss with the immersion time is shown in Figure 4 where it may be observed that the range of weight loss varies from ≅ 3.0 - 4.1% after one day to 9.3 - 12.0% after 42 days.

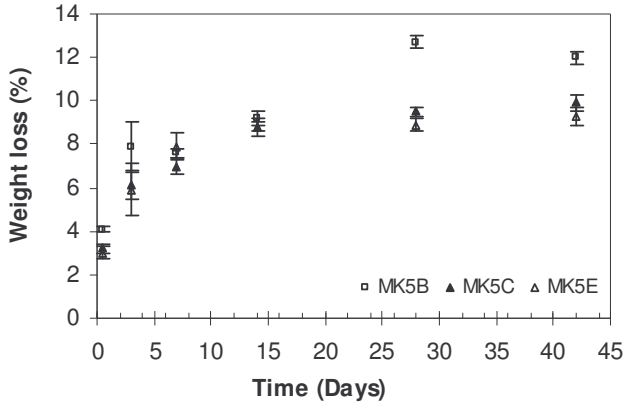

Figure 4 - Weight loss against immersion time for the studied glass ceramics.

The material MK5B showed the highest dissolution among the three glass ceramics under study. MK5C and MK5E showed similar behaviour, i.e., a steady increased weight loss at early immersion times achieving about 9% on day 14, which was then kept constant until 42 days.

Figure 5 depicts the variation of pH of the Tris-HCl solution with immersion time. It was observed a slight increase on pH after half a day of immersion for all glass ceramics, followed by a decrease up to 42 days. The glass ceramic MK5B showed the largest decreases achieving the pH ≅ 6 after 42 days of immersion.

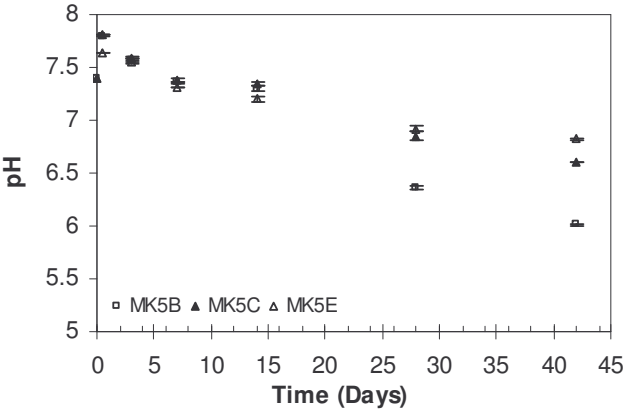

Figure 5 - Variation of pH of the Tris solution with immersion time (standard deviation lower than 0.04).

Figure 6 shows the PO_4^{3-}, K^+, Mg^{2+} and Ca^{2+} ions concentration against immersion time for all studied glass ceramics. The concentration of PO_4^{3-}, K^+ and Mg^{2+} ions in solution had similar trends showing an increase up to day 14, followed by stabilization in ion

concentration up to 42 days. However, for Ca^{2+} ion the higher release was achieved from 0.5 to day 7 (from 110 to 310 ppm) and then a decrease was observed until day 42.

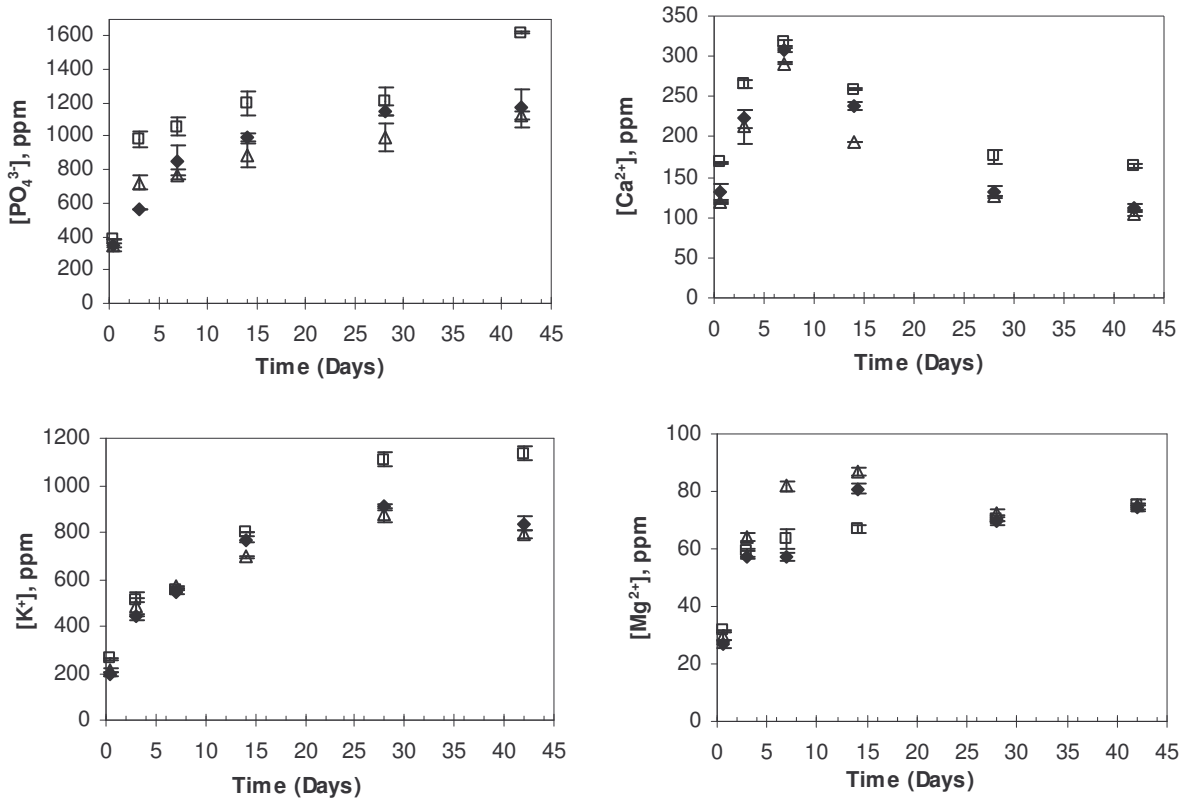

Figure 6 - Ion release from the glass ceramics into Tris-HCl solution (P, Mg, K and Ca) against time of immersion, (□) MK5B, (♦) MK5C and (Δ) MK5E.

The dissolution of K^+ and PO_4^{3-} ions was much higher compared with the other two ions, leading to concentrations from 350 to 1500 ppm, which may be mainly explained by the increased degradation with time of the $KCa(PO_3)_3$ phase, as confirmed by Rietveld analysis, and the residual glassy phase, as confirmed by the presence of the increasing Mg^{2+} ion concentration in the soaking solution.

FTIR results of amorphous glass and crystallized glasses before degradation studies are shown in Figure 7. As expected a broad spectrum was obtained for the glass sample and specific functional groups were identified for glass ceramics that corresponded to metaphosphate and pyrophosphate, $(PO_3)^-$ and $(P_2O_7)^{4-}$. These results are in accordance with functional groups of the crystalline phases identified by XRD: β-$Ca_2P_2O_7$, $KCa(PO_3)_3$, β-$Ca(PO_3)_2$ and $Ca_4P_6O_{19}$. FTIR spectra of MK5B glass ceramic are plotted in Figure 8 before and after degradation testing. Since there is a strong band overlapping for $(PO_3)^-$ and $(P_2O_7)^{4-}$ groups it was very difficult to detect specific changes for each group

with immersion time. However, comparing MK5B before immersion and after 42 days immersion significant band decrease could be detected mainly in the regions of 650-800 cm^{-1} and 950-1300 cm^{-1}, which corresponded to vibration frequencies of meta- and pyrophosphate groups[19].

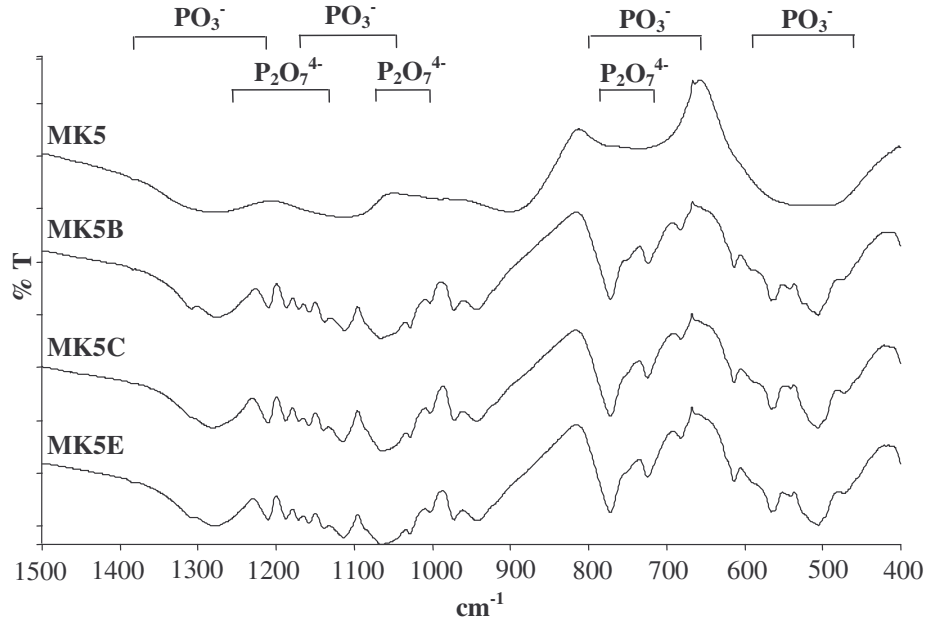

Figure 7 - FTIR spectra of the glass (MK5) and glass ceramics (MK5B, MK5C and MK5E).

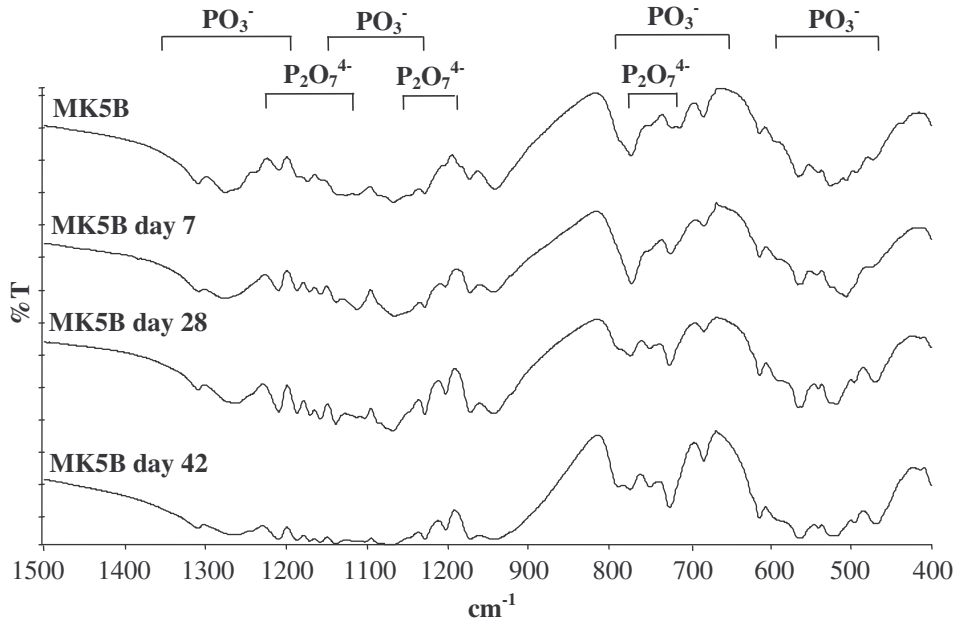

Figure 8 - FTIR spectra of the glass ceramic MK5B before and after immersion in Tris-HCl solution, for 7, 28 and 42 days.

DISCUSSION

Several authors have reported the preparation of $CaO-P_2O_5$ glass ceramics using different nucleating agents to promote volume crystallization[20,21]. Shi and James[22] reported the addition of B_2O_3 to study the effect on the nucleation of $CaO-P_2O_5$ glasses, James et al[20] reported the addition of nucleating agents such as Al_2O_3 and TiO_2 and Abe et al.[7,23] added a few percentage of Na_2O and TiO_2, but using a different preparation route since the glass ceramics were prepared by sintering and crystallization of the glass powder compacts.

In this study, glass ceramics were successfully prepared with $3.0 < O/P < 3.5$ (between the metaphosphate (Q^2) and pyrophosphate (Q^1) region), using a heat treatment for crystallization of the $CaO-P_2O_5$ glasses with two additives that promote volume nucleation and the formation of bioactive and biodegradable phases. In the crystallization heat-treatment cycles volume crystallization could only be obtained when the crystallization treatment was above the first crystallization peak detected by DTA. After heat treatments of crystallization, four phases were precipitated in the glass ceramics. One of them was calcium pyrophosphate β-$Ca_2P_2O_7$ (β-DCP), which is reported in to be bioactive[6]. The biocompatibility of the other three phases $KCa(PO_3)_3$, $Ca_4P_6O_{19}$ and β-$Ca(PO_3)_2$ has not been clearly reported in the literature, however β-$Ca(PO_3)_2$ is considered to be non-toxic[8]. The other two phases are also believed to be harmless since their degradation products are metabolized by cells.

Dissolution studies were carried out in order to investigate the degradation of these glass-ceramics and results confirmed that by controlling the overall composition of the initial glass, namely its O/P ratio, glass ceramics with high degree of degradability may be obtained. In fact, the level of chemical degradation observed for these materials is well-above that reported in literature for bioactive ceramics that are clinically used, namely hydroxyapatite (HA), $Ca_{10}(PO_4)_6(OH)_2$ and tricalcium phosphate (TCP) $Ca_3(PO4)_2$. Several authors have reported that the level of calcium and phosphorus that are leached out from HA and TCP ceramics under similar degradation testing are usually in the range of 6.1-0.36 ppm and 13-5.5 ppm, respectively[24].

The glass ceramics prepared in this work seem to be capable of combining a bioactive behaviour in vivo, due to the bioactive and bioresorbable phases that exist in the microstructure, with the possibility of having good potential as drug delivery system, since the degradability has been shown to be significant. Further studies to examine the in vivo

behaviour of these materials will be conducted to assess this hypothesis.

The ionic release profile showed that initially a high ion concentration was observed in the soaking solutions, particularly for phosphate groups, which tended to reach a plateau after 12h of immersion. A relative decrease in Ca^{2+} ion concentration was detected after 7 days of immersion, which could be attributed to the precipitation of Ca-rich calcium phosphate phase on the samples surface, which was confirmed in block samples of the same composition that were immersed in the same test conditions. Further studies are now being conducted to determine the composition and structure of this precipitated calcium phosphate phase.

The variation of pH can be correlated to the release of ionic species from glass ceramics to the soaking solution. In the first 12h of immersion, there was a slight increase in pH that was due to predominant phosphate group dissolution compared to the cationic species (see Fig. 6). Another stage seemed to occur from 12h to 7days where pH decreases as a result of the leaching of β-$Ca_2P_2O_7$ and $KCa(PO_3)_3$ crystalline phases as well as of the residual glassy phase, as confirmed respectively by the phase quantification performed by XRD analysis and by the sharp increase in Mg^{2+} ion concentration of the soaking solution.

The change in the relative weight fractions of the β-$Ca_2P_2O_7$ and the β-$Ca(PO_3)_2$ phases from 0 to 7 days and from 7 to 42 days, Table 2, implies a change in the dissolution profiles of the materials. During the early stages of soaking (0-7 days), the β-$Ca_2P_2O_7$ phase appeared to be the most soluble phase, with the relative weight fraction decreasing significantly over this time period. As a result, the relative weight fraction of the β-$Ca(PO_3)_2$ phase increased, but this does not correspond to more of this phase forming; the increase is based on a significant amount of the β-$Ca_2P_2O_7$ being lost to dissolution. Correspondingly, from 7 to 42 days soaking, the $Ca(PO_3)_2$ phase showed a large decrease in relative weight fraction, implying that this phase was the most soluble during this time period . It should be noted that from 0 to 7 days the pH of the soaking solution was >7.4, whereas from 7 to 42 days the pH dropped to as low as 6.0; this change in pH would have a strong effect on the relative solubility of different calcium phosphate phases.

It should also be noted that the glass ceramic with the greatest degradability (MK5B), indicated by the largest ion concentrations in the soaking solution (Fig. 6) also showed the biggest drop in pH (Fig. 5). The greater degradation of the material MK5B is a consequence of its phase composition and degree of crystalinity. The low crystallization

temperature used for this glass ceramic (690 ºC) most probably induced a more amorphous structure compared to the other glass ceramics and therefore contributed to its high degradability.

CONCLUSIONS

Glass ceramics with different phases, such as β-$Ca_2P_2O_7$, $KCa(PO_3)_3$, β-$Ca(PO_3)_2$ and $Ca_4P_6O_{19}$ can be obtained, using small additions of nucleating agents such as K_2O and MgO. The MK5B material was shown to be the most soluble material, using a recognized (ISO) dissolution-testing standard. The incorporation of K_2O in a glass ceramics increases the solubility, and offers greater flexibility in terms of tailoring the solubility to suit the potential biomedical application. The straightforwardness of synthesis and the ability to control the degradability of these calcium phosphate glass ceramics makes them potentially clinically helpful for promoting the regeneration of soft as well as hard connective tissue[5].

ACKOWLEDGEMENTS

The authors wish to acknowledge the grant Refª: PRAXIS XXI /BD/ 21458 / 99 financed by FCT (Fundação para a Ciência e a Tecnologia) and the EPSRC (UK) for funding of the X-ray diffractometer at the University of Aberdeen (GR/M89782/01).

REFERENCES

1. Hall, B.K., Bone-fracture repair and regeneration. 1992; **Vol. 5**. CRC.

2. Vidal, J.,Dossa, J., Le tissu osseux. Collection biologie de lápparеil locomoteur. 1990.

3. LeGeros, R.Z., Calcium phosphates in oral biology and medicine. 1991; **Vol. 15**. Karger.

4. Yamamuro, T., Hench, L.L., Wilson, J., Handbook of bioactive ceramics. Bioactive glasses and glass ceramics. 1990; **Vol. 1**. CRC.

5. Hench, L.L., Wilson, J., Handbook of bioactive ceramics. Calcium phosphate and hydroxyapatite ceramics. 1990; **Vol. 2**. CRC.

6. Kitsugi, T., Yamamuro, T., Nakamura, T., Masanori, O. Transmission electron microscopy observations at the interface of bone and 4 types of calcium phosphate

ceramics with different calcium phosphorus molar ratios. Biomaterials, 1995; **16**(14): 1101-1107.

7. Kasuga, T., Abe, Y. Calcium phosphate invert glasses with soda and titania. Journal of Non-Crystalline Solids, 1999; **243**(1): 70-74.

8. Zhang, Y., Santos, J.D. Crystallization and microstructure analysis of calcium phosphate-based glass ceramics for biomedical applications. Journal of Non-Crystalline Solids, 2000; **272**(1): 14-21.

9. Hartmann, P., Vogel, J., Schnabel, B. NMR study of phosphate-glasses and glass-ceramic structures. Journal of Non-Crystalline Solids, 1994; **176**(2-3): 157-163.

10. Brow, R.K. Review: the structure of simple phosphate glasses. Journal of Non-Crystalline Solids, 2000; **263**(1-4): 1-28.

11. Jones, A.R., Winter, R., Greaves, G.N., Smith, I.H. MAS NMR study of soda-lime-silicate glasses with variable degree of polymerisation. Journal of Non-Crystalline Solids, 2001; **293**: 87-92.

12. Clément, J., Manero, J.M., Planell, J.A., Avila, G., Martínez, S. Analysis of the structural changes of a phosphate glass during its dissolution in simulated body fluid. Journal of Materials Science-Materials in Medicine, 1999; **10**: 729-732.

13. Zhang, Y., Lopes, M.A., Santos, J.D. $CaO\text{-}P_2O_5$ class ceramics containing bioactive phases: Crystallisation and in vitro bioactivity studies. Key Engineering Materials, 2000; **192-195**: 643-646.

14. Uo, M., Mizuno, M., Kuboki, Y., Makishima, A., Watari, F. Properties and cytotoxicity of water soluble $Na_2O\text{-}CaO\text{-}P_2O_5$ glasses. Biomaterials, 1998; **19**(24): 2277-2284.

15. Franks, K., Abrahams, I., Knowles, J.C. Development of soluble glasses for biomedical use. Part I: In vitro solubility measurement. Journal of Materials Science-Materials in Medicine, 2000; **11**(10): 609-614.

16. Kasuga, T., Abe, Y. Novel calcium phosphate ceramics prepared by powder sintering and crystallization of glasses in the pyrophosphate region. Journal of Materials Research, 1998; **13**(12): 3357-3360.

17. Franks, K., Abrahams, I., Georgiou, G., Knowles, J.C. Investigation of thermal parameters and crystallisation in a ternary $CaO\text{-}Na_2O\text{-}P_2O_5$-based glass system.

Biomaterials, 2001; **22**(5): 497-501.

18. Hill, R.J., Howard, C.J. Quantitative phase-analysis from neutron powder diffraction data using the Rietveld method. Journal of Applied Crystallography, 1987; **20**: 467-474.

19. Nyquist, R.A., Handbook of infrared and raman spectra of inorganic compounds and organics salts. 1997. Academic Press.

20. Nan, Y., Lee, W.E., James, P.F. Crystallization behavior of CaO-P_2O_5 glass with TiO_2, SiO_2, and Al_2O_3 additions. Journal of the American Ceramic Society, 1992; **75**(6): 1641-1647.

21. Reaney, I.M., James, P.F., Lee, W.E. Effect of nucleating agents on the crystallization of calcium phosphate glasses. Journal of the American Ceramic Society, 1996; **79**(7): 1934-1944.

22. Shi, W., James, P.F. In Physics of Non-Crystalline Solids. 1991University of Cambridge.

23. In XVIII international congress on glass. 1988, American Ceramic Society, Japan.

24. Chun, S., Na, S.W., Lee, J.H., Chung, J.P., Ryu, I.C., Kim, S.Y. Biodegradation study of potassium calcium metaphosphate in the SBF and Tris-buffer solution. Key Engineering Materials, 2002; **218-220**: 149-152.

2.2. Crystallization studies of biodegradable $CaO-P_2O_5$ glass with MgO and TiO_2 for bone regeneration applications

A. G. Dias[1,2], K. Tsuru[3], S. Hayakawa[3], M. A. Lopes[1,2], J. D. Santos[1,2], A. Osaka[3]

[1]Instituto de Engenharia Biomédica (INEB), Laboratório de Biomateriais, Rua do Campo Alegre 823, 4150-180 Porto, Portugal

[2]Universidade do Porto, Faculdade de Engenharia, Departamento de Engenharia Metalúrgica e Materiais, Rua Dr. Roberto Frias, 4200-465 Porto, Portugal

[3]Biomaterials Lab., Faculty of Engineering, Okayama University, Tsushima, Okayama-Shi 700-8530, Japan

Glass Technology 45 (2004) 78 - 79.

ABSTRACT

$CaO-P_2O_5$ glass ceramics with small additions of MgO and TiO_2 were prepared in the ortho- and pyrophosphate regions by powder sintering and crystallization through heat treatment at different temperatures determined from differential thermal analysis (DTA). The glass ceramics were analysed by X-ray diffraction (XRD) and it was observed that α- and β-$Ca_2P_2O_7$ were the first phases to precipitate in the parent glass matrix at a temperature of 681ºC, followed by $CaTi_4(PO_4)_6$ and TiP_2O_7 at temperatures between 703 and 725ºC. The β-$Ca_2P_2O_7$ and $CaTi_4(PO_4)_6$ phases are usually considered as biocompatible and bioactive and therefore these glass ceramics seem to show good potential for bone regeneration applications.

INTRODUCTION

Although glass ceramics are conventionally obtained by controlled crystallisation of the parent glass, sintering and crystallisation of fine glass powders can also be used to fabricate these materials. The parent glass composition is usually chosen to ensure precipitation of desired crystalline phases[(1,2)]. The properties of multiphase systems depend not only on the preparation route but also on the properties and content of each phase precipitated in the glass matrix[(3)]. The aim of this work was to develop and characterize glass ceramics located mainly between ortho- and pyrophosphate region of the $CaO-P_2O_5$-$MgO-TiO_2$ system that could be used in medical applications for bone regeneration. The $CaO-P_2O_5$-$MgO-TiO_2$ system was chosen based on previous studies[(4)]. The glass ceramics

under study were characterised by XRD and the crystallisation process studied using DTA analysis.

MATERIALS AND METHODS

Glass preparation

A calcium phosphate glass (MT13) was prepared with the composition of $37P_2O_5.45CaO.5MgO.13TiO_2$ (mol%), by conventional melting technique at 1550°C for 1h followed by rapid quenching in water. The frit particles were dried at 80°C and then pulverised in a ball mill pot to sub-10 μm using methanol as a liquid medium. The particle size distribution was analysed using laser diffraction (Coulter LS 230, U.K.). All measurements were performed in triplicate.

Glass ceramic preparation

Glass ceramic samples were prepared by powder sintering and crystallisation through heat treatment at different temperatures, ranging from glass transition temperature (T_g) to the crystallization temperature (T_c) as determined by differential thermal analysis (DTA) as shown in Figure 1. The DTA analysis was carried out in a DTA–50 (Shimadzu) with a heating rate of 15°C/min and temperature scanning up to 1200°C, using alumina powder (Al_2O_3) as reference. The pulverised glass powders were uniaxially pressed at 185 MPa to obtain disc shaped compacts. The discs were then heated to either 681, 703 or 725°C at a rate of 4ºC/min and were held at these temperatures for 1h. The resulting glass ceramics are referred to as MT13A, MT13B and MT13C, respectively.

Materials characterization

The density of the glass and glass ceramics was measured using the Archimedes method with water as the immersion liquid and all measurements were performed in triplicate. XRD was used to identify the crystalline phases that precipitated from the parent glass. The samples were ground to a fine powder and analyzed in a Siemens D 5000 diffractometer, using flat plate geometry and CuKα radiation. Data were collected using a scintillation counter and a graphite monochromator, from 10 to 70°(2θ), with a step size of 0.02º and a counting time of 5 s per step.

RESULTS AND DISCUSSION

The pulverised glass particles had unimodal particle size distribution with $D_{0.5}$ = 4.2 μm and $D_{0.9}$ = 7.2 μm. All particles were below 7.2 μm. The mean density values of the glass ceramics MT13A, MT13B and MT13C were approximately 2.90 ± 0,03 g/cm^3 with no statistical difference among them.

The DTA curve obtained for the amorphous glass MT13 is shown in Figure 1 where the glass transition temperature (T_g) was observed at 637ºC and one doublet exothermic peak, attributed to crystallisation, with peak temperatures of T_{C1} = 750ºC and T_{C2} = 762ºC. The presence of two endothermic peaks at 1043 and 1180ºC are attributed to the residual glass matrix and/or partial melting.

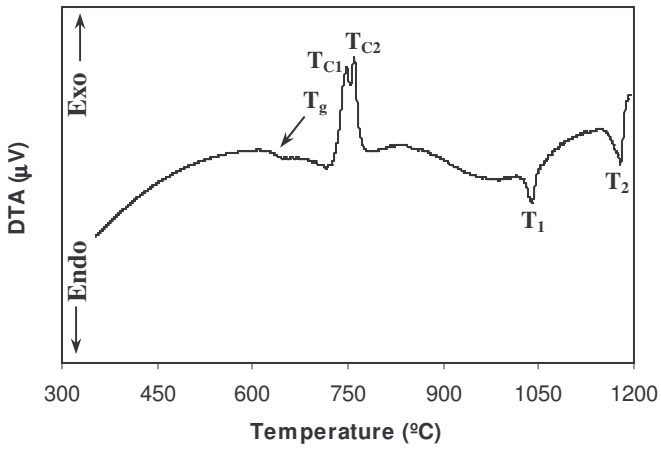

Figure 1 - DTA curve of the $37P_2O_5$-45CaO-5MgO-$13TiO_2$ glass (MT13).

XRD patterns of glass samples after heat treatment shown in Figure 2 revealed that the first phases that precipitated in the glass matrix were α- and β-$Ca_2P_2O_7$ at 681ºC, with the α-phase present in slightly higher percentage than β-phase. Furthermore, higher temperatures induced precipitation of $CaTi_4(PO_4)_6$ and TiP_2O_7 phases. MT13B and MT13C glass ceramics showed similar phase contents, consisting of α- and β-$Ca_2P_2O_7$, $CaTi_4(PO_4)_6$ and TiP_2O_7. Two of these four phases, calcium pyrophosphate β-$Ca_2P_2O_7$ (β-DCP) and $CaTi_4(PO_4)_6$ are reported to be biocompatible and bioactive[5-8]. Dissolution studies are undergoing in order to investigate the *in vitro* degradation of these glass ceramics.

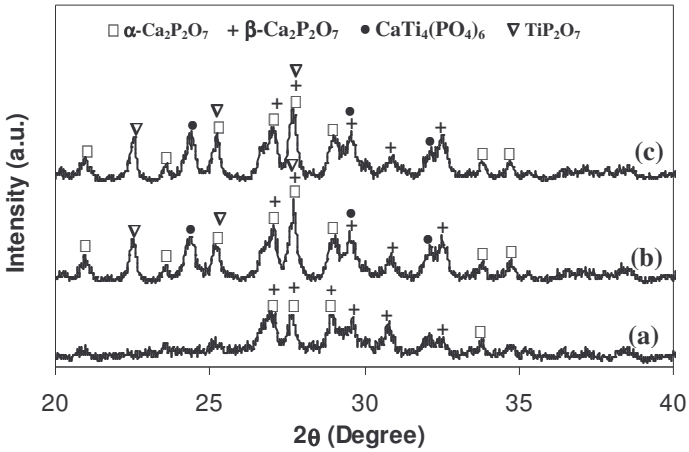

Figure 2 – X-ray diffraction spectra from samples sintered at (a) 681ºC, (b) 703ºC and (c) 725ºC.

CONCLUSIONS

It is possible to induce the precipitation of crystalline phases that show different behaviour (α-$Ca_2P_2O_7$, β-$Ca_2P_2O_7$, $CaTi_4(PO_4)_6$ and TiP_2O_7) in the CaO-P_2O_5-MgO-TiO_2 glass ceramic by controlling the crystallisation conditions.

ACKOWLEDGEMENTS

The authors would like to express their thanks to FCT - Fundação para a Ciência e a Tecnologia for their financial support through the PhD grant PRAXIS XXI/BD/21458/99 and Fundação Calouste Gulbenkian.

REFERENCES

1. Siligardi, C., D'Arrigo, M.C., Leonelli, C. Sintering behaviour of glass-ceramic frits. The American Ceramic Society Bulletin, 2000: 88-92.

2. Clarck, T.J., Reed, J.S. Kinetic process involved in the sintering and crystallization of glass powders. Journal of American Ceramic Society, 1986; **69**(11): 837-846.

3. Karmakar, B., Kundu, P., Jana, S., Dwivedi, N. Crystallization kinetics and mechanism of low-expansion lithium aluminosilicate glass-ceramics by dilatometry. Journal of the American Ceramic Society, 2002; **85**(10): 2572-2574.

4. Zhang, Y., Santos, J.D. Crystallization and microstructure analysis of calcium

phosphate-based glass ceramics for biomedical application. Journal of Non-Crystalline solids, 2000; **272**: 14-21.

5. Ryu, H.S., Youn, H.J., Hong, K.S., Chang, B.S., Lee, C.K., Chung, S.S. An improvement in sintering property of β-tricalcium phosphate by addition of calcium pyrophosphate. Biomaterials, 2002; **23**(3): 909-914.

6. Kitsugi, T.l.T., Yamamuro, T., Nakamura, T., Oka, M. Transmission electron microscopy observations at the interface of bone and four types of calcium phosphate ceramics with different calcium/phosphorous molar ratios. Biomaterials, 1995; **16**(14): 1101-1107.

7. Gross, U., Muller-Mai, C., Voigt, C., Mesgarian, M., Berger, G., Ploska, U. Tissue response in the femur of rabbits after implantation of a new calcium titanium phosphate composition. Key Engineering Materials, 2000; **192-1**: 383-386.

8. Sun, J.S., Tsuang, Y.H., Lin, F.H., Chen, L.T., Hang, Y.S., Liu, H.C. The application potential of sintered β-dicalcium pyrophosphate in total joint arthroplasty. Journal of Arthroplasty, 2003; **18**(3): 352-360.

2.3. *In situ* thermal and structural characterization of bioactive calcium phosphate glass ceramics containing TiO_2 and MgO oxides: High Temperature - XRD studies

A.G. Dias[1,2], J.M.S. Skakle[3], I.R. Gibson[4], M.A. Lopes[1,2], J.D. Santos[1,2]

[1]Instituto de Engenharia Biomédica (INEB), Laboratório de Biomateriais, Rua do Campo Alegre 823, 4150-180 Porto, Portugal

[2]Universidade do Porto, Faculdade de Engenharia, Departamento de Engenharia Metalúrgica e Materiais, Rua Dr. Roberto Frias, 4200-465 Porto, Portugal

[3]Department Chemistry, University of Aberdeen, Meston Walk, Aberdeen AB24 3UE, U.K.

[4]School of Medical Sciences, College of Life Sciences of and Medicine, Institute of Medical Sciences, University of Aberdeen, Foresterhill, Aberdeen AB25 2ZD, U.K.

Journal of Non-Crystalline Solids 351 (2005) 810-817.

KEYWORDS: calcium phosphate glass ceramic, high temperature XRD, phase analysis

ABSTRACT

This study aims to develop glass ceramics in the calcium phosphate system that exhibit suitable properties to be used for biomedical applications. Calcium phosphate glasses with the incorporation of small additions of MgO and TiO_2 oxides were prepared in the pyro- and orthophosphate regions. The glass ceramics were prepared by a controlled powder sintering process through heat-treatment at different temperatures, as defined by results from differential thermal analysis (DTA). The composition of the crystalline phases precipitated in the glassy matrix as a result of heat treatments at different temperatures, ranging from 681 to 725ºC, was determined from X-ray diffraction data. The sequence of phase crystallization in the mother glass was also studied *in situ* using high temperature X-ray diffraction (HT-XRD) analysis. Results showed that the first phases that precipitated in the glass matrix were α- and β-$Ca_2P_2O_7$ at 620ºC. A small amount of $CaTi_4(PO_4)_6$ appeared at 630ºC. At 650ºC the three phases α-$Ca_2P_2O_7$, β-$Ca_2P_2O_7$ and $CaTi_4(PO_4)_6$ were clearly presented with a small amount of TiP_2O_7 and finally at 660ºC all four phases were observed. Glass ceramics were also characterized using Raman and X-ray photoelectron spectroscopy. This study demonstrates that, by altering the heat treatment cycle, it is possible to prepare glass ceramics in the calcium phosphate system that contains

different bioactive and biocompatible phases.

INTRODUCTION

Calcium phosphate glasses have been considered as prospective materials for the reconstruction and repair of bone as a consequence of their biocompatibility and bioactivity, which are of enormous interest in the development of bioabsorbable material for bone healing applications. Therefore, a biocompatible resorbable material with increased resorption rates may be useful; this rate can be high and controllable in some calcium phosphate glass ceramics. Due to this feature and the fact that the composition of glass ceramics may resemble the mineral phase of bone, calcium phosphate glass ceramics may be tailored to be used as a cavity filler for maxillofacial surgery or as a drug delivery carrier, among other applications. However, a balance between their degradation rate and the bone remodelling time must be considered, as some glass systems are too soluble for some purposes. It is well known that by modifying the composition of these glass ceramics, the degradation rate can be controlled, and this can be considerably reduced by the incorporation of some metallic oxides in the glass network, such as TiO_2[1-6]. Previous reports of the preparation of glass and glass ceramics in the CaO-P_2O_5-TiO_2 system have indicated that biocompatible and bioactive phases may be produced[7,8]. With this composition a new family of phosphate glass ceramics appears, with a mixture of soluble and less soluble crystalline phases, such as β-$Ca_2P_2O_7$ and $CaTi_4(PO_4)_6$, respectively[9-11].

The aim of this work is to study the crystallization of the glass in the system CaO-P_2O_5-MgO-TiO_2 prepared between the pyrophosphate (Q^1) and orthophosphate (Q^0) region ($3.5 < O/P < 4.0$). A heat treatment, defined by the results obtained from differential thermal analysis (DTA), was used to achieve nucleation and bulk crystallization. This heat treatment was studied *in situ* using high temperature X-ray diffraction (HT-XRD). Various other properties of the glass ceramics were studied by Raman and X-ray photoelectron spectroscopy and correlated to the changes in the glass structure after heat treatment.

MATERIALS AND METHODS

Glass ceramic preparation

The calcium phosphate glass was prepared with the composition of $37P_2O_5$-45CaO-5MgO-

$13TiO_2$ in mol% (MT13) by the conventional melting technique, using the following analytical chemicals: $CaCO_3$, $MgHPO_4.3H_2O$, TiO_2 and H_3PO_4. Briefly, after water quenching, the glass particles were dried and then pulverized in a ball mill pot by a wet-method using methanol to a mean particle size less than 10 μm[12]. This powder was firstly unixially pressed at 185 MPa to obtain disc shaped compacts followed by sintering/crystallization cycles at different temperatures. The heat treatment temperatures used to obtain the glass ceramics were based on the previous Differential Thermal Analysis (DTA) results, as described elsewhere[12]. Briefly, these results showed that the values obtained for glass transition temperature, T_g, was 637ºC and the onset of crystallization was at 726ºC. Four different heat treatment temperatures (659, 681, 703 and 725°C) that lay between these two values were chosen, Table 1.

Table 1 - Heat treatment cycle applied to amorphous glass to obtain glass ceramics.

Heat treatment	Temperature	Glass ceramic
NC	659ºC	MT13NC
A	681ºC	MT13A
B	703ºC	MT13B
C	725ºC	MT13C

Materials characterization

High temperature X-ray diffraction (HT-XRD) analysis was performed on the mother glass to study the sequence of phase crystallization. For HT-XRD, glass samples were analyzed using a Bruker D8 Advance diffractometer, with flat plate geometry and Cu-K_α radiation. Data were collected using a scintillation counter with primary and secondary Goebel mirrors from 20 to 50º (2θ), with a step size of 0.02º and a counting time of 1.7 s per step. The analysis was performed each 10ºC from 600 to 740 ºC with a heating rate of 4ºC/min and a dwell time of 45 min per scan.

The heat-treated samples as prepared in the section 2.1. were analyzed by X-ray diffraction (XRD) in order to identify and to quantify the percentage of crystalline phases that precipitated in the microstructure at the different treatment temperatures. For the X-ray diffraction measurements glass ceramics were ground to a fine powder and data were collected from 10 to 70º (2θ), with a step size of 0.02º and a counting time of 5 s per step. Satisfactory quantitative phase analysis of these samples using the Rietveld method, using

the software GSAS, was not possible due to the complex powder patterns, in particular the presence of four different phases with differing peak widths/shapes, significant overlapping of peaks, and an amorphous phase. The weight fraction of each crystalline phase that precipitated for the different heat treatments was calculated from an equation that accounts for the scale factor of each phase and the density of each phase[13]. The purpose of these calculations was not to determine definitive values of the phase compositions of these samples, as it is acknowledged that such methods make numerous assumptions. In particular, they will not account for varying degrees of crystallinity of the different phases and preferred orientation effects. However, for the purpose of following trends in the evolution of the crystallization of the four phases with increasing temperature this model is adequate. For each diffraction pattern, a background was fitted and subtracted, using the Bruker DIFFRAC^{plus} EVA software. The uncertainty associated with the composition was less than 5%.

To identify functional groups, the glass and glass ceramic samples were analyzed by FT-Raman spectroscopy (transmission mode) using a system 2000 FTIR spectrometer (Perkin Elmer). The resolution used was 4 cm^{-1} and the number of scans was 200 for each analysis.

X-ray photoelectron spectroscopy (XPS) studies of the mother glass and heat-treated samples was conducted on a VG-Scientific ESCALAB 200A spectrometer using an achromatic Al (Kα) X-ray source operating at 15 KeV (300 W). All elements were identified from survey spectra collected over a range of 0–1300 eV with an analyzer pass energy of 50 eV. For deeper analysis, high-resolution spectra were recorded from individual peaks at 20 eV pass energy. The binding energy (BE) scales were referenced to the adventitious C1s BE at 285.0 eV. The peak deconvolution was performed using XPSPeak4.1 software. The Chi-squared test was used to validate the fitting and the null hypothesis (there is no difference between the fitting and the experimental curves) was rejected for squared-chi values higher than the critical value for P=0.05.

RESULTS

The diffraction patterns of samples heated at 659, 681, 703 and 725^{o}C are presented on Figure 1. Heating the samples at 659^{o}C (MT13NC) did not produce any crystalline phases, as observed by XRD, but did produce a broad background characteristic of an amorphous phase. Two phases were observed in samples heated at 681^{o}C, α- and β-$Ca_2P_2O_7$

(MT13A), and all four phases, α- and β-$Ca_2P_2O_7$, $CaTi_4(PO_4)_6$ and TiP_2O_7, were observed after heating at 703 and 725°C (MT13B and C). The peak positions of the $CaTi_4(PO_4)_6$ phase were shifted to slightly lower 2 theta values, by approximately 0.1-0.2º. The results from the calculation of the phase compositions (wt %) after A, B and C heat treatments of glass samples are shown in Figure 1. The two polymorphs of $Ca_2P_2O_7$ in the MT13A samples were present in comparable amounts, and for the MT13B and MT13C samples, all four phases were present in approximately equal amounts. A glassy phase appeared to be present in all samples, as indicated by a broad background band in the diffraction patterns. The glassy phase was not quantified in the phase quantification analysis.

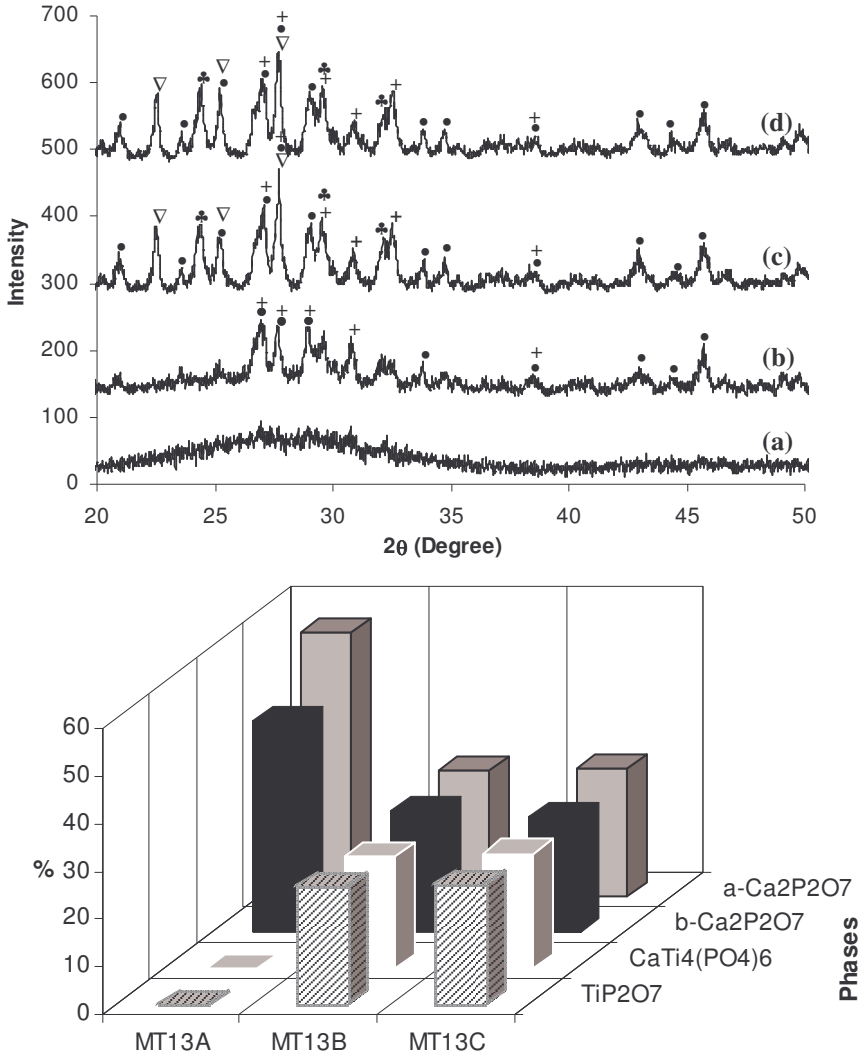

Figure 1 - X-ray diffraction patterns of samples heated at 659 (a), 681 (b), 703 (c) and 725ºC (d) and relative percentage of precipitated phases after heat treatment A, B and C, as described in the materials and methods section. (•) α-$Ca_2P_2O_7$, (+) β-$Ca_2P_2O_7$, (♣) $CaTi_4(PO_4)_6$ and (∇) TiP_2O_7.

Hot-chamber XRD results obtained by heating the mother glass powder at 4ºC/min from 610 to 660ºC are shown in Figure 2; for temperatures above 660ºC, the diffraction patterns showed no differences, and are therefore excluded. The patterns revealed that the first phases that precipitated in the glassy matrix were α- and β-$Ca_2P_2O_7$ at 620ºC and a small content of $CaTi_4(PO_4)_6$ appeared at 630ºC. At 650ºC the three phases, i.e. α-$Ca_2P_2O_7$, β-$Ca_2P_2O_7$ and $CaTi_4(PO_4)_6$ were clearly present with a small content of TiP_2O_7 and finally at 660ºC all four phases were observed. In terms of the sequence of crystalline phase formation these results were in agreement with the phase composition analysis of samples after heat treatment, Figure 1.

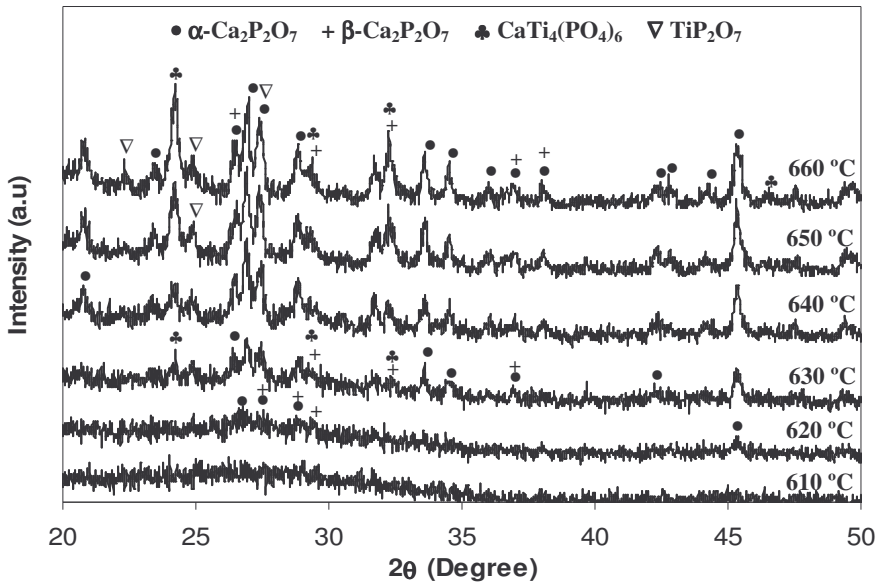

Figure 2 – HT-XRD pattern of mother glass (MT13) at 4ºC/min with an interval of 10ºC, ranging from 610-660 ºC.

Raman spectra of the mother glass (MT13) and the glass ceramics are shown in Figure 3 where a broad bands may be seen at approximately 900 and 1045 cm^{-1}; the latter band may be attributed to the presence of pyrophosphate radical, $P_2O_7^{4-}$. Another specific functional group was identified for glass ceramic MT13B and MT13C samples that correspond to orthophosphate (PO_4^{3-}) group, which was also present at similar wavelengths. The $P_2O_7^{4-}$ group should be assigned to the pyrophosphate group of α- and β-$Ca_2P_2O_7$ and TiP_2O_7, and the PO_4^{3-} group to the $CaTi_4(PO_4)_6$ phase. Generally speaking, it is usually difficult to distinguish the contributions of PO_4^{3-} and $P_2O_7^{4-}$ bands since there is a strong overlapping of the signal of these groups, particularly for glass ceramic samples that are not completely

crystallized.

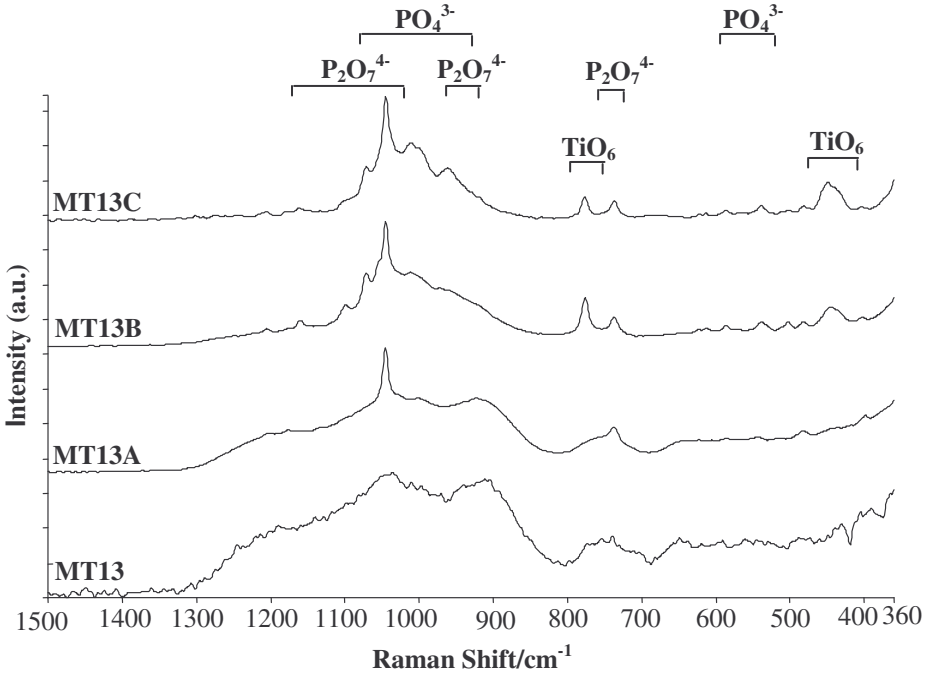

Figure 3 – Raman spectra before (MT13) and after heat treatment A, B and C.

Two Raman peaks characterize the MT13A glass ceramic, one weak peak at approximately 738 and a strong peak at 1045 cm^{-1} assigned to the presence of $P_2O_7^{4-}$ group, which is much more clearly defined than for the previous spectra due to the crystallization treatment. This group corresponds to the presence of $Ca_2P_2O_7$ phase and is related to the P-O-P bridges and P-O stretching, respectively[14]. New bands appear for the MT13B and MT13C glass ceramics, around 440 cm^{-1} and ranging from 950-1020 and 1060-1160 cm^{-1}. The bands located at around the 440 cm^{-1} region can be assigned to the symmetric bending modes of the PO_4 ion, although bands below this position may also involve modes arising from TiO_6 groups[15]. The new bands located at the 1060-1160 cm^{-1} region can be assigned to the presence of the TiP_2O_7 phase. The Raman bands located at approximately 968, 987 and 1008 cm^{-1} are assigned to the asymmetric and symmetric stretching of a P-O bond[16]. The bands at 968 and 1008 cm^{-1} correspond to the PO_4^{3-} group of the $CaTi_4(PO_4)_6$ phase, and it is noteworthy to verify that higher intensity was detected for MT13C than for MT13B. This may be due to there being more crystalline phases in the MT13C glass ceramic, compared to the MT13B sample, or that the $CaTi_4(PO_4)_6$ phase was more crystalline in the former sample. A weak band located at 777 cm^{-1} was also observed in MT13B and MT13C glass ceramics, which can be assigned to the TiO_6 group, as reported

by Krimi et al.[15].

Figure 4 shows the high-resolution XPS spectra of the mother glass. Similar results were obtained for glass ceramics with exception for P2p and Ti2p, which present two peaks, as shown in Figure 5. The binding energies of the Ca2p, P2p, Mg1s, Ti2p, and O1s of the mother glass and glass ceramics determined from the respective high resolution spectra are listed in Table 2.

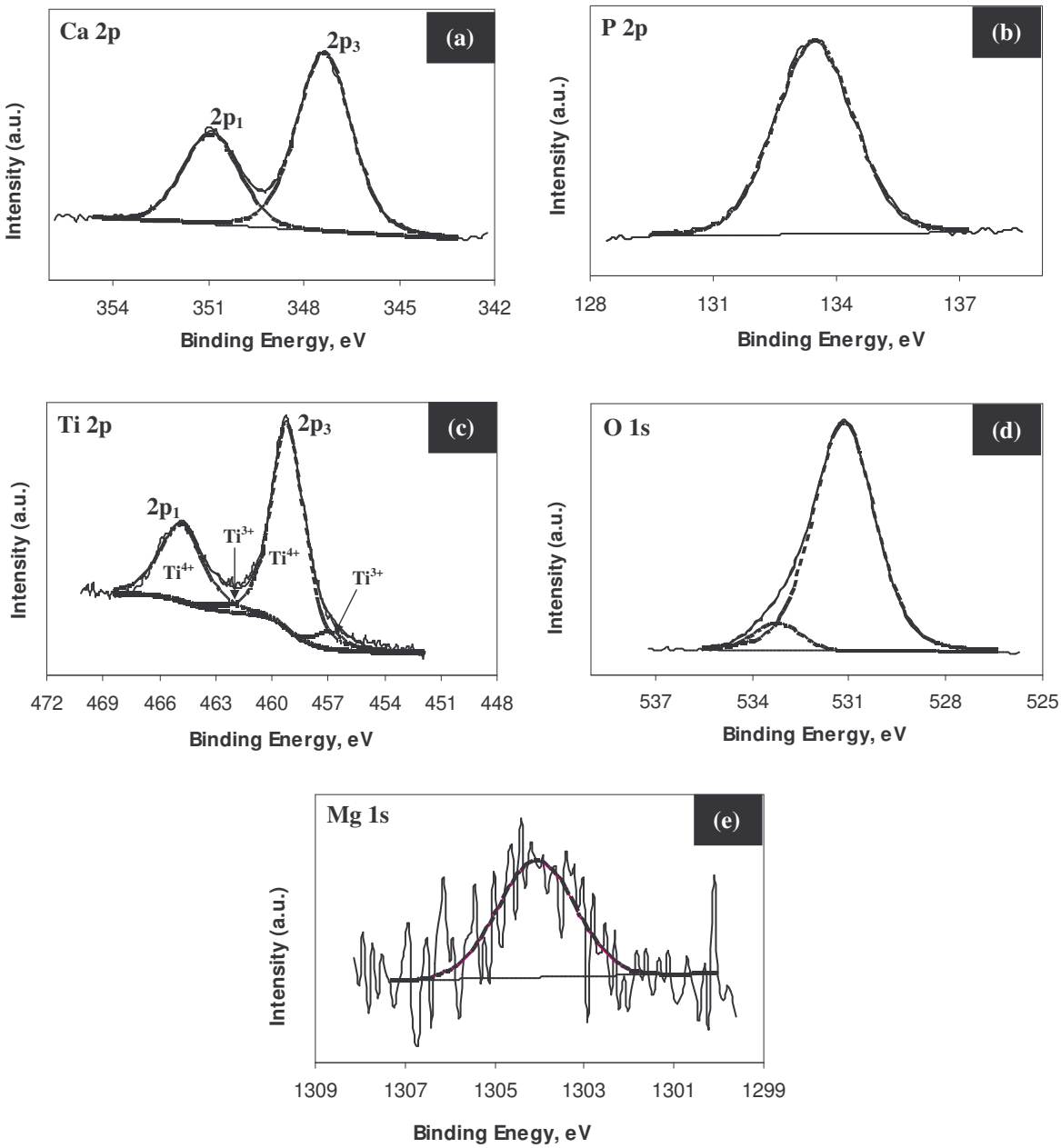

Figure 4 - High-resolution XPS spectra of the mother glass, (a) Ca2p, (b) P2p, (c) Ti2p, (d) O1s and (e) Mg1s.

The Ca2p peak shown in Figure 4 (a) can be deconvoluted to a doublet peak, $Ca2p_1$ located

at 350.8 ± 0.3 eV and $Ca2p_3$ located at 347.1 ± 0.7.

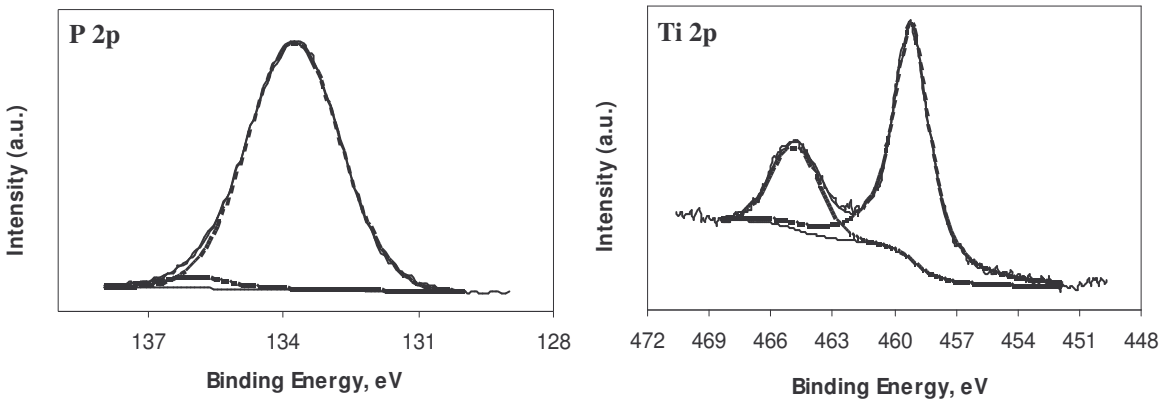

Figure 5 – High-resolution spectra of P2p and Ti2p for glass ceramics.

Table 2 – Binding energy of elements (P, O, Ca, Ti and Mg) detected on the mother glass and glass ceramics surface (values are in eV).

	P 2p		O 1s		Ca 2p		Ti 2p				Mg 1s
Samples	P 2p(1)	P 2p(2)	O 1s(1)	O1s(2)	Ca 2p1	Ca 2p3	Ti 2p1		Ti 2p3		
							Ti^{3+}	Ti^{4+}	Ti^{3+}	Ti^{4+}	
MT13	133.5		531.2	533.2	350.9	347.4	462.4	464.8	456.9	459.2	1304.1
MT13A	133.8	136.0	531.4	533.1	351.1	347.6		464.6		459.2	1304.5
MT13B	133.5	136.0	531.2	533.3	350.8	347.8		464.5		459.1	1304.3
MT13C	133.7	136.0	531.5	533.3	351.1	347.1		464.7		459.3	1304.5

The phosphorus line on the mother glass was a single peak located at 133.5 eV, which is correlated to the $Ca_2P_2O_7$ phase, with a full width half maximum (FWHM) of 2.25 eV indicating a possible overlapping peak. After heat treatment, and crystallization, new phosphate species appear around 136.0 eV, as shown in Figure 5. The nature of the chemical compound in which this element is present is not clearly understood in the literature, but may be attributed to a different structural environment for the $P_2O_7^{4-}$ groups.

The high-resolution spectra of Ti2p depicted in Figure 4 (c) for mother glass showed two doublet peaks. The doublet peak located at 456.9 and 462.4 eV corresponds to Ti in lower oxidation state 3+ (Ti^{3+}) and the doublet at 459.2 and 464.8 eV to titanium in 4+ state (Ti^{4+}). The values are in accordance with NIST XPS database. After heat treatment, only the doublet peak corresponding to Ti^{4+} was detected.

The O1s photoelectron spectrum, depicted in Figure 4 (d) provided important information

by deconvoluting the O1s spectra. In fact, the main peak located at 531.2 ± 0.3 eV was correlated to the pyrophosphate ($P_2O_7^{4-}$) group, as reported in the literature[17]. The second peak was located at 533.1 ± 0.2 eV. Shih et al. reported that for glass ceramic samples the standard O1s peak for P-O-P bonds was located at 533.1 eV[18].

The magnesium line, showed in Figure 4 (e) was a single peak located at 1304.0 ± 0.4 eV and no significant variations was observed for all samples studied.

DISCUSSION

Several authors have carried out a great deal of work on glass and glass ceramics within the composition of CaO-P_2O_5-TiO_2 and realized their enormous importance for the development of glass ceramics with biocompatible and bioactive phases[7,8,14,19]. From this composition, a new family of phosphate glass ceramics have been prepared in this work containing soluble and less soluble crystalline phases, such as β-$Ca_2P_2O_7$ and $CaTi_4(PO_4)_6$ respectively.

In the present study, glass ceramics were successfully prepared between the pyrophosphate (Q^1) and orthophosphate (Q^0) region ($3.5 < O/P < 4.0$). After heat treatment, four different crystalline phases were identified in the glass ceramic structure. Two of them, β-$Ca_2P_2O_7$ (β-DCP) and $CaTi_4(PO_4)_6$ are reported to be biocompatible and bioactive, respectively[14,20,21]. The biocompatibility of the other two phases TiP_2O_7 and α-$Ca_2P_2O_7$ has not been clearly reported so far in the literature. However, previous *in vitro* cell culture studies demonstrated that these materials allow the growth of MG63 osteoblast-like cells[22]. These glass ceramics resulted in good *in vitro* behaviour due to the bioactive and biocompatible phases that exist in the microstructure.

HT-XRD allows us to ensure that the true evolution of phases with temperature can be followed, as quenching/cooling of heated samples can induce artefacts. The HT-XRD patterns revealed that the first phases that precipitated in the glass matrix *in situ* were α- and β-$Ca_2P_2O_7$ at 620ºC with a small amount of $CaTi_4(PO_4)_6$ appearing at 630ºC. The formation of α- and β-$Ca_2P_2O_7$ seems to be a simultaneous process. It is interesting to note that the α-polymorph is normally observed on heating β-$Ca_2P_2O_7$ to temperatures greater than ≅1150ºC but for the glass composition used in this study, it crystallizes at the same time as the β-polymorph, at only 620ºC[23]. At 650ºC the three phases α-$Ca_2P_2O_7$, β-

$Ca_2P_2O_7$ and $CaTi_4(PO_4)_6$ are present with a small content of TiP_2O_7.

In terms of the order of the evolution of phases during heating of the mother glass, these *in situ* results are in agreement with those obtained by conventional phase analysis of samples subjected to different heat treatments, as the first phases precipitated were α- and β-$Ca_2P_2O_7$. The samples with heat treatment B (703ºC) and C (725ºC) consisted of approximately equal amounts of the four phases. However, a discrepancy occurred in the temperature range within which the formation of phases was observed in the two techniques, i.e., XRD and HT-XRD, and from the DTA observations[12]. Comparing the results obtained from the two X-ray diffraction studies, it was observed that phase nucleation/crystallization (β- and α-$Ca_2P_2O_7$) starts at ≅ 620ºC for HT-XRD, while nucleation occurred only at temperatures above 659ºC as a result of the heat treatment process; heat treatment at 659^{o}C resulted in an amorphous diffraction pattern by XRD. Identical results were obtained for the $CaTi_4(PO_4)_6$ phase, which was observed to form 630ºC using HT-XRD, but only appeared at 703ºC after heat treatment. It should be noted that heat treatments were carried out according to the results obtained from DTA analysis[12]. In HT-XRD all phases were present at 650ºC, however from samples that were heat-treated, this was only achieved at 703ºC. The first crystallization temperature from DTA analysis was found to be ≅ 726C, which should correspond to the $Ca_2P_2O_7$ phases, and the second crystallization temperature was ≅ 820^{o}C to the Ti-containing phases.

The main reason for these differences in nucleation temperature should be attributed to the initial size, agglomeration state and time of heat treatment at each temperature. The HT-XRD was performed on fine loose powder packed in a holder and therefore the high surface area favoured a nucleation and crystallization whereas XRD was performed on coarse powder obtained from block samples. On the other hand 45min dwell time at each temperature was applied which accounted for faster phase transformation, justifying the lower crystallization temperature of HT-XRD compared with XRD. It is known that surface area plays an important role in the sintering and phase nucleation mechanisms, with higher surface areas inducing higher rates for both processes[24,25]. It should also be noted that the heating profiles of the two methods are different, and are also different from the heating profile in the DTA analysis, as shown in Figure 6.

The functional groups identified for glass ceramics MT13A, MT13B and MT13C by Raman spectroscopy correspond to the functional groups of the crystalline phases identified by both X-ray diffraction techniques, i.e., orthophosphate (PO_4^{3-}) and

pyrophosphate ($P_2O_7^{4-}$). As indicated before, all functional groups that were identified by Raman analysis correspond to those existing in the crystalline phases α- and β-$Ca_2P_2O_7$, TiP_2O_7 and $CaTi_4(PO_4)_6$ and are in accordance with literature values[14,16]. Also, we obtained in previous studies some reference data from Raman spectroscopy measurements of some of the pure phases crystallized in the glass ceramics, which were as follows: 1044 and 734 cm^{-1} peaks for β-$Ca_2P_2O_7$, 455, 960, 998 and 1009 cm^{-1} peaks for $CaTi_4(PO_4)_6$ and 636, 1021, 1039, 1046 and 1069 cm^{-1} peaks for TiP_2O_7. The evolution of these functional groups in the Raman spectra with increasing treatment temperature corresponds to the results obtained from the XRD analysis, whereby the TiP_2O_7, and $CaTi_4(PO_4)_6$ phases crystallize only after the two polymorphs of $Ca_2P_2O_7$ have crystallized.

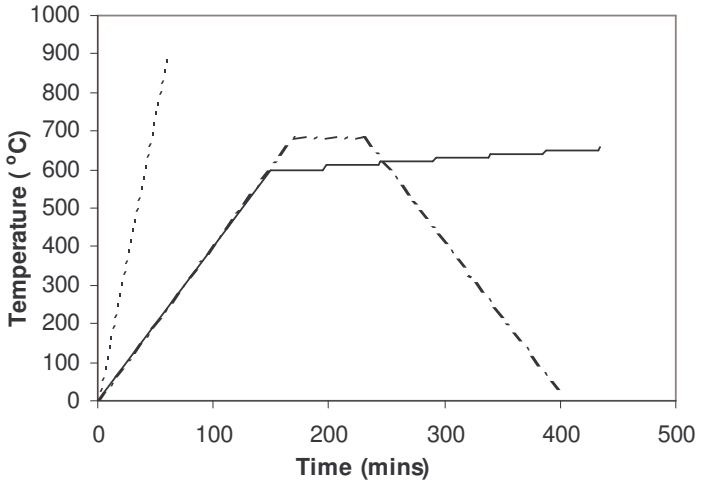

Figure 6 – Heating profiles of XRD (-·-·-), HT-XRD (——) and DTA (- - -) analysis.

A useful parameter to detect changes in the surface composition of glass and glass ceramics is the calcium/phosphorus atomic ratio (Ca/P). According to the oxides used for the mother glass preparation the theoretical value should be Ca/P= 0.60. The experimental value determined by quantitative XPS is around 0.59 for the mother glass, which is very close to the theoretical value. The binding energies for P2p, Ca2p3 and O1s observed at 133.5, 347.1 and 531.2 eV respectively corresponded to the $Ca_2P_2O_7$ phases present in the glass ceramics, as listed in NIST XPS database[17]. The O1s XPS spectrum was deconvoluted into two peaks for the mother glass as well as for the glass ceramics. It is characteristic of a glass to possess bridging (BO) and non-bridging oxygen (NBO) groups. For this reason it is reasonable that the glass before heat treatment presents two distinct contributions, associated with P-O-P vibrations (BO), located around 531 eV and with P-

O-M´ (M´= Mg, Ca and Ti) vibrations at higher binding energy (NBO). The binding energy observed for Ti highlighted the presence of two oxidation states 3+ and 4+ in mother glass. The mother glass showed a violet colour which in accordance to literature should correspond to the presence of $Ti^{3+(26)}$. This observation does not exclude the existence of Ti^{4+}. After crystallization the colour was white which seems to indicate that the majority of Ti is in Ti^{4+} state.

All these considerations allow one to conclude that it was possible to prepare glass ceramics in the calcium phosphate system that contained different bioactive and biocompatible phases and, by altering the heat treatment cycle, materials with different proprieties were obtained.

CONCLUSIONS

This work has demonstrated that depending upon the heat treatment cycle glass ceramics with various contents of α- and β-$Ca_2P_2O_7$, $CaTi_4(PO_4)_6$ and TiP_2O_7 phases were obtained. These phases are biocompatible and known to degrade at different rates in vivo which may be an important factor to cover several clinical applications.

ACKOWLEDGEMENTS

The authors would like to express their thanks to FCT - Fundação para a Ciência e a Tecnologia for their financial support through the PhD grant PRAXIS XXI/BD/21458/99. JMSS would like to thank EPSRC for funding the D8 Advance and HTXRD system.

REFERENCES

1. Franks, K., Abrahams, I., Georgiou, G., Knowles, J.C. Investigation of thermal parameters and crystallisation in a ternary CaO-Na_2O-P_2O_5-based glass system. Biomaterials, 2001; **22**(5): 497-501.

2. Rizkalla, A.S., Jones, D.W., Clarke, D.B., Hall, G.C. Crystallization of experimental bioactive glass compositions. Journal of Biomedical Materials Research, 1996; **32**: 119-124.

3. Navarro, M., Clément, J., Ginebra, M.P., Martínez, S., Avila, G., Planell, J.A.

Improvement of the stability and mechanical properties of resorbable phosphate glasses by the addition of TiO_2. Key Engineering Materials, 2002; **218-220**: 275-278.

4. Zhang, Y., Lopes, M.A., Santos, J.D. $CaO-P_2O_5$ class ceramics containing bioactive phases: Crystallisation and in vitro bioactivity studies, In: Bioceramics. 2000.

5. Navarro, M., Clément, J., Ginebra, M.P., Avila, G., Martínez, S., Planell, J.A. *In vitro* biocompatibility pf titanium containing soluble phosphate glasses. In 17th European Conference on Biomaterials. 2002Barcelona, Spain.

6. Ohtsuki, C., Osaka, A., Kokubo, T. Effects of Al_2O_3 and TiO_2 on bioactivity of $CaO-SiO_2$ glasses. Bioceramics, 1994; **7**.

7. Suzuki, T., Toriyama, M., Hosono, H., Abe, Y. Application of a microporous glass-ceramics with a skeleton of $CaTi_4(PO_4)_6$ to carriers for immobilization of enzymes. Journal of Fermentation and Bioengineering, 1991; **72**(5): 384-391.

8. Abe, Y., Hosono, H., Hosoe, M. Development of calcium phosphate glass-ceramics for surgical and dental use. Phosphorus and Sulfur, 1987; **30**: 337-340.

9. Schneider, K., Heimann, R.B., Berger, G. Plasma-sprayed coatings in the system $CaO-TiO_2-ZrO_2-P_2O_5$ for long-term stable endoprostheses. Materialwissenschaft Und Werkstofftechnik, 2001; **32**(2): 166-171.

10. Lin, F.H., Lin, C.C., Lu, C.M., Liu, H.C., Sun, J.S., Wang, C.Y. Mechanical-properties and histological-evaluation of sintered β-$Ca_2P_2O_7$ with $Na_4P_2O_7.10H_2O$ addition. Biomaterials, 1995; **16**(10): 793-802.

11. Lin, C.C., Liao, C.J., Sun, J.S., Liu, H.C., Lin, F.H. Prevascularized bone graft cultured in sintered porous β-$Ca_2P_2O_7$ with 5 wt% $Na_4P_2O_7.10H_2O$ addition ceramic chamber. Biomaterials, 1996; **17**(11): 1133-1140.

12. Dias, A.G., Tsuru, K., Hayakawa, T., Lopes, M.A., Santos, J.D., Osaka, A. Crystallisation studies of biodegradable $CaO-P_2O_5$ glass with MgO and TiO_2 for bone regeneration applications. Glass Technology, 2004; **45**(2): 78-79.

13. Bish, D.L., Howard, S.A. Quantitative phase-analysis using the Rietveld method. Journal of Applied Crystallography, 1988; **21**: 86-91.

14. Gimenez, I.D., Mazali, I.O., Alves, O.L. Application of Raman spectroscopy to the study of the phase composition of phosphate based glass-ceramics. Journal of Physics and

Chemistry of Solids, 2001; **62**(7): 1251-1255.

15. Krimi, S., Eljazouli, A., Rabardel, L., Couzi, M., Mansouri, I., Leflem, G. Glass-formation in the Na_2O-TiO_2-P_2O_5 System. Journal of Solid State Chemistry, 1993; **102**(2): 400-407.

16. Barj, M., Lucazeau, G., Delmas, C. Raman and infrared-spectra of some chromium NASICON-type materials: Short-range disorder characterization. Journal of Solid State Chemistry, 1992; **100**(1): 141-150.

17. NIST standard reference database.

18. Shih, P.Y., Yung, S.W., Chin, T.S. Thermal and corrosion behaviour of P_2O_5-Na_2O-CuO glasses. Journal of Non-Crystalline Solids, 1998; **224**(2): 143-152.

19. Reaney, I.M., James, P.F., Lee, W.E. Effect of nucleating agents on the crystallization of calcium phosphate glasses. Journal of the American Ceramic Society, 1996; **79**(7): 1934-1944.

20. Ryu, H.S., Youn, H.J., Hong, K.S., Chang, B.S., Lee, C.K., Chung, S.S. An improvement in sintering property of β-tricalcium phosphate by addition of calcium pyrophosphate. Biomaterials, 2002; **23**(3): 909-914.

21. Kitsugi, T., Yamamuro, T., Nakamura, T., Masanori, O. Transmission electron microscopy observations at the interface of bone and 4 types of calcium-phosphate ceramics with different calcium phosphorus molar ratios. Biomaterials, 1995; **16**(14): 1101-1107.

22. Dias, A.G., Costa, M.A., Lopes, M.A., Santos, J.D., Fernandes, M.H. Biological activity of two glass ceramics in the meta- and pyrophosphate region: a comparative study. Key Engineering Materials, 2004; **254-256**: 825-828.

23. Bian, J.J., Kim, D.W., Hong, K.S. Microwave dielectric properties of $Ca_2P_2O_7$. Journal of the European Ceramic Society, 2003; **23**(14): 2589-2592.

24. Clark, T.J., Reed, J.S. Kinetic processes involved in the sintering and crystallization of glass powders. Journal of the American Ceramic Society, 1986; **69**(11): 837-846.

25. Siligardi, C., D'Arrigo, M.C., Leonelli, C. Sintering behaviour of glass-ceramic frits. American Ceramic Society Bulletin, 2000; **79**(9): 88-92.

26. Chowdari, B.V.R., Rao, G.V.S. XPS and ionic conductivity on Li_2O-Al_2O_3-(TiO_2 or

GeO_2)-P_2O_5 glass ceramics. Solid State Ionics, 2000; **136-137**: 1067-1075.

2.4. Physicochemical degradation studies of calcium phosphate glass ceramic containing TiO_2 and MgO oxides

ABSTRACT

The *in vitro* degradation behaviour of MT13B ($45CaO\text{-}37P_2O_5\text{-}5MgO\text{-}13TiO_2$, mol %) glass ceramic in two possible physiological conditions at pH=7.4 and pH=3.0 are reported. The incorporation of TiO_2 in the glass structure leads to the precipitation of specific crystalline phases in the glass matrix, namely α- and β-$Ca_2P_2O_7$, TiP_2O_7 and $CaTi_4(PO_4)_6$.

The *in vitro* testing was carried out at 37ºC during periods of 42 days in pH 7.4 solution and during 24h in pH 3.0 solution. The degradation testing at pH 3.0 showed a higher weight loss compared with degradation testing at pH 7.4; the weight loss under the acidic condition was about ten times higher after 42 days of immersion at pH 7.4. The ionic release profile of Ca^{2+}, PO_4^{3-}, Mg^{2+} and Ti^{4+} showed a continuous increase in concentration over all immersion times for both testing solutions. At pH 7.4 the level of dissolution of MT13B was low, leading to the low release of ions. For Mg^{2+}, Ca^{2+}, PO_4^{3-} after 24h of immersion at pH 3.0, the concentration levels were about six times higher than the levels after 42 days of immersion at pH 7.4. The structural changes at the surface of materials during degradation have been analyzed by Raman spectroscopy and scanning electron microscopy (SEM). Results suggest that the degradation is dependent on the medium and pH used in the dissolution test. This material seems to offer an attractive alternative for slowly resorbable materials in biomedical applications.

INTRODUCTION

The research on bioresorbable materials for tissue regeneration applications has been increasing significantly[1] because these materials do not require a second surgery to retrieve the implant, which happens to bioinert materials in many cases. However, the variety of available degradable biomaterials is still too restricted to cover an adequate range of diverse material properties[1-3]. Hence, the development of new degradable biomaterials is currently an important research challenge in the biomaterials field. In this perspective, calcium phosphate glass ceramics seems to be a motivating choice for this purpose as their solubility can be tailored by controlling the chemical composition of the

base glass and choosing the correct heat treatment cycle, and thus short-term or long-term soluble phosphate glass ceramics may be obtained[2-6].

Considering the solubility in the physiological environment, these materials must be seen as multiphase systems in which each phase has a unique degradable characteristic. The solubility of glass ceramics was reported to be influenced by several factors: 1) composition of the crystalline phases, 2) structure and density of the crystalline phases, 3) volume fraction of crystalline phases, and 4) grain size of crystalline phases[7-11].

Generally the biodegradation of calcium phosphates may be caused by three major factors: 1) physicochemical dissolution, which depends on the solubility product of the material and the local pH of its environment; 2) physical disintegration into small particles as a result of preferential chemical attack of grain boundaries, and 3) biological factors, such as phagocytosis[1,8,9,11].

Calcium phosphate glass ceramics, and particularly those in the P_2O_5-CaO-MgO-TiO_2 system, have been demonstrated to support cell growth and differentiation *in vitro* and to provide osteoconductivity with *in vivo* degradation compatible with new bone formation[12-15]. The aim of this work was to evaluate the *in vitro* degradation behaviour of the 45CaO-37P_2O_5-5MgO-13TiO_2 (mol %) glass ceramic at two different physiological conditions of pH 7.4 and 3.0.

MATERIALS AND METHODS

Glass ceramic preparation

Glass ceramic MT13B with the composition of 45CaO-37P_2O_5-5MgO-13TiO_2, mol % was prepared by the powder sintering technique. The sintering of glass powder was performed according to differential thermal analysis (DTA) results of the base glass, as described elsewhere[16,17]. Briefly, MT13 base glass was sintered at 703ºC for 1h, with a heating rate of 4ºC/min and naturally cooled inside the furnace. The prepared glass ceramic was then crushed, ground and sieved in the range of 355-425 μm.

In vitro degradation studies

The degradation testing was performed in triplicate, according the standard ISO 10993-14 "Biological evaluation of medical devices- Part 14: Identification and quantification of

degradation products from ceramics". Two sets of experiments were performed at different pH. The first set was conducted at pH 3.0 using citric acid and it was referred as extreme solution testing, and the second experiment was performed at pH 7.4 using Tris-HCl solution, referred to as simulation solution testing.

The samples were incubated for 6, 12 and 24h in the extreme solution testing and for 7, 14, 28 and 42 days in the simulation solution testing. At these time points, granules were collected by filtering (0.22 μm), washed in deionised water and dried to constant weight. At the end of each immersion time the pH value of the soaking solution was measured at 37 ± 0.1ºC. A relative weight loss percentage (W_L) after a certain time of immersion, t, of the samples was calculated from the following equation:

$$W_L = [(W_0 - W_t)/W_0] \times 100$$

where W_0 and W_t stand for initial and final weight after a specific immersion time, respectively.

Ionic concentration measurement

The quantitative determination of the released ions into the testing solution was measured using two different techniques. Calcium, magnesium and titanium ions were measured by flame atomic absorption spectroscopy (AAS) (GBC 90AA), whereas the phosphate ion concentration was measured by ultraviolet spectroscopy using the molybdenum blue method (Philips, Model PU 8620, UV-Vis Nir). According to this method, pyrophosphate groups were converted to orthophosphate by a heating procedure using sulphuric acid and ammonium persulphate. All results are presented as arithmetic means ± standard deviation.

Materials characterization

The granule samples were ground to a fine powder form in order to be analyzed by Raman spectroscopy (transmission mode) using a system 2000 FTIR spectrometer (Perkin Elmer) before and after the degradation testing. The resolution used was 4 cm^{-1} and the number of scans was 200. A JEOL scanning electron microscope (JSM-35C) was used to observe the external surface of the granule samples before and after dissolution periods.

RESULTS

Figure 1 shows the variation of sample weight with immersion period for both testing solutions. A similar trend was observed for both conditions, with a steady weight loss with the immersion period. After 42 days of immersion in simulation solution (pH 7.4) a weight loss variation of ≅ 0.05-0.2 was obtained and ≅ 0.4-1.6 % for 1 day in extreme solution (pH 3.0).

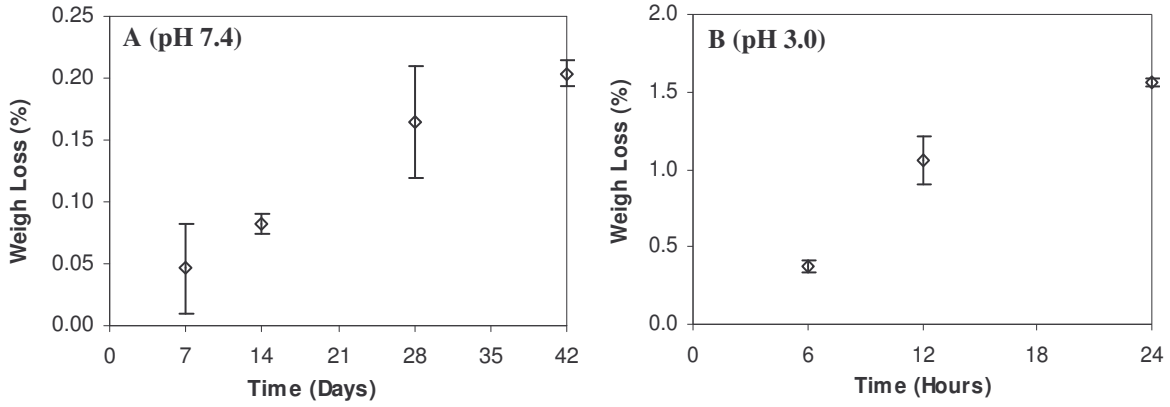

Figure 1 – Weight loss percentage against immersion time for MT13B glass ceramic in: (A) simulation and (B) extreme testing condition.

The variation in pH of the two testing solutions with immersion time is shown in Figure 2. In the pH 7.4 testing solution (Figure 2A), no significant variation of pH could be observed while for the extreme testing solution (Figure 2B) a slight increase in pH was observed up to 12h achieving a pH value of 3.3 ±0.1, which was then followed by stabilization.

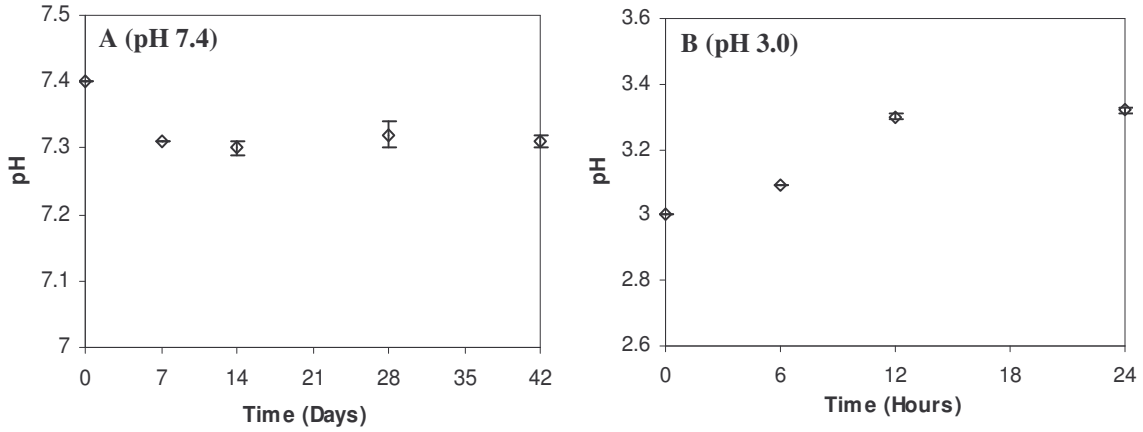

Figure 2 – Variation of pH of the (A) simulation and (B) extreme testing solution with immersion time.

Figures 3 and 4 show the variation of the Ca^{2+}, PO_4^{3-}, Mg^{2+} and Ti^{4+} ionic concentrations against immersion time in both testing solutions. The variation of the concentration of the ions released in both testing solutions showed a similar trend, continuously increasing throughout the immersion time but with a lower degradation rate for most of the ions analyzed at pH 7.4. The level of concentration attained for Ca^{2+} was higher than the PO_4^{3-} in both testing solutions.

Despite the very short immersion time used in the extreme condition, when compared to the physiological pH 7.4 solution, a higher amount of each ion was released into the former except for titanium ions.

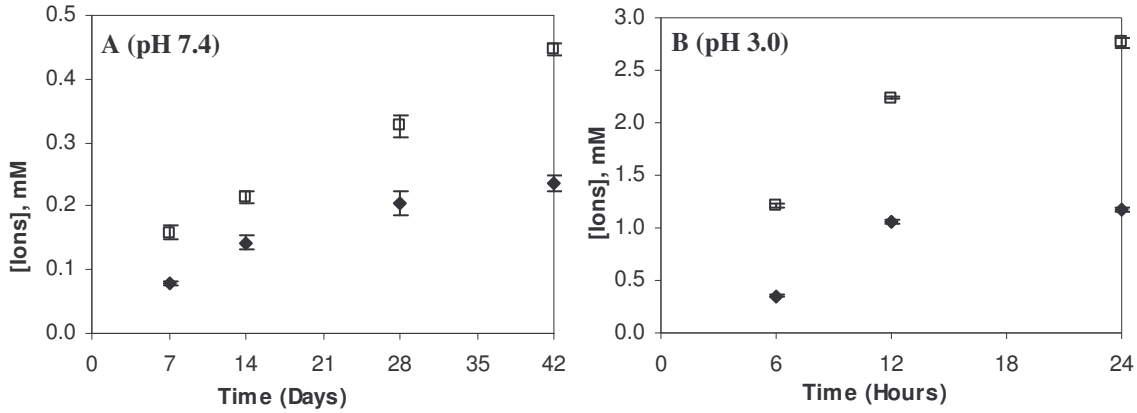

Figure 3 – Ca^{2+} (□) and PO_4^{3-} (♦) ion concentration in simulation A) and extreme testing solution (B) against immersion time.

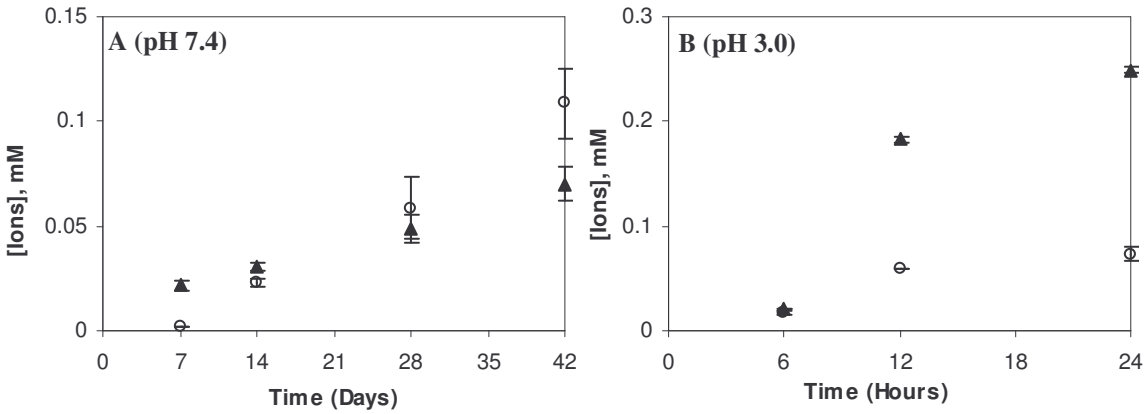

Figure 4 – Mg^{2+} (▲) and Ti^{4+} (○) ion concentration in simulation (A) and extreme testing solution (B) against immersion time.

The SEM results of MT13B glass ceramic granules before and after degradation testing are

shown in Figure 5. SEM observations revealed important differences in the progress of surface degradation in both solutions. A much more degraded surface was observed in the experiment conducted at pH 3.0 just after 6h (Fig. 5C) of immersion compared with the experiment performed at pH 7.4 (Fig. 5B) after 7 days.

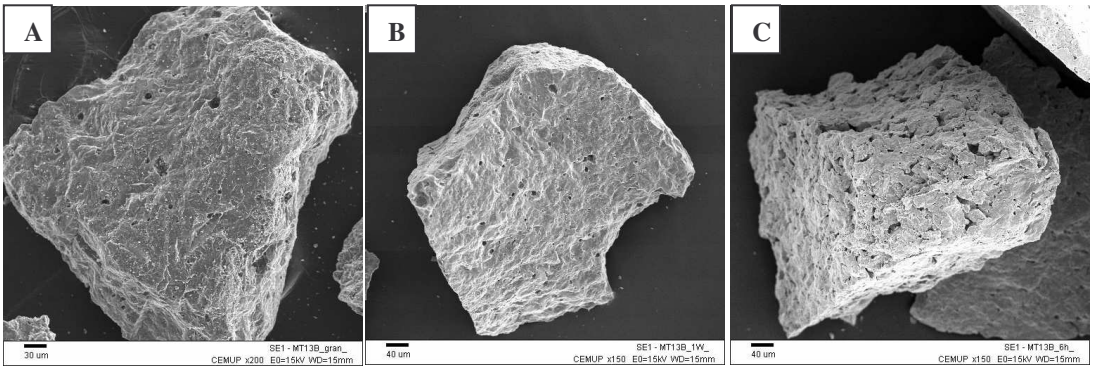

Figure 5 –SEM images of the glass ceramic MT13B before (A) and after immersion in simulation (B) and extreme testing solution (C).

Raman spectra of MT13B glass ceramic before and after degradation testing in both solutions are plotted in Figure 6.

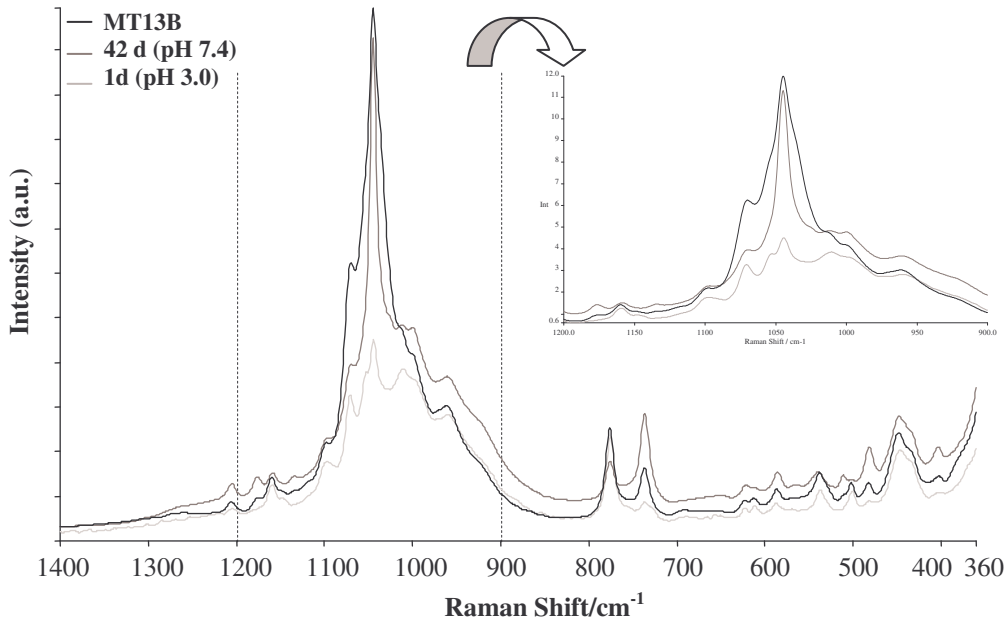

Figure 6 – Raman spectra of the glass ceramic MT13B before and after immersion during 7 and 42 days at pH 7.4 and 1 day at pH 3.0.

Comparing MT13B spectrum before and after immersion, significant band changes could be detected mainly in the region of 900-1160 cm^{-1}, as observed in the detailed figure. The associated vibrations correspond to ortho- and pyrophosphate groups[18,19], correlated to those crystalline phases existing in the glass ceramic, namely α- and β-$Ca_2P_2O_7$, TiP_2O_7 and $CaTi_4(PO_4)_6$. After soaking for 42 days in pH 7.4 solution a slightly decrease was observed in the band located at 1069 cm^{-1} correlated to the $P_2O_7^{4-}$ groups present in the TiP_2O_7 phase. Strong band changes were observed for 24h soaking in pH 3.0 solution, and this was more pronounced in the band located at approximately 1045 cm^{-1} assigned to the presence of $P_2O_7^{4-}$ groups.

DISCUSSION

In this work a base glass with the composition 45CaO-37P_2O_5-5MgO-13TiO_2 (mol %) was prepared and converted into a glass ceramic by a sintering technique. As previously published, four crystalline phases were precipitated in the glass matrix, α and β–$Ca_2P_2O_7$ (α- and β-DCP), $CaTi_4(PO_4)_6$ (CTP) and TiP_2O_7 (TP) phases[18,20]. Two of them, β-DCP and CTP, are reported to be biocompatible, with the former being present in commercial graft materials such as Bioresorb® and Vitoss®[21]. However, the biocompatibility of the other two phases is not clearly reported in the literature. Literature also reports that CTP is almost insoluble in normal physiological conditions, although Ploska et al.[22] state that the presence of TP as a minor phase in the CTP matrix can improve its degradation rate. β-DCP was reported as not dissolving in distilled water[23], while for TP and α-DCP pure phases no results have been reported so far in the literature.

Despite the controversy regarding the *in vitro* acellular tests for assessing biodegradation, since calcium phosphate ceramics can either undergo chemical and/or cellular degradation *in vivo* conditions, a number of authors believe these experiments can give insights about the biodegradation behaviour of MT13B glass ceramic[10,11,13].

The chemical degradation studies, following the ISO 10993, consisted of two tests. The first test, an extreme solution conducted at pH 3.0 used a citric acid buffer solution that mimics the acid environment produced by osteoclasts. Literature reports that direct pH measurements of the extracellular fluid from bone-resorbing cells showed that the pH was as low as 3[24]. The second test simulates a more frequently encountered *in vivo* pH 7.4 using TRIS-HCl buffer. Using these two soaking mediums with different pH values the

mechanisms of degradation, which may not be the same at normal body pH as it is for the case of extremely low pH 3.0, were also evaluated.

When performing the degradation testing at pH 3.0, a higher weight loss was quantified as expected. Based on the weight loss obtained, the dissolution of MT13B at pH 7.4 is comparable to HA as reported in the literature, being relatively insoluble in neutral solution and readily soluble in acid solution[25,26]. One of relevant parameter on the study of glass dissolution kinetics is the kind of medium used. The pH and ionic strength of the medium have an important role on the rate at which the glasses dissolve[10,27]. In fact, the weight loss observed after 24h of immersion at pH 3.0 was about ten times higher than in 42 days at pH 7.4. SEM observations also showed that the superficial degradation mechanism is higher in acidic solution than in neutral solution. As compared with the granule samples before soaking, no significant superficial degradation changes were observed in the granules samples after soaking at pH 7.4.

The ionic release profiles found from MT13B dissolution showed a continuous increase in the concentration of the evaluated ions over all immersion time, even though their appeared to be a reduction in the dissolution rate in the extreme testing solution after about 12 hours. It should be noted that the degradation of MT13B during the immersion time revealed the presence of a residual glassy phase probably at grain boundaries. In fact, despite not detecting a chemical phase containing magnesium in MT13B glass ceramic composition by XRD, Mg^{2+} ions were continuously released into both testing solutions over the entire immersion time evaluated.

At pH 7.4 minor dissolution of MT13B occurred leading to low release of ions. As a consequence of higher dissolution of MT13B at lower pH testing solution, increases in ion concentration release were observed. For Mg^{2+}, Ca^{2+}, PO_4^{3-} after 24h of immersion at pH 3.0, the ion concentration levels were about six times higher than the values observed after 42 days of immersion at pH 7.4.

The citric acid (CA) used as soaking medium in the pH 3.0 testing solution may also have had a role in the dissolution process. Literature reports that the presence of CA may inhibit, stimulate or have no effect on the dissolution of some calcium phosphate materials, depending on the type of molecular events that take place on crystal surface[28-31]. The fact that Ti^{4+} concentration levels detected on test solution at pH 3.0 were lower compared to those observed with the pH 7.4 solution should be related to the interaction of Ti^{4+} with CA, which seemed to weaken bonds between Ti^{4+} and pyrophosphate groups in the crystal

surface. As a consequence of this, similar molar levels of Ca^{2+} and PO_4^{3-} were attained in this extreme pH medium, in contrast to what happened at pH 7.4. This interaction might also be followed by protonation of citrate groups in the surface contributing to the small pH increase observed with this solution. The residual glassy phase should also have contributed to the release of some Ti^{4+} ions into both testing solutions.

The different degradation behaviours in terms of pH changes observed for the 2 testing solutions is a response to the cations and anions released into each solution as a result of partial dissolution of some chemical phases present in the MT13B glass ceramic.

CONCLUSIONS

The results obtained in this work demonstrated that the degradation of MT13B material is dependent on the medium and pH used in the dissolution test. A stronger degradation was observed using pH 3.0 citric acid buffer solution compared to the normal physiological pH 7.4, where is the glass ceramic was relatively insoluble, with results that were comparable to hydroxyapatite. Therefore, opportunities exist to use this material as a bone graft in certain clinical applications, such as cranioplasty, where relative slow resorption and replacement by bone is quite acceptable.

ACKNOWLEDGMENTS

The authors would like to express their thanks to FCT - Fundação para a Ciência e a Tecnologia for their financial support through the PhD grant PRAXIS XXI/BD/21458/99.

REFERENCES

1. Laurencin, C.T., ed. Bone graft substitutes. 2003. ASTM International.

2. Ratner, B.D., Hoffmam, A.S., Schoen, F.J., Lemons, F.J., eds. Biomaterials science: an introduction to materials in medicine. 2nd ed. 2004. Elsevier Academic Press.

3. Hench, L.L., Wilson, J., eds. Introduction to bioceramics. 1993. World Scientific: Singapore.

4. Burnie, J., Gilchrist, T., Duff, S.R.I., Drake, C.F., Harding, N.G.L.,Malcolm, A.J. Controlled release glasses (CRG) for biomedical uses. Biomaterials, 1981; **2**(4): 244-246.

5. Burnie, J., Gilchrist, T. Controlled release glass (C.R.G.) - A new biomaterials, In: Ceramics in Surgery, Vicenzi, P., Editor. 1983, Elsevier Scientific Publishing Company.

6. Vogel, J., Wange, P., Hartmann, P. Phosphate glasses and glass-ceramics for medical applications. Glastechnische Berichte-Glass Science and Technology, 1997; **70**(7): 220-223.

7. Dorozhkin, S.V., Epple, M. Biological and medical significance of calcium phosphates. Angewandte Chemie-International Edition, 2002; **41**(17): 3130-3146.

8. Lettuec, J.C., Clément, D., Lesprit, E., Faber, J. The use of calcium phosphates, their biological properties. European Journal of Orthopaedic Surgery and Traumatology, 2000; **10**: 223-229.

9. Grambow, B. Geochemical approach to glass dissolution, In: Corrosion of glass, ceramics and ceramic superconductors, Clark, D.E.,Zoitos, B.K., Editors. 1992, Novel Publications.

10. Legeros, R.Z. Biodegradation and bioresorption of calcium phosphate ceramics. Clinic Materials, 1993; **14**: 65-88.

11. McCracken, W.J. Corrosion of glass-ceramics, In: Corrosion of glass, ceramics and ceramic superconductors, Clark, D.E., Zoitos, B.K., Editors. 1992, Novel Publications.

12. Jantzen, C.M. Thermodynamic approach to glass corrosion, In: Corrosion of glass, ceramics and ceramic superconductors, Clark, D.E., Zoitos, B.K., Editors. 1992, Novel Publications.

13. Koerten, H.K., Van der Meulen, J. Degradation of calcium phosphate ceramics. Journal of Biomedical Materials Research, 1999; **44**(1): 78-86.

14. Dias, A.G., Lopes, M.A., Santos, J.D., Fernandes, M.H. The influence of pre-incubation treatment in the *in vitro* biological performance of degradable $CaO\text{-}P_2O_5$ glass ceramics. Key Engineering Materials, 2005; **284-286**: 565-568.

15. Dias, A.G., Costa, M.A., Lopes, M.A., Santos, J.D., Fernandes, M.H. Biological activity of two glass ceramics in the meta- and pyrophosphate region: a comparative study. Key Engineering Materials, 2004; **254-256**: 825-828.

16. Dias, A.G., Lopes, M.A., Afonso, A.A., Tsuru, K., Hayakawa, S., Takashima, S., Kurabayashi, Y., Osaka, A., Santos, J.D. *In vivo* performance of biodegradable calcium

phosphate glass ceramics using the rabbit model: histological and SEM observation. Journal of Biomaterials Applications (*In press*).

17. Dias, A.G., Lopes, M.A., Santos, J.D., Fernandes, M.H. In vitro studies of calcium phosphate glass ceramics with different solubility using human bone marrow cells. Journal of Biomedical Materials Research (*In press*).

18. Dias, A.G., Skakle, J.M.S., Gibson, I.R., Lopes, M.A., Santos, J.D. *In situ* thermal and structural characterization of bioactive calcium phosphate glass ceramics containing TiO_2 and MgO oxides: HT-XRD studies. Journal of Non-Crystalline Solids (Accepted).

19. Nyquist, R.A., Handbook of infrared and raman spectra of inorganic compounds and organics salts. 1997. Academic Press.

20. Dias, A.G., Tsuru, K., Hayakawa, T., Lopes, M.A., Santos, J.D., Osaka, A. Crystallisation studies of biodegradable $CaO\text{-}P_2O_5$ glass with MgO and TiO_2 for bone regeneration applications. Glass Technology, 2004; **45**(2): 78-79.

21. Tadic, D., Epple, M. A thorough physicochemical characterisation of 14 calcium phosphate-based bone substitution materials in comparison to natural bone. Biomaterials, 2004; **25**(6): 987-994.

22. Ploska, U., Berger, G. Solubility of compositions in the system $CaTixZr_4\text{-}x(PO_4)_6$ with x = 0-4. Biomaterials, 1997; **18**(24): 1671-1675.

23. Lin, F.H., Liao, C.J., Chen, K.S., Sun, J.S., Liu, H.C. Degradation behaviour of a new bioceramic: $Ca_2P_2O_7$ with addition of $Na_4P_2O_7.10H_2O$. Biomaterials, 1997; **18**(13): 915-921.

24. Athanasou, N.A. Cellular biology of bone-resorbing cells. The Journal Of Bone And Joint Surgery. American Volume, 1996; **78**(7): 1096-1112.

25. Aoki, H., Science and medical applications of hydroxyapatite. 1991. Takayama Press System center Co., Inc. Tokyo.

26. Aoki, H., Medical aplications of hydroxypatite. 1994. Ishiyaku EuroAmerica, Inc. Tokyo.

27. Zyman, Z., Dedukh, N.V., Glusko, V.I., Shcherbyna, S.V. In 17th European Society for Biomaterials. 2002Barcelona.

28. Misra, D.N. Interaction of citric-acid with hydroxyapatite - formation of calcium

citrate. Journal of Dental Research, 1995; **74**: 72-72.

29. Hennequin, M., Douillard, Y. Effects of citric-acid treatment on the Ca, P and Mg contents of human dental roots. Journal of Clinical Periodontology, 1995; **22**(7): 550-557.

30. Misra, D.N. Interaction of citric acid with hydroxyapatite: Surface exchange of ions and precipitation of calcium citrate. Journal of Dental Research, 1996; **75**(6): 1418-1425.

31. Hennequin, M., Pajot, J., Avignant, D. Effects of different pH values of citric-acid solutions on the calcium and phosphorus contents of human root dentin. Journal of Endodontics, 1994; **20**(11): 551-554.